ISSN. 0377 - 2969
Vol. 42(4) Dec. 2005

PROCEEDINGS

OF THE PAKISTAN ACADEMY OF SCIENCES

The Pakistan Academy of Sciences
Islamabad Pakistan

PAKISTAN ACADEMY OF SCIENCES

Founded 1953

President: Prof. Dr. Atta-ur-Rahman, N.I., H.I., S.I, T.I.

THE PROCEEDINGS OF THE PAKISTAN ACADEMY OF SCIENCES is an international publication and is the official journal of the Academy published quarterly. It publishes original research papers and reviews on a broad range of topics in basic and applied sciences. All papers are refereed externally. Authors are not required to be members or fellows of the Academy.

Annual Subscription for 2005

Pakistan: Institutions: Rupees 2000/-
Individuals: Rupees 1000/-
Other countries: US$ 100.00 (Price includes air-lifted delivery overseas)

Published quarterly by **The Pakistan Academy of Sciences**, 3 Constitution Avenue, G-5/2, Islamabad, Pakistan.
Tel:- 92-51-9207140 & 9207789 Fax: 92-51-9206770 E-mail: pasisb@yahoo.com

Website of the Academy: www.paspk.org

Proceedings of the
Pakistan Academy of Sciences

Contents Volume 42 No. 4 December 2005

Research Articles

Life Sciences

Analysis of some residual antibiotics in muscle, kidney and liver samples of Broiler Chicken by various methods 223
— *Habib Amjad, Javed Iqbal and Muhammad Naeem*

Distribution of ABO and RH blood group alleles in Gujrat region of Punjab, Pakistan 233
— *Mohammad Anees and Mohammad Shabir Mirza*

Physical Sciences

Fermions in Kerr-Newman-Kasuya Space-time 239
— *Elias Uddin Biswas*

Pocklington equation and the method of moments 243
— *J. Sosa-Pedroza, V. Barrera-Figueroa and J. López-Bonilla*

Some applications of a Lovelock's Theorem 249
— *M. Acevedo, J. López-Bonilla and S. Vidal-Beltrán*

Determination of triprolidine-HCl by spectrophotometric method in pure and pharmaceutical preparations using dichloronitrobenzene as a new chromogenic reagent 253
— *Amina Mumtaz, Asrar A. Kazi, Tehseen Aman, M. Usman Sabri and Fauzia Noureen*

Landau Lifshitz Energy Momentum Pseudotensor for metrics with spherical symmetry 261
— *J. H. Caltenco, J. I. López-Bonilla, R. Peña-Rivero and J. Rivera-Rebolledo*

On certain class of Analytic Functions 265
— *Nailah Abdul rahman Al Dihan*

Seismic hazard assessment of NW Himalayan Fold and Thrust Belt using probabilistic approach 287
— *MonaLisa, Azam A. Khwaja, M. Javed, Ywer S. Ansari and M. Qasim Jan*

Enginering Sciences & Technology

Design Structure Matrix (DSM): New Directions 297
– *A.H.M. Shamsuzzoha and Nadia Bhuiyan*

Reviews

Present status and future needs of Tea Industry in Bangladesh 305
– *G.M.R. Islam, M. Iqbal, K.G. Quddus and M.Y. Ali*

Adverse effects of pesticides amd related chemicals on enzyme and hormone systems of fish, amphibians and reptiles: A Review 315
– *M. Zaheer Khan and Francis C.P. law*

Instructions to Authors 325

Submission of manuscripts: Manuscripts should be submitted in duplicate including the original, **through a Fellow of the Academy** preferably to *Sectional Editors* (see instructions). Authors should consult the ***Instructions to Authors*** on pages 325-326 of this issue and the Website, www.paspk.org.

Proc. Pakistan Acad. Sci. 42(4):223-231.2005

ANALYSIS OF SOME RESIDUAL ANTIBIOTICS IN MUSCLE, KIDNEY AND LIVER SAMPLES OF BROILER CHICKEN BY VARIOUS METHODS

Habib Amjad*, Javed Iqbal and Muhammad Naeem

**Institute of Chemistry, University of the Punjab, Lahore, Pakistan, and Applied Chemistry Research Centre, PCSIR Labs. Complex, Ferozepur Road, Lahore, Pakistan*

Received February 2005, accepted September 2005

Communicated by Prof. Dr. A. R. Shakoori

Abstract: The present study was conducted for the analysis and comparison of selected residual antibiotics in broiler chicken available in local market. The broiler samples included muscle, kidney and liver. The quinolones included in this study were, oxolinic acid, nalidixic acid, flumequine, enrofloxacin, norfloxacin and ciprofloxacin. An assessment of variation of these analytes (residues) in these samples was made. The intertissue/organ comparison within each analytical technique and intermethod comparison of results obtained by HPLC, UV spectroscopy and ion association complex techniques were made. TLC was used to separate and identify the quinolone residues. Infrared (IR) was also used for identification of the residues. HPLC with ODS column and UV detector and UV/ visible spectroscopy were used for quantification of the residues. Oxolinic acid, nalidixic acid and norfloxacin residues were absent in all the samples. The "ciprofloxacin–brilliant blue G" ion association complex was used for ciprofloxacin determination using ion association complex technique. Good compatibility of the spectrophotometric results was found with those of high pressure liquid chromatography.

Keywords: Maximum Residue Limits (MRL's), Ion Association Complex Technique (IAC) and HPLC.

Introduction

Recently the scale of growth of chicken, swine and fish has expanded throughout the world. The density of the chicken, swine and fish growth is so high at farms that infection often occurs. Large amount of quinolone antibacterials are applied in poultry industry, to prevent infectious diseases. The poultry birds are treated with quinolone antibiotics, which inhibit the DNA gyrase formation [1,2]. Ciprofloxacin (CPRF), enrofloxacin (ENRF), norfloxacin (NRF), flumequine (FLUM), nalidixic acid (NAL) and oxolinic acid (OXOL) are the fluoroquinolones/quinolones frequently applied to treat the diseases. These drugs treat gonorrhoea, bacterial gastroenteritis, skin and soft tissue infections, complicated and uncomplicated urinary tract infections caused by gram positive and gram negative organisms. These drugs find extensive applications in the field of medicine and chemical analysis [3].

The quinolones have been classified according to their antibacterial spectrum; potency and pharmacology. There is no widely accepted classification at present [4,5]. These are divided into two categories. The first generation quinolones include, NAL, OXOL, FLUM and piromidic acid (PIRM), which have good antibacterial activity against gram negative bacteria [6]. Their antibacterial effect is no longer good as drug resistant bacteria have evolved [7]. The second category (the second and third generation) includes fluoroquinolones containing fluorine at C-6 position and piperazinyl

Corresponding Address:
Habib Amjad C/O Prof. Dr. Javed Iqbal, Institute of Chemistry, University of the Punjab, Lahore. Institute of Chemistry, University of the Punjab, Lahore.

ring at C-7 position, such as marbofloxacin (MARB), ofloxacin (OFL), danofloxacin (DNF), ENRF, sarafloxacin (SRF), NRF and levofloxacin (LEVOF). These have broad antibacterial spectrum. They are safe drugs and are effective against gram positive, gram negative bacteria and mycoplasma. So their antibacterial activity is good [3,7,8].

The ever increasing use of quinolones, fluoroquinolones in poultry industry has caused their residual deposition in the poultry products resulting in the drug resistant bacteria. It has become a matter of foremost importance to screen the poultry birds of these residual antibiotics, down to the safer MRL's (Maximum Residue Limits) set by international fora Table 1 [9,10,11]. Various analytical techniques such as atomic absorption, spectrometry, polarography, AC-oscillopolarographic titration, differential pulse polarography, capillary zone electrophoresis, spectrofluorometry and high performance liquid chromatography have been used for determination of these drugs. But these techniques are either very expensive or not available at all at most poultry products quality control laboratories. The ultraviolet spectroscopy and other spectrophotrometic techniques are the most preferred and easy ones for assay of the different drugs in biological samples. Both these methods are simple and easy to apply. The present communication is aimed at testing the validity of these techniques in the quantificatin of some residual antibiotics extracted from different organs of broiler birds.

Materials and Methods

The samples were collected randomly from local markets situated in Lahore. The broiler birds came from the broiler poultry farms situated in the outskirts of Lahore. The samples were collected during the summer of 2004.

The quinolones were extracted, purified with

Table 1.
Maximum Residue Limits (MRL's) for quinolones in force in Europe [9,10,11].

Substance	Marker Residue	Species	MRL (μg/kg)	Tissue
Enrofloxacin	Sum of	Bovine	30	Muscle
	enrofloxacin &	Porcine	30	Liver
	ciprofloxacin	Poultry	30	Kidney
Ciprofloxacin	Sum of	Bovine	30	Muscle
	enrofloxacin &	Porcine	30	Liver
	ciprofloxacin	Poultry	30	Kidney
Flumequine	Flumequine	Bovine	50	Muscle
		Ovine	100	Liver
		Porcine	300	Kidney
		Poultry	50	Fat, Skin
		Salamander	150	Muscle, Skin

bond elute cartridges and separated from one another on large TLC separating plates spread with the silica gel and cellulose using various solvent systems such as Me_2CO: Et_2O (7:3 V/V) with silica gel plates and BuOH: isopropyl alcohol: H_2O (4:4:2 V/V), H_2O: BuOH: HOAc (5:4:1 V/V), MeCN: H_2O: Me_2 CO:α-Chlorohydrin (70:2.5:10:5.25 V/V) and $CHCl_3$: MeOH: NH_4OH (2:1:1) with the cellulose plate [12]. NRF, OXOL and NAL were absent. Known fractions of total volume of each sample were used for TLC.

The UV spectroscopy and ion association complex spectrophotometric techniques were then applied which are highly accurate and selective methods. Their limits of detection were generally sufficient for determination of residues. HPLC was used as the standard method to validate these. The IAC spectrophotometric technique was restricted only to NRF and CPRF. It selectively forms blue coloured chloroform-soluble ion association complexes due to their interaction with brilliant blue G (BBG) in NaOAc-AcOH buffer of pH 4 [13].

Extraction of the Residues from Broiler Tissues

Broiler liver and muscle samples (10g each) and 5g samples of broiler kidney were used for extraction of quinolones. Phosphate buffer with acetonitrile was added to each sample with magnetic stirring. The extracts were filtered by whatman filter paper. This procedure was repeated thrice for each sample. Then activated charcoal was used for decolouration and anhydrous sodium sulphate was used for dehydration of the sample extracts. Defatting was done by n-hexane saturated with acetonitrile in a separation flask. Each sample was made up to mark to 50ml by addition of deionised water. Cleaning of the basic fluoroquinolones was performed with a bond elute (Varian, Walton-on-Thames, UK) strong cation exchange (SCX) solid phase extraction cartridge and that of acidic quinolones with AGMP-1 resin (Bio-Rad Richmond, CA, USA); anion exchange cartridge.

Preparation of 0.05% Chromogen Brilliant Blue G (BBG) Solution

Stock solution of BBG was prepared by dissolving 50mg of BBG in a few drops of acetone and made up to mark (100ml) in a measuring flask with double distilled water.

Preparation of Ion Association Complex Standards of ciprofloxacin and norfloxacin

A series of working standards of 1, 2, 3, 4, 5, 6 ppm for CPRF and 2, 4, 6, 8, 10 ppm for NRF were prepared from the 100 ppm stock standard by taking their respective volumes in ml equal to their respective ppm's and making them up-to mark in 100 ml measuring flasks. One ml from each flask was taken into a series of 125 ml separating flasks. A sodium acetate / acetic acid buffer of pH 4 was prepared and 5 ml of this buffer was added into each flask having CPRF and 2 ml of it into each separating flask having NRF was added. To each of the flasks for both CPRF and NRF, 1 ml of 0.05% chromogen BBG was added. Then 10 ml chloroform was added into each flask and shaken well. The chloroform layer was dried by running it into anhydrous sodium sulfate.

Preparation of Samples for Ion Association Complex (IAC) Technique

The NRF scratchings NRF spots of each sample on TLC plates were taken to dissolve them in a few drops of acetone. But NRF was not located in any of the 15 samples of layer liver, kidney and muscle. CPRF scratchings of each sample was dissolved in 1 ml of deionised water. 5 ml of the buffer were added followed by 1 ml BBG into each flask. Then 10 ml chloroform was added into each flask and shaken well. Chloroform layer was retained, dehydrating it with anhydrous sodium sulfate.

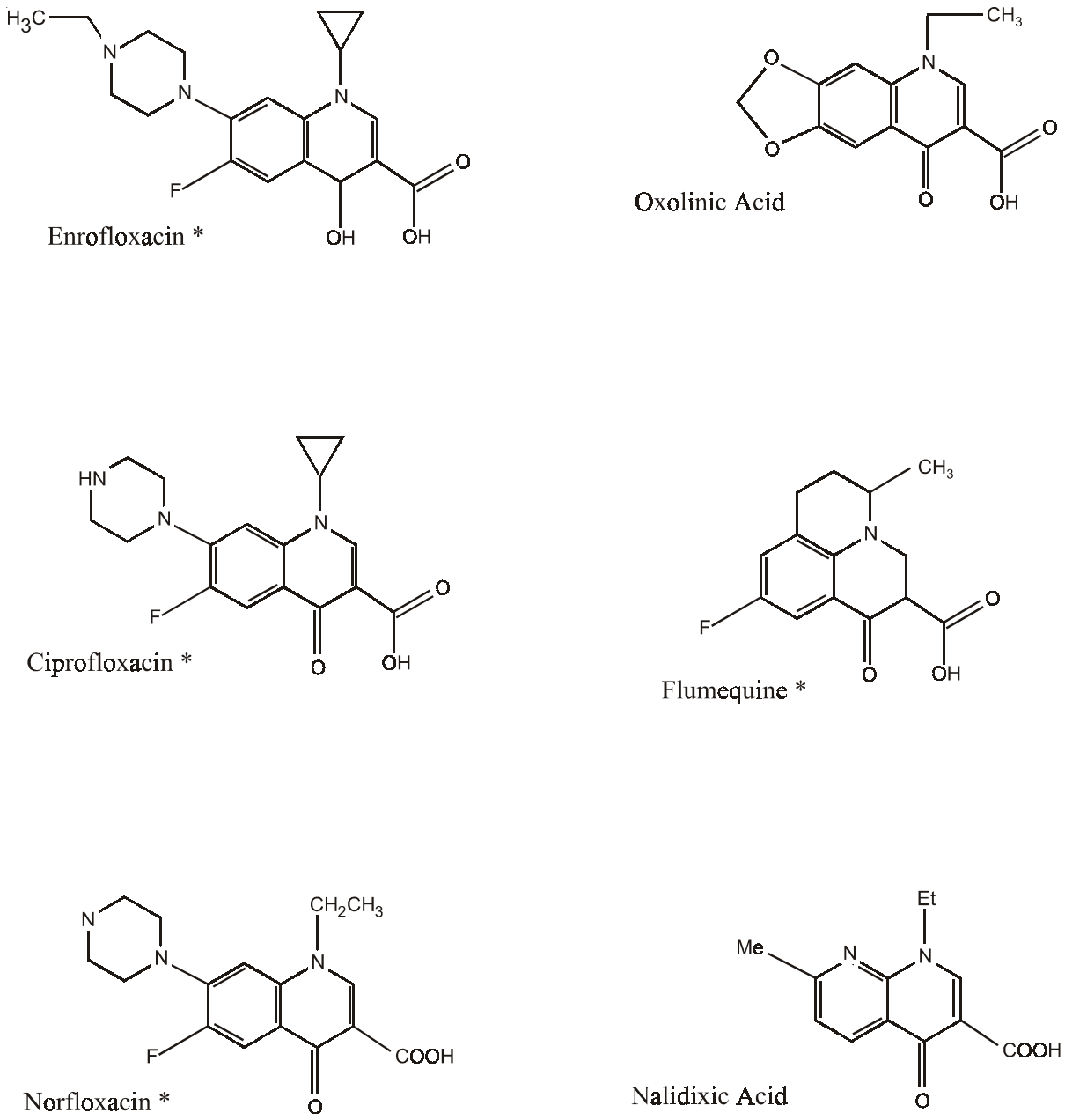

Fig 1. Chemical structures of quinolones (* = fluoroquinolones) involved in residual analysis.

Analysis of the (IAC) Samples

The absorbance of the standards and samples of CPRF were recorded at 610 nm and those for NRF standards only (as NRF was absent on TLC plate) at 614 nm. Standard calibration curves were plotted and concentrations of samples of CPRF from layer's liver, kidney and muscle were calculated. The minimum limits of detection for CPRF and NRF were 0.5 and 0.4 ppm and those maximum were 6 and 8 ppm respectively.

Analysis by HPLC

HPLC systems consisted of LC-9A pump (Shimadzu), SPO-6AB, UV/visible spectro-

photometric detector (Shimadzu), CTO 6A oven (Shimadzu), SCL-6B system controller, and CSW-32 software. The ultrasonic cleaner (EYELA Tokyo Rikakai Co. Ltd.) was used for degassing the samples, standards and mobile phase. Sartorius filtration assembly (Germany) was used for filtration with nylon filter of 0.45 ìm pores (Germany). The pH of the mobile phase was set by pH meter (Hanna HI-8418). The extractants, solvents and mobile phase constituents were of HPLC grade.

The standards of 5, 10, 15, 20, 25, 30, 35 and 40 ppm were prepared in HPLC mobile phases which were also used for UV analysis. The mobile phase consisted of MeCN: phosphate buffer (35:65 v/v) added with 3.5 mM SDS. The wavelengths used were 279, 284 and 241 nm for CPRF, ENRF and FLUM respectively. The injection volume was 20 ìl, the detector worked at ambient temperature and flow-rate 1 ml per minute for CPRF and ENRF and 1.5 ml per minute for FLUM. The mobile phase for FLUM consisted of 0.01 M Oxalic Acid: Acetonitrile: methanol (6:3:1). As oxalinic acid (OXOLN), NAL and NORF were not identified in TLC technique, these were not estimated on HPLC.

Analysis of Samples by UV Technique

The samples from HPLC analysis were taken off, dried gently on water bath, separated by TLC, spots for CPRF, ENRF and FLUM were scratched and redissolved in the respective mobile phases of HPLC, and working standards from HPLC technique were used. Absorbance was recorded on U-2000 Hitachi Spectrophotometer Tokyo (Japan) at 279, 284 and 241 nm for CPRF, ENRF and FLUM respectively. Calibration plots were drawn and sample residue concentrations were calculated.

Identification and Quantification of Residues

Quinolones (NRF, CPR, ENRF, OXOL, NAL, and FLUM) were identified in the samples by comparing their IR spectra, migration values and retention times of standards with those of unknown substances in the samples using their respective mobile phases in case of HPLC and UV detection. Estimations were made (1) by using standard calibration curves, and (2) by using the relation of "peak area /ppm" calculation from the standard calibration curve values of the peak area and concentrations. NRF, NAL and OXOL were not located and identified by TLC technique. These could not be identified by IR as well. Hence these were absent. Only FLUM, ENRF and CPRF were present.

Statistical Treatment

The statistical treatment given to the analyzed data were (i) F test, (ii) Student "t" test, and (iii) comparison of correlation coefficients of the analyzed residues. All the three statistical treatments of the analyzed residual data validate the test techniques with reference to an accepted reference technique (HPLC). The correlation coefficient is used as a measure of correlation between two sets of data (residues).

A correlation coefficient "r" can be calculated for a calibration curve to ascertain the degree of correlation between them. As a general rule, $0.90 < r < 0.95$ indicates a fair correlation, $0.95 < r < 0.99$ a good correlation, and $r > 0.99$ indicates excellent correlation. An $r > 0.99$ can sometimes be obtained with care. "r" may range from +1 to –1. It is common practice in the clinical chemistry literature when comparing two methods to analyze a series of samples over a range of concentrations by both methods and calculate a correlation of results of one method with those of the other. In this paper the correlation coefficients between the residual data obtained by UV and IAC techniques were separately calculated. The coincidence between the "r" values with respect to sign and numerical value shows the degree of agreement and conformity between the

two techniques. Hence this treatment gives us a finger print comparison between the test and reference techniques. F test and "t" test decide that the test technique differs within permissible limits internationally accepted. The correlation coefficient gives a finger print agreement of a test technique (UV and IAC) with the reference technique (HPLC). Hence the numerical value of correlation coefficient holds the same statistical significance as the F test and "t" test [14].

Results

The results (Table 2) show average residual concentration of antibiotics; CPRF, ENRF and FLUM in broiler samples. FLUM was not found in muscle but was detectable to a small extent in liver and kidney. CPRF was detected in liver, kidney and muscle but to a lesser extent as compared to ENRF. There was slight intra-analyte residual difference between the UV and IAC test methods and standard HPLC method. The concentration of the residues of various antibiotics in various samples according to HPLC and UV in decreasing order was: CPRF: BL>BK>BM, ENRF: BK>BL>BM, FLUM: BK>BL (FLUM was absent in broiler's muscle). The order of concentration of CPRF residues according to IAC technique was: BL>BK>BM. OXOLN, NAL and NRF were absent in all samples. Moreover the level of concentration of these quinolones was dependant upon their lipophylicity. Thus the more lipohyhyllic ENRF was in higher concentration and the less lipophyllic CPRF was in lower concentration. The least lipophyllic FLUM had the least concentration.

Discussion

The validity of the UV and IAC techniques was established by "F" test and "t" test of the results. Table 3 shows F-Test data for the test techniques (UV and IAC). The tabulated F-Test value for 4 degrees of freedom is 6.39 and all the calculated values in the Table are below this value, showing that variances of both methods (UV and IAC) do not have statistically significant differences from those of the standard method (HPLC) for the intra-analyte residues of all the three broiler samples. It also means that the standard deviations are due to manual handlings and not due to the determinate errors including those in sample preparation. Hence student "t" test was performed to test the validity of both the test methods. Table 4 shows the student "t" test values for both the test techniques for CPRF residues and for only one technique (UV spectroscopy) for ENRF and FLUM residues involving liver, kidney and muscle samples. All the calculated values (2.776) for 4 degrees of freedom and 95% confidence level.

Table 2.

Mean residual antibiotic concentration (mg/kg) in the liver, kidney and muscle of broiler chicken.

Antibiotic residues	HPLC Technique			UV Technique			IAC Technique		
	Broiler Liver	Broiler Kidney	Broiler Muscle	Broiler Liver	Broiler Kidney	Broiler Muscle	Broiler Liver	Broiler Kidney	Broiler Muscle
CPRF	250.25	146.08	87.81	24.49	140.32	85.29	245.34	143.602	85.39
ENRF	1430.41	2143.79	709.87	1425.86	2136.88	703.72	*N.D.	N.D.	N.D.
FLUM	30.60	52.4	Nil	29.65	50.97	Nil	N.D.	N.D.	N.D.

Hence both the test techniques were statistically valid, at the same time not differing significantly from the standard (HPLC) technique.

Tables 5 shows intra-residue inter-organ correlation coefficient for HPLC, UV and IAC techniques. For example in case of CPRF estimated from broiler liver and kidney, the values of "r" were -0.7949, -0.6972 and -0.7672 for the above three techniques respectively. All the three "r" values were negative and of about the same order. But in case of ENRF and FLUM estimated from different organs, the two techniques HPLC and UV show "r" values of the same magnitude and sign. Table 6 shows intra-organ inter-residue correlation coefficient in which the same organ has the same value and sign even if estimated under different techniques. For example, for broiler kidney the "r" values for ENRF/CPRF residues under UV and HPLC techniques were – 0.18292 and -0.17569. Hence there was very fine complementarity and symmetry of the sign and the degree of the correlation, proving the validity of the test techniques according to the internationally acceptable standards. The higher CPRF residual concentrations in liver as compared to these in kidney and muscle are attributable to (i) the metabolite formation from ENRF to CPRF by de-ethylation, (ii) higher rates of excretion of CPRF from the kidney as compared to that of ENRF due to its lower lipophylicity than ENRF (iii) the lower capacity of binding of CPRF than that of ENRF and (iv) unsophisticated amounts of dosages administered to the poultry birds. In case of inter-tissue/organ difference of ENRF residues the relatively lower

Table 3.

F-Test values for the two test techniques (UV and Ion Association Complex Techniques).

Antibiotic	**IAC Technique**			**UV Spectroscopy**		
Residues	Broiler Liver	Broiler Kidney	Broiler Muscle	Broiler Liver	Broiler Kidney	Broiler Muscle
CPRF	1.2417	1.0654	1.3820	1.1766	1.0720	1.0572
ENRF	N.D.	N.D.	N.D.	1.3356	1.0020	1.0266
FLUM	N.D.	N.D.	N.D.	1.0591	1.0552	Nil

ND: not detectable

Table 4.

The student "t" test values for the UV and IAC Techniques.

Antibiotic	**IAC Spectroscopy**			**UV Technique**		
Residues	Broiler Liver	Broiler Kidney	Broiler Muscle	Broiler Liver	Broiler Kidney	Broiler Muscle
CPRF	1.4855	0.5008	0.8417	1.5	0.2148	0.9249
ENRF	0.02701	0.01353	0.11964	N.D	N.D	N.D
FLUM	0.04763	0.03946	Nil	N.D	N.D	N.D

Table 5.
Correlation coefficients for residual antibiotics estimated in broiler liver, kidney and muscle using different analytical techniques.

Antibiotic Residues	Inter-Tissue Correlation Correlation	HPLC Technique	UV Spectroscopy	IAC Technique
CPRF	Broiler Liver/Broiler Kidney	-0.7949	-0.6972	-0.7672
	Broiler Muscle/ Broiler Liver	-0.7672	-0.754	-0.75497
	Broiler Muscle/ Broiler Kidney	+0.8588	+0.8365	+0.8427
ENRF	Broiler Liver/Broiler Kidney	+0.701935	+0.496378	N.D.
	Broiler Muscle/ Broiler Liver	+0.7741	+0.787252	N.D.
	Broiler Muscle / Broiler Kidney	-0.12089	-0.10502	N.D.
FLUM	Broiler Liver/Broiler Kidney	+1.00	+0.994871	N.D.
	Broiler Muscle/ Broiler Liver	Nil	Nil	N.D.
	Broiler Muscle / Broiler Kidney	Nil	Nil	N.D

Table 6.
Intra-organ inter-residual coefficient of correlation.

Inter-residual Correlation	UV Spectroscopy			HPLC Technique		
	Broiler Liver	Broiler Kidney	Broiler Muscle	Broiler Liver	Broiler Kidney	Broiler Muscle
ENRF/CPRF	-0.76444	-0.18292	+0.369166	-0.72765	-0.17569	+0.433429
ENRF/FLUM	+0.023683	-0.3628	Nil	+0.030345	-0.34816	Nil
CPRF/FLUM	-0.05929	-0.32938	Nil	+0.054266	-0.32809	Nil

ENRF in liver is attributable to its primary metabolite formation [15] and its higher kidney residue levels are due to its higher lipophylicity [16]. The decreasing order of residual amounts of quinolones was ENRF>CPRF>FLUM. This is exactly in accordance with their decreasing order of lipophylicity as shown by their log D values. The decreasing order is also in accordance with the residual amounts of quinolones in kidney, liver and muscle [17]. The essence of the work is that the results obtained by test techniques do not differ significantly from the reference (HPLC) technique thereby providing authentication of these easily applicable and cheaper techniques.

This work enables the common laboratories to monitor the quinolone residues in poultry products. The validation tests "F test" and "t test" have shown the test techniques (UV and IAC) to be statistically equivalent for the determination of the residues. Also,

the value, sign and symmetry of correlation obtained by different test techniques show their degree of accuracy and equivalence with the reference technique. Those samples are deviating samples which have some residue larger that MRL's set internationally. The ENRF and CPRF in the analyzed samples were higher than MRL's. However these samples do not have any residual NAL and NORF. FLUM residues were detected only in liver and kidney of the broiler birds and not in the broiler muscle samples. The FLUM residual level of kidney and liver was below safer maximum residue limits internationally accepted (Table 1). These should be strictly monitored by sufficient washing time periods. The samples should also be monitored for the quinolone resistant pathogenic bacterial species related to the respective residue.

References

1. **Yorke, J.C. and Froc, P.** 2000. Quantitation of nine quinolones in chicken tissues by HPLC with fluorescence detection. *J. Chromatogr*. (A) 882:63 – 67.
2. **Gigosos, P.G., Revesado, P.R., Cadahia, O., Fente, C.A., Vazquez, B.I., Franco, C.M. and Cepeda, A.** 2000. Determination of quinolones in animal tissues and eggs by HPLC with photodiode-array detection. *J. Chromatogr*. (A) 871:31-36.
3. **Katrizky, A.R. and Boulton, A.J**. 1968. The chemistry of quinolones. In: *Advances in heterocyclic chemistry*. Academic Press, New York.
4. **Wolfson, J.S. and Hooper, D.C.** 1989. Fluoroquinolone antimicrobial agents. *Clin. Microbiol. Rev*. 2:378-424.
5. **Perez, R. T., Martinez, L.C., Sanz, A. and Bravo, E.** 1999. Separation and simulataneous determination of quinolone antibiotics by capillary zone electrophoresis. *Chromatographia* 49:419-423.
6. **Martin, A.R.** 1998. In: *Textbook of organic medicinal and pharmaceutical chemistry*. Eds. Delygado, J.M. and Removes, W.A., pp. 196-202. New York, USA.
7. **Horie, M., Saito, K., Nose, N. and Nakazawa, H**. 1992. Simultaneous determination of quinolone antibacterials in fish and meat by HPLC. *J. Food. Hyg. Soc. Japan* 33:442-448.
8. **Horie, M., Saito, K., Nose, N. and Nakazawa, H**. 1995. Simultaneous determination of eight quinolone antibacterials in meat and fish by HPLC. *J. Food. Hyg. Soc. Japan* 36:62-67.
9. **Rose, M.D., Bygrave, J. and Stubbing, G.W.F.** 1998. Extension of multi-residue methodology to include the determination of quinolones in food. *The Analyst* 123:2790-2791.
10. **EEC**. 1990. *Council regulation No. 2377/90*.
11. **EEC**. 1993. *Council regulation No. 93/256*/EC.
12. **Siewert, E. and Saga, B.** 1979. *Studies on the qualitative analysis of antibiotic residues*. Inst. Vet. Med. Berlin (1), p 22.
13. **Gowda, B. G. and Seetharamapa, J**. 2003. Extractive spectrophotometric determination of fluorouinolones and antiallergic drugs in pure and pharmaceutical formulations. *Anal. Sci*. 19:461-464.
14. **Christian, G.D**. 1994. Data handling. In: *Analytical Chemistry*. 5th ed., pp. 14-64. John Wiley and Sons Inc., New York.
15. **Ariens, E.J., Simonis, A. M. and Offermeier, J**. 1976. The toxicological action. In: *Introduction to General Toxicology*. 2nd ed., pp 13-78. Academic Press. New York, San Francisco and London.
16. **Gabriel, Z., Annegret, B., Martina, K.S., Fritz, S. and Ulrike, H**. 1998. Plasma protein binding of gyrase inhibitors. *J. Pharm. Sci*. 87:215- 220.
17. **Izumi, T. and Kitagawa, T**. 1989. Protein binding of quinolone carboxylic acids. *Chem. Pharm. Bull*. 37:742-745.

Proc. Pakistan Acad. Sci. 42(4):233-238.2005

DISTRIBUTION OF ABO AND RH BLOOD GROUP ALLELES IN GUJRAT REGION OF PUNJAB, PAKISTAN

***Mohammad Anees and Mohammad Shabir Mirza**

Department of Biological Sciences, The University of Gujrat, G.T. Road College, Gujrat, Pakistan and Aziz Bhatti Shaheed Hospital, Gujrat, Pakistan.

Received August 2005, accepted November 2005

Communicated by Prof. Dr. M. A. Hafeez

Abstract: A study has been carried out on blood groups, representing a random population sample from urban and rural areas of Gujrat region, Province of the Punjab, Pakistan. Blood samples were collected from the patients visiting the Aziz Bhatti Shahid Hospital, Gujrat. The objective of this study was to determine the frequency of different blood groups and their alleles in this region, which would not only help in blood transfusion services, but also eliminate the risk of erythroblastosis and some other diseases. Blood grouping was carried out over a period of 12 months from January 2004 to December 2004, and encompassed 2647 subjects, in which 80.59% were male and 19.41% female. The blood groups were categorized according to ABO/Rh system and allele frequency was determined according to Hardy-Weinberg law. The distribution of phenotypes in the total sample was 0.2489, 0.3691, 0.0688 and 0.3132 for groups A, B, AB and O respectively, with Rh-positive (R) 0.7958 and Rh-negative (r) 0.2042. The distribution of the alleles in the total sample was 0.1740, 0.2229, 0.0435 and 0.5596, for IA, IB, IAIB and i, respectively. From these studies it was concluded that phenotypically B group was dominant in the Gujrat region, with a high allelic frequency of O group.

Keywords: Alleles, gene frequency, blood groups, Rh factor, transfusion

Introduction

The regulation of ABO blood group system is under the control of ABO gene expression [1]. A loss of blood group A antigen expression has been reported in Bladder cancer, caused by the allelic loss or methylation of ABO gene [2]. Research on ABO group system has been of immense interest, due to its medical importance in different diseases. The ABO blood group system is not only important in blood transfusions, cardiovascular diseases, organ transplantation, erthroblastosis in neonates, but also one of the strongest predictors of national suicide rate and a genetic marker of obesity [3-8]. A significant deficit of group O has suggested that there may be susceptibility to develop osteoarthrosis in normal hip-joint and spinal osteochondrosis [9,10].

The genetic history of a person can be known by studying the blood groups [11]. For instance, type O blood is the oldest blood and shows a connection to the hunter-gatherer cultures. This blood type is strongly aligned with high animal protein consumption; individuals generally produce higher stomach acids and experience more incidence of gastric ulcer disease than the other groups. Blood group A is primarily associated with vegetarian food sources and individuals in this group secrete smaller amounts of stomach acid and have lesser chances for gastric ulcers, heart diseases, cancer and diabetes [12].

The carbohydrate antigens A, B and O appear to be located on the long arm of the autosomal locus at chromosome number 9 [13], which constitute the four blood types. The gene symbols IA, IB, IAIB and i are often used to denote these alleles. Two alleles, R and r, are responsible for the inheritance

*Author for correspondence.

E-mail address: anees_4_9@hotmail.com

of rhesus blood groups, with R denoting Rh positive, and r being Rh negative allele. Gene frequency takes into consideration the numbers of various genotypes in the population, and the relative allele frequencies are determined by application of the Hardy-Weinberg Law [14].

The present study is carried out to record the phenotypic and genotypic frequency of various alleles in the blood groups of a sample of the population in the Gujrat region, Punjab, Pakistan. The study has suggested that the blood group frequencies of this region are similar to the Asian communities [15], in the sequence of B>O>A>AB, with the highest allele frequency of Rh positive in the studied Pakistani populations. These figures are reported in the hope that they may be used as reference for studies of ABO blood groups by health planners, while making an effort to face future health challenges in this region.

Materials and Methods

Subjects

A total of 2647 subjects, comprising 2133 (80.59%) male and 514 (19.41%) females, were screened for blood grouping. The subjects belonged to both rural and urban areas of Gujrat, Punjab, Pakistan.

Collection of blood samples

A 2.0 ml sample of blood was drawn from the antecubital vein of each subject in a disposable syringe, and transferred immediately to a tube containing ethylene diamine tetra acetic acid (EDTA).

Determination of blood groups

Blood grouping was done by the antigen-antibody agglutination test. The antisera used were obtained from Plasmatic (Kent, UK). Plasmatic ABO monoclonal reagents are *in vitro* culture supernatants of hybridized immunoglobulin secreting mouse cell-line. For determination of Rh factor, plasmatic anti D (1.0g) Lo-Du and LO-Du2 monoclonal reagents, prepared from different antibody producing human B-lymphocyte cell lines, were used.

Results

Table 1 shows the phenotypic frequency of ABO blood groups in the studied population, with gender distribution. The distribution of phenotypes in the total sample was 0.2489, 0.3691, 0.0688 and 0.3132 for groups A, B, AB and O respectively. Phenotypically B group was dominant and AB was rare in both males as well as females. Table 2 depicts the distribution of allele frequencies of ABO antigens in the studied population, in comparison with certain

Table 1.
Phenotypic frequencies of various blood groups (ABO and Rh) in the studied.

Blood Groups	Total Subjects			Male Subjects			Female Subjects		
	Complete	Rh+	Rh-	Complete	Rh+	Rh-	Complete	Rh+	Rh-
A	0.2489	0.2475	0.2830	0.2705	0.274	0.2683	0.2289	0.2329	0.2207
B	0.3691	0.3652	0.4622	0.3623	0.3687	0.3092	0.3636	0.3571	0.3158
AB	0.0688	0.0680	0.0849	0.0346	0.0210	0.1680	0.0893	0.1021	0.0981
O	0.3132	0.3193	0.1699	0.3326	0.3362	0.2545	0.3182	0.3079	0.3654
Total	1.0000	1.0000	1.0000	1.0000	1.0000	1.0000	1.0000	1.0000	1.0000

earlier studies. The distribution of the alleles in the total sample was 0.1740, 0.2229, 0.0435 and 0.5596 for IA, IB, IAIB and i respectively, indicating that the allelic frequency of O positive group was higher than the other blood groups. Table 3 compares the distribution of allele frequencies of Rh factor antigens in the Gujrat population with earlier studies on different populations. The distribution of Rh alleles was 0.7958 and 0.2042 for R and r gene, suggesting the dominance of Rh positive. The studied population exhibited the frequency in the order of i> IB > IA > IAIB and R>r respectively.

Discussion

In the study under discussion, the relative frequency of the various blood group alleles does not seem to deviate from those which have been recorded in the past for most of the Pakistani regions (Table 2). This study has demonstrated that phenotypically, there was a dominance of B blood group (B=0.3652, O=0.3322, A=0.2475), but the allele frequency of O blood group was higher (O=0.5596, A=0.1901, B=0.2503), than the other blood groups. These findings are inconsistent with the results obtained in earlier studies carried out in Wah Cantt (O=0.5400, A=0.1813. B=0.2450) and Punjab division (O=0.5760, 0.2440, B=0.1380), but significantly higher from the other regions of Pakistan (Bannu, O=0.2507, A=0.3103, B=0.3623, Peshawar O=0.3100, A=0.2800, B=0.3400, Swabi, O=0.3220, A=0.2760, B=0.3040, Hazara,

Table 2.
Allelic frequency of blood groups (ABO) studied in different populations.

Populations	Frequency of blood groups A	B	AB	O	References
American Indian	0.0390	0.0110	0.000	0.9500	16
Turky	0.1220	0.1213	0.0085	0.7398	17
Nairobi (Kenya)	0.1580	0.1261	0.0239	0.6900	15
Sudan	0.1814	0.1235	0.0268	0.6683	18
Kuwait	0.1608	0.1400	0.0265	0.6678`	19
W.Germany	0.2565	0.081	0.0225	0.6400	20
Ukraine	0.2360	0.2250	0.0704	0.5760	21
Hungary	0.2766	0.1218	0.0423	0.5593	22
Nigeria	0.2443	0.2388	0.0275	0.4894	23
Kenya	0.2620	0.2200	0.0440	0.4748	15
Britain (UK)	0.4170	0.0860	0.0300	0.4670	25
India	0.2470	0.3750	0.0530	0.3250	25
Bannu (Pakistan)	0.3103	0.3623	0.0767	0.2507	26
Peshawar (Pakistan)	0.2800	0.3400	0.0700	0.3100	27
Swabi (Pakistan)	0.2760	0.3040	0.0880	0.3220	28
Hazara (Pakistan)	0.2400	0.3200	0.1100	0.3300	29
Bahawalpur (Pakistan)	0.2100	0.3600	0.0600	0.3700	30
Wah cant (Pakistan)	0.1813	0.2450	0.0517	0.5400	31
Punjab (Pakistan)	0.2440	0.1380	0.0420	0.5760	32
Gujrat (Pakistan)	**0.1740**	**0.2229**	**0.0435**	**0.5596**	**Present study**

Table 3.
Frequency of Rh antibody allele in different populations.

Populations	Allele frequency R	r	References
Nigeria	0.9430	0.0570	23
Azad Jammu and Kashmir	0.8480	0.1520	33
Kenya	0.8030	0.1970	24
Sudan	0.7436	0.2564	18
Bannu (Pakistan)	0.6720	0.3280	26
Lahore (Pakistan)	0.7170	0.2830	34
Islamabad (Pakistan)	0.7290	0.2710	35
Wah Cantt (Pakistan)	0.7300	0.2710	31
Peshawar (Pakistan)	0.7680	0.2320	27
Gujrat (Pakistan)	**0.7958**	**0.2042**	**Present study**

O=0.3300, A=0.2400, B=0.3200, Bahawalpur, O=0.3700, A=0.2100, B=0.3600). However, the data for the American Indians, Turkey, Nairobi (Kenya), Sudan, Kuwait, W.Germany, Ukraine, Hungary, Nigeria, Kenya and Britain, presented in the same Table, reveals that there is dominance of O group, in these populations in contrast to the Indo-Pak sub-continent, in which both B and O groups show comparable frequency. The least reported group in all the populations has been AB. These studies suggest that the heterogeneity in these populations is due to the genetic and environmental factors which are responsible for varying frequency of the blood groups [26]. Perhaps the environment of the Indo-pak region helps in the expression of blood group B alleles, which are progressively dominating in this region, rather than the oldest O blood group.

In terms of presence of Rh antibody alleles, the data from several studies on Pakistani as well as African, British and other countries populations is compared in Table 3. The present study has shown 0.7958 Rh positive alleles and 0.2042 Rh negative cases, which are very close to those for Kenya (R=0.8030 r=0.1970) and Peshawar (Pakistan, R=0.7680, r=0.2320) populations, suggesting that there is no significant difference between the frequencies for these populations. However the frequency of Rh positive alleles was less than the Nigerian population (R= 0.9430, r=0.0570). These findings suggest that Gujrat population seems to show the highest rate of Rh positive alleles compared to the other regions of Pakistan studied so far (Table 3).

It is well known that blood groups are associated with several diseases, like cardiovascular, obesity, osteoarthrosis, erthroblastosis in neonates and many other diseases especially, osteoporosis and suicide rate in different nations [2-12]. The prevalence of osteoporosis in the proximal femur and lumbar spine averaged 2.3- and 1.7-fold higher in women with blood type AB than in those with blood type O. Thus, ABO blood group status seems to have a significant relationship to the prevalence of osteoporosis in postmenopausal women [36]. Lester [7] has recently demonstrated that Blood types are one of the strongest predictors of national suicide rates. He studied that in a sample of 51 nations, the suicide rates were negatively associated with the proportion of people with Type O blood, while

homicide rates were positively associated with A and B blood groups. The data generated in the present study may be useful for health planners, while making efforts to face the future health challenges in the region. In short, generation of a simple database of blood groups, not only provides data about the availability of human blood in case of regional calamities, but also serves to enable insight into possibilities of future burden of diseases.

Acknowledgements

I wish to express my gratitude to Mrs Naseem, Incharge Blood Bank, Aziz Bhatti Shahid Hospital, Gujrat, for providing help in collection of blood group data.

References

1. **Kominato, Y., Hata, Y., Matsui, K., and Takizawa, H.** 2005. Regulation of ABO gene expression. *Leg. Med.* 3:371-8511.
2. **Chihara, Y., Sugano, K., Kobayashi, A., Kanai, Y., Yamamoto, H., Nakazono, M., Fujimotom., H., Kakizoe, T., Fujimoto, K., Hirohashi, S. and Hirao, Y.** 2005. Loss of blood group A antigen expression in bladder cancer caused by allelic loss and/or methylation of the ABO gene. *Lab Invest.* 9:158-167.
3. **Molison, P.L**. 1979. *Blood transfusion in clinical medicine*. 6th edition, Blackwell Scientific Publication, Oxford, U.K. pp 239-666.
4. **Egawa, H., Oike, F., Buhler, S., Minamiguchi, S., Haga, H., Uryuhara, K., Kiuchi, T., Kaihara, S. and Tanaka, K.** 2004. Impact of recipient age on outcome of ABO-incompatible living-donor liver transplantation. *Transplantation* 15:403-11.
5. **Shamim, A., Hafeez, M.A. and Ahmad, M.M**. 2002. ABO and Rh blood groups I: Markers of cardiovascular risk and association with lipids and other related risk co variables in a Pakistani population. *Proc. Pakistan Acad. Sci.* 39:47-66.
6. **Komar-Szymborska, M., Szymborski, J., Sleboda, A., Bajkacz, M. and Cioch, E**. 1993. RH and ABO incompatibility in newborns treated in a pediatric hospital. *Wiad Lek.* 46:644-50.
7. **Lester, D.** 2005. Predicting suicide in nations. *Suicide Res*. 9:219-23.
8. **Hein, H.O., Suadicani, P. and Gyntelberg, F**. 2005. The Lewis blood group-a new genetic marker of obesity. *Int. J. Obes. Relat. Metab. Disord*. 29:540-52.
9. **Lourie, J.A**.1983. Is there an association between ABO blood groups and primary osteoarthrosis of the hip? *Ann. Hum. Biol*. 10:381-383.
10. **Nevropatol, Z.P**. 1979. Analysis of the distribution of ABO system blood groups among patients with spinal osteochondrosis syndrome. *Ann. Hum. Biol*. 79:409-413.
11. **Sokolov, R**. 1993. *Why We Eat What We Eat: How Columbus Changed the Way the World Eats*. New York: Simon & Schuster. pp 1-50.
12. **Viola, H., J. and Carolyn, M**. 1991. *Seeds of change: five hundred years since Columbus*. 2nd ed., Washington and London, Smithsonian Institution. pp. 110-153.
13. **Hoffbrand, A.V.** 1981. *Postgraduate hematology*. 2nd edition, Heinemann Professional Publishing Ltd., London, U.K. pp. 270-350.
14. **Strickberger, M.W.** 1976. *Dominance relations and multiple alleles in diploid organisms*. 2nd edition, McMillan Publishing Company Inc., New York, N.Y., U.S.A. pp. 164-180.
15. **Lyko, J., Gaertner, H., Kaviti, J.N., Karithi,M.W. and Akoto, B.** 1992. The blood groups antigens ABO and Rh in Kenyans. *Hamdard Medicus* 35:59-67.
16. **Mourant, A.E., Kipec, A.C., and Domanjewska, S. K.** 1976. *The distribution of human blood groups*. Oxford University Press, London. pp.10-19.
17. **Akbas, F., Aydin, M. and Cenani, A**. 2003. AB0 blood subgroup allele frequencies in the Turkish population. *Anthropol. Anz*. 61:257-60.
18. **Khalil, I.A., Phrykian, S. and Farr, A.D**. 1989. Blood group distribution in Sudan. *Gene Geogr.* 3:7-10.
19. **Al-Bustan, S., El-Zawahri, M., Al-Azmi, D., Al-Bashir, A.A., Miser, A., Geraci, T.K. and Wennberg, R.P.** 2002. Allele frequencies and molecular genotyping of the ABO blood group system in a Kuwaiti population. *Int. J. Hematol*. 75:147-53.
20. **Wagner, F.F., Kasulke, D., Kerowgan, M. and Flegel, W.A**. 1995. Frequencies of the bloods group ABO, Rhesus D category VI. Kell and of clinically relevant high frequency antigens in southwestern Germany. *Infusions her Transfusions med*. 22:285-290.
21. **Mukhin, V.N., Chinakh, D.G, Avdeev, A.V., Kuleba, V.V. and Afanas'ev, M.V**. 2003. Gene frequencies and heterozygosity of the AB0 and RH blood group alleles in the populations of two cities of the Donetsk region, Ukraine. *Rus. J. Genetics* 39:530-43.
22. **Tuaszik, T.** 1995. Hetrogenetiy in the distribution of ABO blood groups in Hungary. *Gene Geogr.* 9:169-176.
23. **Falusi, A.G., Ademowo, O.G., Latunji, C.A., Okeke, A.C., Olatunji, P.O., Onyekwere, T.O, Jimmy, E.O.,**

Raji, Y., Hedo, C.C., Otukonyong, E.E. and Itata, E.O. 2000. Distribution of ABO and Rh genes in Nigeria. *Afr. J. Med. Sci*. 29:23-6.

24. **Lyko, J., Gaertner. H., Kaviti, J.N., Karithi, M.W., Akoto, B**. 1992. The blood groups antigens ABO and Rh in Kenyans. *Hamdard Medicus* 35:59-67.
25. **Talib, V.H**. 1991. *Handbook of medical laboratory technology*. 2nd edition. New Delhi, CBS Publishers, pp. 23-47.
26. **Khan, M.S., Subhan, F., Tahir, F., Kazi, B.M., Dil, A.S., Sultan, S., Deepa, F., Khan, F. and Sheikh, M.A.** 2004. Prevalence of blood groups and Rh factor in Bannu region (NWFP) Pakistan. *Pak. J. Med. Res*. 43:8-10.
27. **PMRC**. 1982. Some normal parameters of Pakistani are in the Peshawar area. Peshawar. *Pak. Med. Res. Council*, KMC. 1976-1982.
28. **Khurshid, B., Naz, M., Hassan, M. and Mabood, S.F**. 1992. Frequency of ABO and Rh (D) blood groups in district Swabi N.W.F.P (Pakistan). *J. Sci. Tech. Univ., Peshawar* 16:5-6.
29. **Khaliq, M.A, Khan, J.A., Shah, H. and Khan, S.P.** 1984. Frequency of ABO and Rh (D) blood groups in Hazara Division (Abbottabad). *Pak. J. Med. Res*. 23:102-3.
30. **Yousaf, M., Yousaf, N. and Zahid, A**. 1988. Pattern of ABO and Rh (D) blood group distribution in Bahawalpur Division. *Pak. J. Med. Res*. 27:40-51.
31. **Khan, I.M., Khan, G.A. and Akbar, A.** 1982. Gene frequency of ABO and Rh blood group system in Wah Cantonment. Botany Department, Peshawar University, Pakistan.
32. **Shami, S.A. and Rasmuson, M.** 1994. Genetic heterogeneity and gene diversity in the population of Punjab, Pakistan, based on ABO and Rh (D) blood group frequencies. *Hum. Hered.* 44:214-9.
33. **Rashid, M.** 1983. Gene frequency of ABO, blood groups in Azad Kashmir. MSc thesis, Department of Botany, University of Peshawar, Peshawar, Pakistan.
34. **Parveen, N**. 1983. Incidence of ABO and Rh system in Lahore area. MPhil thesis, University of Peshawar, Peshawar, Pakistan.
35. **Subhan, F., Tahir, F., Sultan, S. and Dil, A.S**. 2000. Bad obstetric history: cytogenetic and haematological parameters. *Pak. J. Med. Res*. 39:139-44.
36. **Jong, W.C. and Soo, H.P.** 2004. Associations between ABO blood groups and osteoporosis in postmenopausal women. *Ann. Clin. Lab. Sci.* 34:150-153.

Proc. Pakistan Acad. Sci. 42(4):239-242.2005

FERMIONS IN KERR-NEWMAN-KASUYA SPACE-TIME

Elias Uddin Biswas

Department of Mathematics, Shahjalal University of Science and Technology, Sylhet, Bangladesh

Received August 2005, accepted November 2005

Communicated by Prof. Dr. M. Iqbal Choudhary

Abstract: The aim of this paper is to build up the U(1)- gauge theory for fermions in the curve space-time such as Kerr-Newman-Kasuya space-time. The Kerr-Newman-Kasuya space-time is not a black hole space-time but it has the common feature with the black hole space-time that it has horizon.

Keywords: Gauge theory, black hole space-time, horizon, magnetic monopole charge, null complex tetrads

Introduction

Carmeli and Carmeli derived the Klein-Gordan, Weyl, and Dirac-type equations on $R\times S^3$ topology by simply going from the momen-tum to the angular momentum representation [1,2,3]. Sen [4] obtained the most general Lagrangians for the Dirac, Weyl, and Majorana fermions. Sen's work offers an excellent description of fermions in the space-time $R\times S^3$. Dariescu *et al.* [4] developed a U(1)-gauge theory for massive fermionic fields minimally coupled to a curved space-time such as Kerr-Newman black hole space-time. Dariescu and Dariescu [5] also developed the tetradic Lorentz-gauge invariant formulation of the SU(2)×U(1) theory in $R\times S^3$ space-time. To develop a U(1)-gauge theory for massive fermionic fields on curved space-time such as Kerr-Newman black hole space-time, they used the Dirac-type equation and the U(1)-gauge invariant Lagrangian. In this paper, the U(1)-gauge theory for massive fermionic fields minimally coupled to a Kerr-Newman-Kasuya space-time is studied. The Kerr-Newman-Kasuya space time is the Kerr-Newman space-time involved with extra magnetic monopole charge. This monopole hypothesis was propounded by Dirac relativity long ago.

The Kerr-Newman-Kasuya space-time

The Kerr-Newman-Kasuya space-time is described by the metric

$$\begin{aligned} ds^2 &= \left(r^2+h^2\cos^2\theta\right)\left(\frac{dr^2}{r^2-2mr+e^2+h^2+l^2}+d\theta^2\right) \\ &+\sin^2\theta\left\{r^2+h^2+\frac{h^2\sin^2\theta\left(2mr-e^2-l^2\right)}{r^2+h^2\cos^2\theta}\right\}d\varphi^2 \\ &-\left(1-\frac{2mr-e^2-l^2}{r^2+h^2\cos^2\theta}\right)dt^2-\frac{2h\sin^2\theta\left(2mr-e^2-l^2\right)}{r^2+h^2\cos^2\theta}dt\,d\varphi \end{aligned} \tag{1}$$

where m, h, e and l are the mass, angular momentum per unit mass, electric charge and magnetic monopole charge parameters respectively. This is a solution to the Einstein-Maxwell equations with electromagnetic vector potential

$$A_\mu dx^\mu = \frac{er\left(dt-h\sin^2\varphi\, d\varphi\right)}{r^2+h^2Cos^2\theta} \tag{2}$$

The space-time given by (1) encompasses all the black hole space-times, which are asymptotically flat. Specially, the metric (1) includes:

e-mail: ebiswasmat@yahoo.cpm

(i) Kerr-Newmann black hole space-time when l=0.
(ii) Kerr black hole space-time for l =e=0.
(iii) Reissner-Nordstrom black hole space-time if l=h=0.
(iv) Schwarzchild black hole space-time when l=e=h=0.

This metric can be transformed to Boyer coordinates under the proper coordinate transformation such as

$$\{x^{\mu}\}=\left\{p=h\cos\theta\,;\sigma=-\frac{\varphi}{h}\,;q=r\,;\tau=t-h\varphi\right\} \quad (3)$$

with the suitable adjustment of the parameter

$$X(p)=h^2-p^2\,;Y(q)=q^2-2mq+e^2+h^2+l^2 \quad (4)$$

Therefore, the metric (1) can be written as

$$ds^2=\frac{p^2+q^2}{X}dp^2+\frac{X}{p^2+q^2}(d\tau+q^2d\sigma)^2+ \frac{p^2+q^2}{Y}dq^2-\frac{Y}{p^2+q^2}(d\tau-p^2d\sigma)^2 \quad (5)$$

This metric represents the Kerr-Newman-Kasuya space-time in Boyer coordinates, which has been studied in detail by Plebanski [7]. After a suitable choice of the null complex tetrads $\{\omega^a\}$ which consists of two complex conjugate null vectors $m,\overline{m}$ and two real null vectors

$k_1,k_2\,;\{\omega^a\}=\{m,\overline{m},k_1,k_2\}$:

$$\begin{aligned}
\omega^1=m&=\frac{1}{\sqrt{2}}\left[\sqrt{\frac{p^2+q^2}{X}}dp+i\sqrt{\frac{X}{p^2+q^2}}\left(d\tau+q^2d\sigma\right)\right]\\
\omega^2=\overline{m}&=\frac{1}{\sqrt{2}}\left[\sqrt{\frac{p^2+q^2}{X}}dp-i\sqrt{\frac{X}{p^2+q^2}}\left(d\tau+q^2d\sigma\right)\right]\\
\omega^3=k_1&=\frac{1}{\sqrt{2}}\left[\sqrt{\frac{Y}{p^2+q^2}}\left(d\tau-p^2d\sigma\right)-\sqrt{\frac{p^2+q^2}{Y}}dq\right]\\
\omega^4=k_2&=\frac{1}{\sqrt{2}}\left[\sqrt{\frac{Y}{p^2+q^2}}\left(d\tau-p^2d\sigma\right)+\sqrt{\frac{p^2+q^2}{Y}}dq\right]
\end{aligned} \quad (6)$$

the metric (1) becomes in the simple form

$$ds^2=2(\omega^1\omega^2-\omega^3\omega^4)=g_{ab}\omega^a\omega^b \quad (7)$$

with

$$(g_{ab})=\begin{pmatrix}0&1&0&0\\1&0&0&0\\0&0&0&-1\\0&0&-1&0\end{pmatrix} \quad (8)$$

Field equations

For the massive fermionic complex fields ψ the U(1)-gauge invariant Lagrangian is given by

$$L=\overline{\psi}\gamma^{\mu}D_{\mu}\psi+M\overline{\psi}\psi+\frac{1}{4}F_{\mu\nu}F^{\mu\nu} \quad (9)$$

where γ^{μ} is the generalized Dirac gamma metrics, the U(1)-gauge field-strength tensor is defined as

$$F^{\mu\nu}=g^{\mu\alpha}\partial_{\alpha}A^{\nu}-g^{\nu\alpha}\partial_{\alpha}A^{\mu}-\left(g^{\mu\alpha}\partial_{\alpha}g^{\nu\beta}-g^{\nu\alpha}\partial_{\alpha}g^{\mu\beta}\right)g_{\beta\sigma}A^{\sigma} \quad (10)$$

and the gauge-covarint derivative is defined as

$$D_{\mu}\psi=\nabla_{\mu}\psi+igA_{\mu}\psi\,,\ \text{and its h.c.} \quad (11)$$

here $\nabla_{\mu}\psi$ be the Levi-Civita covarint derivative and g is the gauge coupling constant. Under these assumptions, the Dirac-type equation is obtained in the covarint expression

$$\gamma^{\mu}\left(\partial_{\mu}+igA_{\mu}\right)\psi-\frac{1}{4}\Gamma_{\alpha\beta\mu}\gamma^{\mu}\gamma^{\alpha}\gamma^{\beta}\psi+M\psi=0 \quad (12)$$

The Dirac-type equation governs the particle in curved space-time, and the Maxwell equations with sources can be expressed in the standard form

$$\gamma^{\mu}\left(\partial_{\mu}+igA_{\mu}\right)\psi-\frac{1}{4}\Gamma_{\alpha\beta\mu}\gamma^{\mu}\gamma^{\alpha}\gamma^{\beta}\psi+M\psi=0 \quad (13)$$

which will be generalized for the case of a null tetradic base $\{e_a\}, a=1,4$. To build up a U(1)-gauge theory of a massive fermionic complex

field in the curved space-time described by the metric (7) we use the U(1)-gauge invariant Lagrangian. The general expression for the covarint derivative (11) becomes,

$$D_a\psi = \nabla_a\psi + igA_a\psi \text{ , and its h.c.} \tag{14}$$

and the Lagrangian (9) as

$$L = \overline{\psi}\gamma^a D_a\psi + M\overline{\psi}\psi + \frac{1}{4}F_{ab}F^{ab} \tag{15}$$

The electromagnetic tensor F^{ab} can be expressed in the base of coordinate (p,q,σ,τ)

$$F^{ab} = \omega^a_\mu\omega^b_\nu F^{\mu\nu} \tag{16}$$

Therefore, the essential components $F^{\mu\nu}$ are given below

$$F^{12} = \frac{X}{p^2+q^2}A_p{}^2 - \frac{p^2+q^2}{q^4X-p^4Y}A_\sigma{}^1 - \frac{p^2+q^2}{q^2X+p^2Y}A_\tau{}^1 - \left[\frac{X(q^4X-p^4Y)}{(p^2+q^2)^2}\left(\frac{p^2+q^2}{q^4X-p^4Y}\right)_p + \frac{X(q^2X+p^2Y)}{(p^2+q^2)^2}\left(\frac{p^2+q^2}{q^2X+p^2Y}\right)_p\right]A^2 \tag{17.1}$$

$$F^{13} = \frac{X}{p^2+q^2}A_p{}^3 - \frac{Y}{p^2+q^2}A_q{}^1 - \frac{X}{Y}\left(\frac{Y}{p^2+q^2}\right)_p A^3 + \frac{Y}{X}\left(\frac{X}{p^2+q^2}\right)_q A^1 \tag{17.2}$$

$$F^{14} = \frac{X}{p^2+q^2}A_p{}^4 - \frac{p^2+q^2}{q^2X+p^2Y}A_\sigma{}^1 - \frac{p^2+q^2}{X-Y}A_\tau{}^1 - \left[\frac{X(q^4X-p^4Y)}{(p^2+q^2)^2}\left(\frac{p^2+q^2}{q^2X-p^2Y}\right)_p + \frac{X(q^2X+p^2Y)}{(p^2+q^2)^2}\left(\frac{p^2+q^2}{X-Y}\right)_p\right]A^2 - \left[\frac{X(X-Y)}{(p^2+q^2)^2}\left(\frac{p^2+q^2}{X-Y}\right)_p + \frac{X(q^2X+p^2Y)}{(p^2+q^2)^2}\left(\frac{p^2+q^2}{q^2X+p^2Y}\right)_p\right]A^4 \tag{17.3}$$

$$F^{23} = -\frac{Y}{p^2+q^2}A_q{}^2 + \frac{p^2+q^2}{q^4X-p^4Y}A_\sigma{}^3 + \frac{p^2+q^2}{q^2X+p^2Y}A_\tau{}^3 + \left[\frac{Y(q^4X-p^4Y)}{(p^2+q^2)^2}\left(\frac{p^2+q^2}{q^4X-p^4Y}\right)_q + \frac{Y(q^2X+p^2Y)}{(p^2+q^2)^2}\left(\frac{p^2+q^2}{q^2X+p^2Y}\right)_q\right]A^2 \tag{17.4}$$
$$+ \left[\frac{Y(X-Y)}{(p^2+q^2)^2}\left(\frac{p^2+q^2}{q^2X+p^2Y}\right)_q + \frac{Y(q^2X+p^2Y)}{(p^2+q^2)^2}\left(\frac{p^2+q^2}{q^4X-p^4Y}\right)_q\right]A^4$$

$$F^{24} = \frac{p^2+q^2}{q^4X-p^4Y}A^4{}_{,\sigma} + \frac{p^2+q^2}{q^2X+p^2Y}A^4{}_{,\tau} - \frac{p^2+q^2}{q^2X+p^2Y}A^2{}_{,\sigma} - \frac{p^2+q^2}{X-Y}A^2{}_{,\tau} \tag{17.5}$$

$$F^{34} = \frac{Y}{p^2+q^2}A_q{}^4 - \frac{p^2+q^2}{q^2X+p^2Y}A_\sigma{}^3 - \frac{p^2+q^2}{X-Y}A_\tau{}^3 - \left[\frac{Y(q^4X-p^4Y)}{(p^2+q^2)^2}\left(\frac{p^2+q^2}{q^2X-p^2Y}\right)_q + \frac{Y(q^2X+p^2Y)}{(p^2+q^2)^2}\left(\frac{p^2+q^2}{X-Y}\right)_q\right]A^2 \tag{17.6}$$
$$- \left[\frac{Y(X-Y)}{(p^2+q^2)^2}\left(\frac{p^2+q^2}{X-Y}\right)_q + \frac{Y(q^2X+p^2Y)}{(p^2+q^2)^2}\left(\frac{p^2+q^2}{q^2X+p^2Y}\right)_q\right]A^4$$

These components of $F^{\mu\nu}$ allow us to put the Maxwell equations (13) in the expression

$$e_a F^{ba} = J^b \tag{18}$$

Finally the Dirac-type equation is derived for the spinorial massive complex field ψ coupled to the Kerr-Newman-Kasuya space-time. Using the U(1)-gauge invariant Lagarangian (15) the Dirac-type equation is obtained in the general form

$$\gamma^a(\partial_a + igA_a)\psi - \frac{1}{4}\Gamma_{bca}\gamma^a\gamma^b\gamma^c\psi + M\psi = 0 \tag{19}$$

Hence, by working out the above Dirac-type equation for the metric (5) can be expressed in the form

$$\gamma^a(\partial_a + igA_a)\psi + M\psi - \frac{1}{4\sqrt{2(p^2+q^2)^3}}\times \left\{\begin{bmatrix}(p^2+q^2)\left(\frac{\partial X}{\partial p}\right) - 2pX \\ \sqrt{X}\end{bmatrix}(\gamma^1+\gamma^2) + \begin{bmatrix}(p^2+q^2)\left(\frac{\partial Y}{\partial q}\right) - 2qY \\ \sqrt{Y}\end{bmatrix}(\gamma^3-\gamma^4)\right] \\ -8i\left[p\sqrt{Y}\gamma^1\gamma^2(\gamma^3+\gamma^4) - q\sqrt{X}(\gamma^1-\gamma^2)\gamma^3\gamma^4\right]\Bigg\}\psi = 0 \tag{20}$$

Using (3) and (4) into the equation (20) we obtain the Dirac-type equation for the metric (1) in the following form

$$\gamma^a(\partial_a + igA_a)\psi + M\psi + \left[\frac{\{(r^2+h^2)h\cos\theta\}(\gamma^1+\gamma^2)}{2h\sin\theta\sqrt{2\{r^2+h^2\cos^2\theta\}^3}}\right]\psi - \left[\frac{\{h^2\cos^2\theta(r-m)+r(rm-e^2-h^2-l^2)\}(\gamma^3-\gamma^4)}{2\sqrt{2\{r^2+h^2\cos^2\theta\}^3}(r^2-2mr+e^2+h^2+l^2)}\right]\psi + \left[\frac{2i\{h\cos\theta(\sqrt{r^2-2mr+e^2+h^2+l^2})\}(\gamma^3+\gamma^4)\gamma^1\gamma^2}{\sqrt{2\{r^2+h^2\cos^2\theta\}^3}}\right]\psi - \left[\frac{2irh\sin\theta(\gamma^1-\gamma^2)\gamma^3\gamma^4}{\sqrt{2\{r^2+h^2\cos^2\theta\}^3}}\right]\psi = 0 \tag{21}$$

The result obtained in this paper corresponds to the result obtained in the case of the Kerr Newman black hole space-time when l =0. Under this observation, we like to claim that this study encompasses the known result of Dariescu *et al.* [4] in the context of Kerr-Newman black hole. So, it is interesting to note that the

U(1)-gauge theory for fermions not only exists in the Kerr-Newman black hole space-time, but also in the Kerr-Newman Kasuya space-time. The Kerr-Newman-Kasuya space-time is not a black hole space-time but it has the common feature with the black hole space-time that it has horizon.

References

1. **Carmeli, M**. 1985. Field theory on RÍS^3 topology. I: The Klein-Gordon and Schrödinger equation. *Foundations of Phys*. 15:175-184.
2. **Carmeli, M. and Carmeli, S**. 1985. Field theory on $R \times S^3$ topology. II: The Weyl equation. *Foundations of Phys.* 15:185-191.
3. **Carmeli, M. and Malin, S**. 1985. Field theory on topology. III: The Dirac equation. *Foundations of Phys*. 15:1019-1029.
4. **Sen, D.** 1986. Fermions in space-time $R \times S^3$. J. Math. Phys. 27:472-482.
5. **Dariescu, M., Dariescu, C. and Gottlieb, I**. 1995. Fermions in a Kerr-Newman space-time. *Foundations of Phys.* 25:1523-1528.
6. **Dariescu, C. and Dariescu, M**. 1994. Gauge theory of Bosonic and Fermionic fields in space-time. *Foundations of Phys.* 24:1577-1582.
7. **Plebanski, J.F.** 1975. A class of solutions of Einstein-Maxwell equations. *Ann. Phys.* 90:196-255.

Proc. Pakistan Acad. Sci. 42(4):243-247.2005

POCKLINGTON EQUATION AND THE METHOD OF MOMENTS

J. Sosa-Pedroza, V. Barrera-Figueroa and J. López-Bonilla

Instituto Politécnico Nacional, Escuela Superior de Ingeniería Mecánica y Eléctrica, Sección de Estudios de Postgrado e Investigación, Edif. Z-4, 3er. piso, col. Lindavista, C.P. 07738, México D.F.

Received November 2005, accepted November 2005

Communicated by Prof. Dr. M. Iqbal Choudhary

Abstract: In this paper the authors make an analysis of different function combinations for application in the method of moments, especially to dipole antenna, in order to select the most suitable pair of functions which could provide better results in getting the current distribution along the antenna.

***Keywords*:** Pocklington equation; dipole antenna; method of moments; base and weight functions comparative analysis

Introduction

Method of Moments (MM) is widely used in the solution of field equations to obtain current distribution of wire antennas. Both, Hallén equation defined by magnetic and electric potentials and the electric field Pocklington equation, use the MM procedure. Since the beginning, when Harrington [1] established the method, a main task has been the selection of base and weight functions to obtain a computational efficient and reliable solution. Even though the actual articles write mainly about MM applications, we think that there is a pendent issue related with the analysis of the best combination of base and weight functions. This paper presents a comparative analysis of 16 combinations for the four more used functions; as a matter of comparison we use the feed point impedance obtained for the classical analysis and the MM solution of Pocklington's general equation for arbitrary bent wires [2], applied to the well known half wavelength dipole.

The Pocklington general equation

Starting with Maxwell equations, it is possible to obtain the simplified general equation for arbitrary bent wires [3], given by:

$$E^i_{\tan} = -\frac{1}{j\omega\varepsilon}\int_{s'}\left[R^2\left(k^2R^2-1-jkR\right)\mathbf{s}\bullet\mathbf{s}' + \left(3+3jkR-k^2R^2\right)(\mathbf{R}\bullet\mathbf{s})(\mathbf{R}\bullet\mathbf{s}')\right]\frac{e^{-jkR}}{4\pi R^5}I(s')ds'. \quad (1)$$

Pocklington's procedure applied to wire antennas, supposes the current to be located over a thin filament over the conductor, while the rest of it is part of the free space (Fig. 1), considering constant the transversal current distribution. As Fig. 1 shows, $\mathbf{s}'$ represents a unit vector parallel to the conductor surface and $\mathbf{s}$ a unit vector over the conductor axis, the conductor axis $\mathbf{r}(s)$ and the current filament $\mathbf{r}'(s')$ are given by:

$$\mathbf{r}(s) = x(s)\mathbf{i} + y(s)\mathbf{j} + z(s)\mathbf{k}\,, \qquad \mathbf{r}'(s') = \mathbf{r}(s') + a\mathbf{n}(s)\,, \quad (2)$$

where $\mathbf{n}(s)$ represents a unit normal vector to the wire axis.

As is seen, both the filament curve and axis curve are parallel to each other. Although it is possible to choose an infinite number of filaments, in practice the one which makes the easiest calculation is selected. The Pocklington's general equation, given

E-mail: jsosa@ipn.mx; vbarreraf@ipn.mx; jlopezb@ipn.mx

by (1) can be used for any geometry. The MM solution is obtained after definition of unit vectors of equation (2). The dot product $\mathbf{s} \bullet \mathbf{s}'$ and position of any point over the conductor's surface $|\mathbf{r} - \mathbf{r}'|$ is:

$$R = |\mathbf{R}| = |\mathbf{r} - \mathbf{r}'| = \sqrt{[x(s) - x'(s')]^2 + [y(s) - y'(s')]^2 + [z(s) - z'(s')]^2} \quad (3)$$

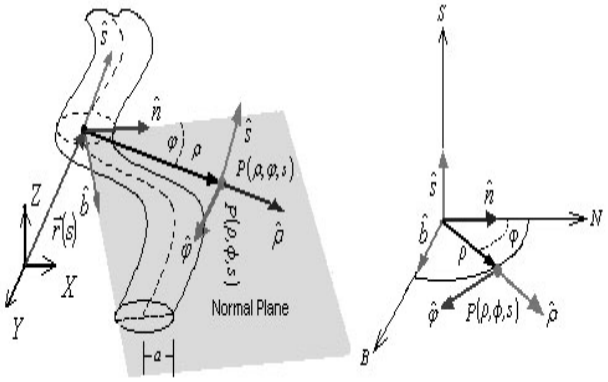

Fig. 1. Geometry for an arbitrary thin wire.

The method of moments

Equation (1) has the form [4]:

$$Lf = g. \quad (4)$$

where L represents the integral linear operator, g is a known function (electric field) and f the unknown function (the current), which should be determined and MM represents the unknown f, by a set of functions in the L domain, ($f_1, f_2, f_3, \cdots$), as a linear combination:

$$f = \sum_n \alpha_n f_n . \quad (5)$$

The α_n are constants to be determined and the f_n, named base or expansion functions, are arbitrarily selected. Substituting (4) in (5) and considering the linearity of L, we have:

$$\sum_n \alpha_n L f_n = g . \quad (6)$$

Equation (6) has N unknowns and it is necessary to have N independent linear equations, which are obtained taking the internal product of (6) with other set of functions, named weight functions, in the L domain, then:

$$\sum_n \alpha_n \langle w_m, Lf_n \rangle = \langle w_m, g \rangle . \quad (7)$$

The internal product is usually an integral of area. Equation (7) can be written in matrix form as:

$$[\langle w_m, Lf_n \rangle][\alpha_n] = [\langle w_m, g \rangle], \quad [l][\alpha_n] = \mathbf{g} . \quad (8)$$

If the inverse of $[l]$ exists the a_n are obtained by:

$$[\alpha_n] = [l]^{-1}[\langle w_m, Lf_n \rangle]. \quad (9)$$

Comparing (8) and (1), and using the linearity of integral operator, the matrix of (9) can be written as:

$$[Z_{mn}](I_n) = (V_m), \quad (10)$$

where $[Z_{mn}]$ and (V_m) are known as impedance and voltage matrices, respectively, and are defined by [5]:

$$Z_{mn} = -\frac{1}{j\omega\varepsilon} \int_{s_m} w_m \int_{s'_n} \alpha_n \left[R^2 \left(k^2 R^2 - 1 - jkR\right)\mathbf{s} \bullet \mathbf{s}' + \left(3 + 3jkR - k^2 R^2\right)(\mathbf{R} \bullet \mathbf{s})(\mathbf{R} \bullet \mathbf{s}')\right] \frac{e^{-jkR}}{4\pi R^5} ds ds' , \quad (11)$$

$$V_m = \int_{s_m} w_m E^i_{\tan} ds \quad (12)$$

Using (11) and (12), the current is:

$$(I_n) = [Z_{mn}]^{-1}(V_m) \quad (13)$$

To solve (13) it is necessary to define the base and weight functions; as is known, both functions are selected arbitrarily. The most widely used subdomain functions have been a subject of research. Some discussion of these may be found in [6,7], but the more often used functions are Dirac´s delta, pulse, triangle and piecewise sinusoidal. This paper make 16 combinations of these functions to solve equation (13), trying to find the best one. As a matter of comparison, we use the feed impedance of a half wavelength dipole obtained by the well

known analytical method for thin wire antennas.

The four functions

The purpose of this paper is to show the performance of combining the four most used base and weight functions to establish the best combination, considering a time and resources computational efficiency, and reliable solution. The used functions are described in the following paragraphs.

Dirac's delta: This function is the most used as weight function, because it reduces in one the number of integrations:

$$\int_{\Delta s} \delta(s-s_m)ds = \begin{cases} 1 & \text{if} \quad s_m \in \Delta s \\ 0 & \text{elsewhere} \end{cases} \tag{14}$$

Pulse function: This is the most common base function in the literature, and is given by:

$$i_n(s') = \begin{cases} 1 & \text{if} \quad (n-1)\Delta s' \le s' < n\Delta s' \\ 0 & \text{elsewhere} \end{cases} \tag{15}$$

Linear or triangular function: It attempts to use a softer function at the cost of greater complexity, and is defined by:

$$i_n(s') = \begin{cases} \dfrac{s'-s'_{n-1}}{s'_n - s'_{n-1}} & \text{if} \quad s'_{n-1} \le s' \le s'_n \\ \dfrac{s'_{n+1}-s'}{s'_{n+1}-s'_n} & \text{if} \quad s'_n \le s' \le s'_{n+1} \\ 0 \quad \text{elsewhere} \end{cases} \tag{16}$$

Piecewise sinusoidal: It is a more complicated function with a higher computational complexity, but many authors suppose that it gives a more exact solution. It is represented by:

$$i_n(s') = \begin{cases} \dfrac{sen\left[k\left(s'-s'_{n-1}\right)\right]}{sen\left[k\left(s'_n - s'_{n-1}\right)\right]} & \text{if} \quad s'_{n-1} \le s' \le s'_n \\ \dfrac{sen\left[k\left(s'_{n+1}-s'\right)\right]}{sen\left[k\left(s'_{n+1}-s'_n\right)\right]} & \text{if} \quad s'_n \le s' \le s'_{n+1} \\ 0 \quad \text{elsewhere} \end{cases} \tag{17}$$

Computational results

The following Figures show the results for the 16 combinations we make, for real and imaginary components; they are presented in eight figures using one as weight function and the other four as base functions. The horizontal coordinate shows the relationship between the length and wire's radius. The horizontal straight line is the reference impedance for a half wavelength dipole, using the analytical method. As is known, the real part in this case is 73 Ω and 43 Ω for imaginary part.

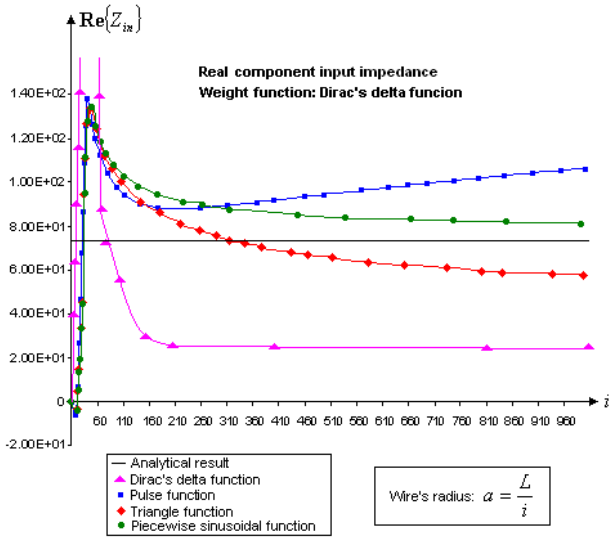

Fig. 2. Real component input impedance for Dirac's delta as weight function.

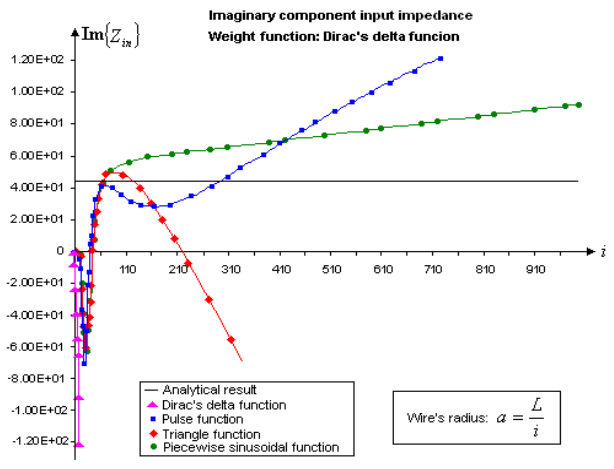

Fig. 3. Imaginary component input impedance for Dirac's delta as weight function.

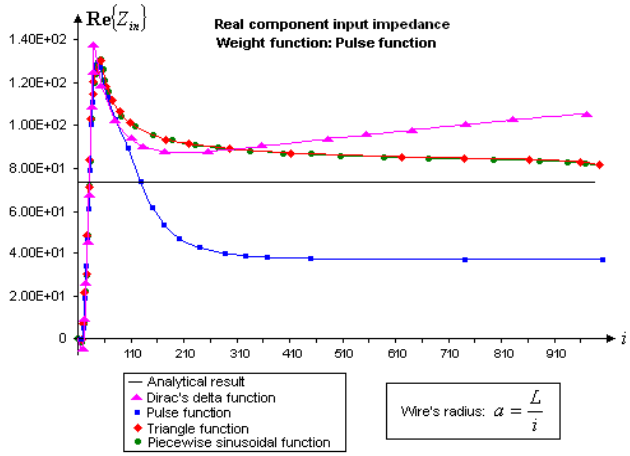

Fig. 4. Real component input impedance for pulse function as weight function.

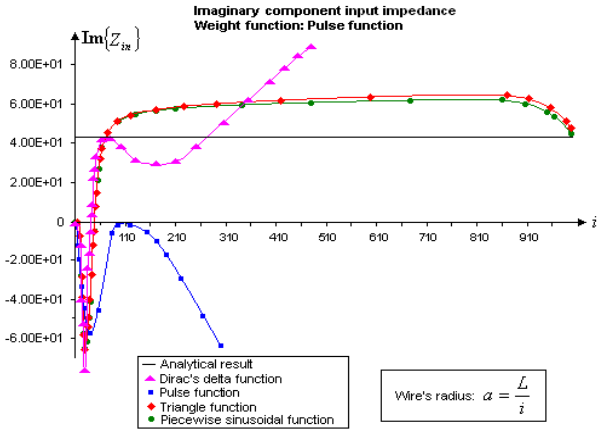

Fig. 5. Imaginary component input impedance for pulse function as weight function.

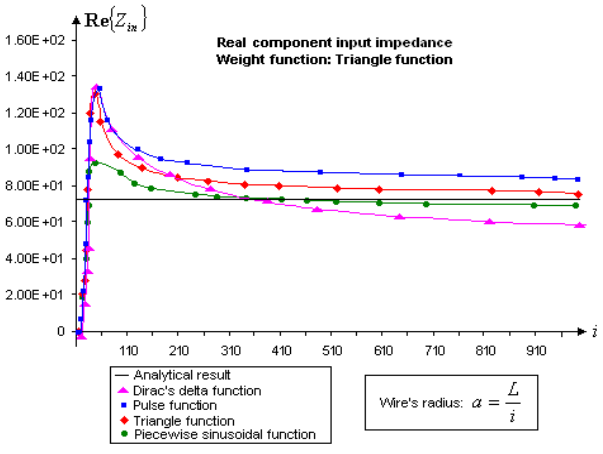

Fig. 6. Real component input impedance for triangular function as weight function.

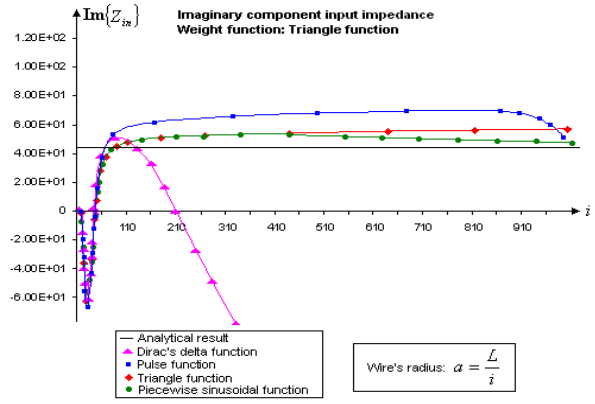

Fig. 7. Imaginary component input impedance for triangular function as weight function.

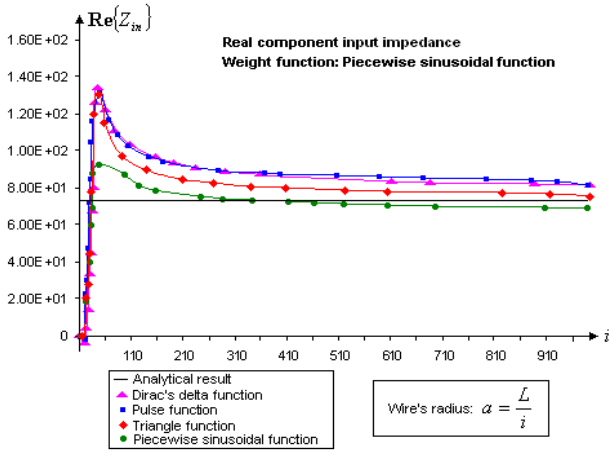

Fig. 8. Real component input impedance for piecewise sinusoidal function as weight function.

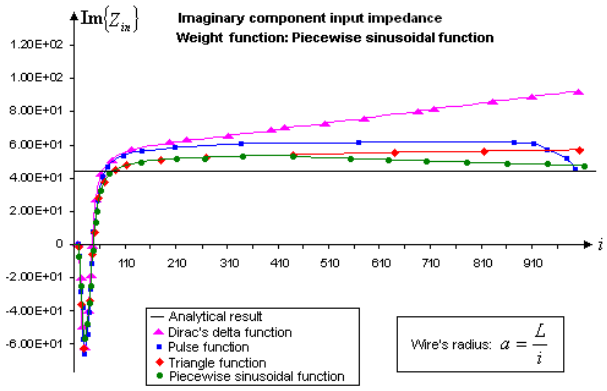

Fig. 9. Imaginary component input impedance for piecewise sinusoidal function as weight function.

As we can see, in computational results the less reliable is de Dirac's delta as weight function, although pulse, triangular and sinusoidal base functions are close to the analytical solution. The curves for the pulse weight functions are closer and softer than the former. It is interesting to see that the triangular and sinusoidal base functions respond almost in the same way, but there is a 15% to 30% deviation.

The triangular and sinusoidal weight functions respond almost in the same way, but Dirac's delta has higher desviation, mainly for the triangle function. It is very easy to conclude that the best solution is the piecewise sinusoidal function for both, the base and weight functions (Galerkin procedure), but the computational time is very high, compared with the pulse or delta procedures, Table 1 shows the computational time difference using a personal computer Pentium 4 running to 1.8 GHz and 256 MB of RAM. We use the pulse as a base and delta as a weight functions and reference time of approximately one minute.

Table 1.
Time comparison

		Base Functions			
Weight Functions		Delta	Pulse	Linear	Sine
	Delta	0.1	1	2	2
	Pulse	1	40	80	80
	Linear	2	80	160	160
	Sine	2	80	160	160

The conclusion is evident. We have presented a comparison analysis for the most popular base and weight functions, considering the reliability and computer time consumption. As can be seen, the reliability runs contrary to time consumption. Under our machine conditions, it takes almost fifteen minutes for the best solution. This is something that requires attention, although we think that it is necessary to search for a more efficient integration procedure than the Simpson's rule we are using. Actually we are working with other integration methods to reduce the inefficient times.

References

1. **Harrington, R.F**. 1980. Origin and development of the Method of Moments for field computation. In: *Applications of the Method of Moments to Electromagnetic Fields*. Ed. Strait, B. J., SCEE Press, New York, Chap. 1.
2. **Barrera-Figueroa, V., Sosa-Pedroza, J. and López-Bonilla, J**. 2005. Simplification of Pocklington's integral equation for arbitrary bent thin wires. In: *Boundary Elements XXVII.* Eds. Kassab, A., Brebbia, C.A., Divo, E. and Poljak, D., WIT Press, England, pp. 563-574,
3. **Sosa-Pedroza, J., López-Bonilla, J. and Barrera-Figueroa, V**. 2005. La ecuación generalizada de Pocklington para antenas de alambre de forma arbitraria. *Mex. J. Electr. Eng.* 9:83-86.
4. **Balanis, A**. 1980. *Antenna theory, analysis and design.* 2nd edition, John Wiley & Sons, New York, Chap. 8.
5. **Stutzman, W.L. and Thiele, G.A**. 1998. *Antenna Theory and Design.* John Wiley & Sons, New York.
6. **Butler, Ch. M. and Wilton, D.R**. 1975. Analysis of various techniques applied to thin wire scatterers. *IEEE Trans. Antennas Propag.* AP-23: 422-428.
7. **Sarkar, T.K.** 1985. A note on the choice weighting functions in the Method of Moments. *IEEE Trans. Antennas Propag.* AP-33:436-441.

Proc. Pakistan Acad. Sci. 42(4):249-252.2005

SOME APPLICATIONS OF A LOVELOCK'S THEOREM

M. Acevedo, J. López-Bonilla and S. Vidal-Beltrán

SEPI-ESIME-Zacatenco, Instituto Politécnico Nacional, Edif. Z-4, 3er Piso, Col Lindavista, CP 07738, México DF

Received March 2005, accepted September 2005

Communicated by Prof. Dr. Kamaluddin Ahmad

Abstract: Here we employ a Lovelock´s result for a) to obtain the general structure of the second fundamental form of intrinsically rigid spacetimes of class one, b) to show a known identity between the Riemann tensor and its double dual, and c) to construct a Lanczos potential for the Gödel metric.

Keywords: Embedding of Riemannian spaces; Lanczos potential; Gödel solution; Lovelock's theorem, **PACS Nos.** 04.20.- q; 04.90. +e

Introduction

We shall use the notation and quantities of [1]. Lovelock [2,3] proved the following interesting theorem valid only in four dimensions.:

"If the tensor $A_i^{\ j}$ depends exclusively on the metric tensor g_{ab} and on its first and second partial derivatives

$$A_i^{\ j} = A_i^{\ j}(g_{ab}; g_{ab,c}; g_{ab,cd}), \tag{1}$$

and if it also satisfies the continuity equation

$$A_i^{\ j}{}_{;j} = 0, \tag{2}$$

then necessarily

$$A_i^{\ j} = \alpha\delta_i^{\ j} + \beta G_i^{\ j},\ \alpha, \beta = \text{constants}, \tag{3}$$

where $G_{ab} = R_{ab} - \frac{R}{2} g_{ab}$ is the Einstein tensor".

Notice that $_{\rm r}$ denotes covariant derivative and besides [1] $\delta_i^{\ j}{}_{;j} = G_i^{\ j}{}_{;j} = 0$. In (1) the symmetry $A_{ij} = A_{ji}$ neither required nor needed that $A_i^{\ j}$ be linear in $g_{ab,cd}$. We do not know specific applications of this Lovelock's theorem to general relativity, except as stated by Harvey [4].

Here we shall employ (1), (2), and (3) to (a) deduce the structure of the second fundamental form of spacetimes embedded into E_5 for the case of intrinsic rigidity [1], (b) give a plain but illustrative demonstration of a Lanczos identity [5] between the curvature tensor and its double dual [1], and (c) obtain a Lanczos generator [6] in Gödel geometry [1,7].

(a) Spacetime of class one with intrinsic rigidity.

A R_4 can be embedded into E_5 if and only if there exists the second fundamental form $b_{ac} = b_{ca}$ fulfilling the Gauss-Codazzi equations [1]

$$R_{acij} = \varepsilon(b_{ai}b_{cj} - b_{aj}b_{ci}), \tag{4}$$

$$b_{ji;c} = b_{jc;i}, \tag{5}$$

where $\varepsilon = \pm 1$ and R_{acij} is the Riemann tensor, thus we say that such 4-space has class one. From the Gauss relation (4), it is possible to deduce the identity [8]

$$pb_{ij} = \frac{K_2}{48} g_{ij} - \frac{1}{2} R_{iacj} G^{ac}, \tag{6}$$

e-mail: jlopezb@ipn.mx

with the presence of the Lanczos invariant [5]

$$K_2 = {}^*R^{*ijac} R_{ijac}, \tag{7}$$

in terms of the double dual [1,6] of curvature tensor ${}^*R^{*ij}{}_{ac} = \frac{1}{4}\eta^{ijrm} R_{rm}{}^{nr} \eta_{nrac}$, being η_{ijac} the Levi-Civita tensor; besides [8]

$$p^2 = -\frac{\varepsilon}{6}\left(\frac{R}{24}K_2 + R_{imnj}G^{ij}G^{mn}\right) \geq 0, \tag{8}$$

If $p \neq 0$, then (6) permits to construct explicitly a b_{ij} verifying (4), and then from (6) and (8) it is clear that the intrinsic rigidity [9]

$$b_i{}^j = b_i{}^j(g_{ab}; g_{ab,c}; g_{ab,cd}), \tag{9}$$

If into Codazzi equation (5) we sum c with j

$$(b_i{}^j - b\delta_i{}^j)_{;j} = 0, \quad b = b^r{}_r, \tag{10}$$

then (9) and (10) imply that the tensor $A_i{}^j = b_i{}^j - b\delta_i{}^j$ satisfies the conditions (1) and (2) of the Lovelock's theorem. Thus it must have the structure (3) and therefore

$$b_{ij} = (\alpha + b)g_{ij} + \beta G_{ij}, \tag{11}$$

where α, β are constants. But the scalar curvature $R = -G_i{}^i$, then (11) gives us that $b = \frac{1}{3}(\beta R - 4\alpha)$, thus finally (11) takes the general expression for the second fundamental form of a spacetime with intrinsic rigidity

$$b_{ij} = \beta R_{ij} - \frac{1}{6}(2\alpha + \beta R)g_{ij}, \tag{12}$$

such that $R_{ij} = R^a{}_{ija}$ is the Ricci tensor.

Without the Lovelock's result, it is very difficult to suspect the existence of (12). In other paper we will study the important consequences that (12) has in the local and isometric embedding of R_4 into E_5, when is present the intrinsic rigidity.

(b) A Lanczos identity

We shall employ the Lovelock's theorem to show the following Lanczos relation [5]

$${}^*R^{*jbpq} R_{ibpq} = \frac{K_2}{4}\delta_i^j, \tag{13}$$

which usually is proved via the generalized Kronecker´s delta [3]. However, we believe that its deduction with the aid of (1), (2) and (3) will be attractive in general relativity.

Bianchi's identities for the curvature tensor in every spacetime are [1]

$$R_{pqab;i} + R_{pqbi;a} + R_{pqia;b} = 0 \tag{14}$$

or in terms of the double dual [6]

$${}^*R^{*pqab}{}_{;b} = 0; \tag{15}$$

Besides, its known that $\eta_{pqab;c} = 0$, then from (7)

$$K_{2;i} = 2{}^*R^{*pqab} R_{pqab;i} \overset{(14)}{=} -2{}^*R^{*pqab}(R_{pqbi;a} + R_{pqia;b}),$$

$$= 2{}^*R^{*pqab}(R_{ibpq;a} - R_{iapq;b}),$$

$$= 4{}^*R^{*pqab} R_{ibpq;a} \overset{(15)}{=} (4{}^*R^{*abpq} R_{ibpq})_{;a},$$

Thus we see that (1) and (2) are verified with $A_i{}^j = {}^*R^{*jbpq} R_{ibpq} - \frac{K_2}{4}\delta_i{}^j$, then (3) implies

$${}^*R^{*jbpq} R_{ibpq} = \left(\frac{K_2}{4} + \alpha\right)\delta_i^j + \beta G_i{}^j, \tag{16}$$

whose contraction of i and j gives us

$$\beta R - 4\alpha = 0. \tag{17}$$

if $\beta \neq 0$ then $R = \frac{4\alpha}{\beta} =$ constant, which could be

valid for some particular spacetimes; similarly $R = 0$ corresponds to an specific case. But we wish a universal identity for any R_4 without restrictions on its geometry, and by (17) this is possible only if $\alpha = \beta = 0$, thus (16) implies the Lanczos identity (13), q.e.d.

(c) Lanczos potential for the Gödel solution

The analysis of the invariant (7) led [6] to discover, for arbitrary spacetime, the potential K_{abc} with the properties:

$$K_{abc} = -K_{bac}\,,\; K_{abc} + K_{bca} + K_{cab} = 0, \tag{18}$$

$$K_a{}^r{}_r = 0, \tag{19}$$

$$K_{ab}{}^c{}_{;c} = 0, \tag{20}$$

which generates the Weyl tensor through the expression [10]

$$C_{aijr} = K_{aij;r} - K_{air;j} + K_{jra;i} - K_{jri;a} + g_{ar}K_{ij} - g_{aj}K_{ir} + g_{ij}K_{ar} - g_{ir}K_{aj}, \tag{21}$$

where $K_{ij} = K_i{}^r{}_{j;r} = K_{ji}$.

Given the conformal tensor, it may be very difficult to obtain a Lanczos potential by integrating directly (21), but here we shall show that the Lovelock's result permits to determine one solution of (21) for the Gödel metric [1,7](signature +2)

$$ds^2 = -(dx^1)^2 - 2e^{x^4}dx^1dx^2 - \frac{1}{2}e^{2x^4}(dx^2)^2 + (dx^3)^2 + (dx^4)^2, \tag{22}$$

with the interesting structure

$$K_{abc} = Q_{ca;b} - Q_{cb;a}\,,\; Q_{ab} = Q_{ba}\,, \tag{23}$$

which verifies (18); thus the symmetric tensor Q_{ij} is a generator of the Lanczos potential.

The Lanczos algebraic gauge (19) may be satisfied if in (23) we ask the conditions

$$Q^r{}_r = constant, \tag{24}$$

$$Q_i{}^j{}_{;j} = 0 \tag{25}$$

Besides, if we accept that Q_{ij} depends locally on the intrinsic geometry of R_4

$$Q_{ir} = Q_{ir}(g_{ab}; g_{ab,c}; g_{ab,cd}), \tag{26}$$

then (25) and (26) imply, via the Lovelock's theorem, that

$$Q_{ab} = \alpha g_{ab} + \beta G_{ab}, \tag{27}$$

thus $Q^r{}_r = 4\alpha - \beta R$ is in accord with (24) because $R = 1$ for the Gödel solution (22). If now we put (27) into (23), it results in

$$K_{abc} = \alpha\left(R_{ca;b} - R_{cb;a}\right), \tag{28}$$

which also verifies the Lanczos differential gauge (20). Finally with the help of (21), (22) and (28), we conclude that $\alpha = -\frac{1}{9}$, that is,

$$K_{ijr} = \frac{1}{9}\left(R_{rj;i} - R_{ri;j}\right). \tag{29}$$

This means that, in the Gödel cosmological model, the Ricci tensor generates one Lanczos potential.

References

1. **Kramer, D., Stephani, H., MacCallum, M. and Herlt, E.** 1980. *Exact solutions of Einstein's field equations*. Cambridge Univ. Press, Cambridge.
2. **Lovelock, D.** 1972. The four-dimensionality of space and the Einstein tensor. *J. Math. Phys.* 13:874-876.
3. **Lovelock , D. and Rund, H.** 1975. *Tensors, differential forms and variational principles*. John Wiley and Sons, New York.
4. **Harvey, A**. 2002. *Is the Universe's expansion accelerating?* Physics Today, February 2002.
5. **Lanczos, C**. 1938. A remarkable property of the

Riemann tensor in four dimensions. *Ann. Math*. 39:842-850.

6. **Lanczos, C.** 1962. The splitting of the Riemann tensor. *Rev. Mod. Phys*. 34:379-389.
7. **Gödel, K.** 1949. An example of a new type of cosmological solutions of Einstein's field equations of gravitation. *Rev. Mod. Phys.* 21:447-450.
8. **López-Bonilla, J., Morales, J. and Ovando, G**. 2000. An identity for R_4 embedded into E_5. *Indian J. Math.* 42:309-312.
9. **Goenner, H.F.** 1976. Intrinsically and energetically rigid spacetimes of class one. *Tensor New Series* 30:15 .
10. **López-Bonilla, J., Morales, J. and Ovando, G.**, 1999. A potential for the Lanczos spintensor in Kerr geometry. *Gen. Rel. Grav*. 31:413-415.

Proc. Pakistan Acad. Sci. 42(4):253-259.2005

DETERMINATION OF TRIPROLIDINE-HCl BY SPECTROPHOTOMETRIC METHOD IN PURE AND PHARMACEUTICAL PREPARATIONS USING DICHLORONITROBENZENE AS A NEW CHROMOGENIC REAGENT

Amina Mumtaz, Asrar A. Kazi*,Tehseen Aman, M. Usman Sabri and Fauzia Noureen

Applied Chemistry Research Centre, Pakistan Council of Scientific and Industrial Research Laboratories Complex, Ferozepur Road, Lahore-54600, Pakistan

Received August 2005, accepted October 2005

Communicated by Dr. M. Iqbal Choudhary

Abstract: In the present study it is demonstrated that H_1- blockers such as triprolidine–HCl can be determined by a very simple, sensitive and accurate spectrophotometric procedure. The method consisted of interaction of triprolidine-HCl with dichloronitrobenzene in alkaline medium. Absorbance of resulting orange colour was measured at 440 nm .The reaction turned out to be selective for triprolidine –HCl with 0.005 $mgml^{-1}$ as the visual limit of identification and provided a basis for a new spectrophotometric determination. The reaction obeyed Beer's law from 0.05 mg to 0.15 $mgml^{-1}$ for triprolidine–HCl and the relative standard deviation was 0.60 %. The quantitative assessment of other drugs was also studied.

Keywords: Triprolidine–HCl determination, dichloronitrobenzene, colour stability, analytical pharmacy

Introduction

Triprolidine hydrochloride (Fig.1) is a pyridine derivative with the properties of antihistamine. It is a potent histamine H_1-receptor antagonist (H_1-blocker), with a rapid onset and long duration action, almost up to 12 hours. It is probably effective for the symptomatic treatment of seasonal and perennial allergic rhinitis, vasomotor rhinitis, allergic conjunctivitis due to allergens, foods and prevention of allergic reactions to blood or plasma [1]. The most common side effects are sedation, dizziness, incoordination, gastrointestinal disturbances, nausea, vomiting and diarrhea. It may also produce blurred vision, dryness of mouth, tightness of chest, blood disorders including agranulocytosis and haemolyticanaemia [2].

In view of the importance of antihistamine considerable analytical work has been carried out. In the reversed phase HPLC [3,4] and HPLC photodiode procedures [5], 12.5 cm Nucleosil 100 $t-5C_{18}$ bonded phase column with a mobile phase consisting of methanol acetonitrile was used. A 0.01M potassium dihydrogen phosphate solution was employed to adjust the pH to 6.8 [3] and UV detection was carried out at 254 and 280 nm [4]. In another HPLC method different UV absorption characteristics of triprolidine hydrochloride have been used to facilitate its determination in a mixture [6]. A wavelength switching programme has to be employed in this procedure. In the micro extraction capillary GC procedure [7] headspace solid-phase extraction was carried out followed by capillary gas chromatography with flame ionization detection. The recoveries in blood extraction were 4 - 51 folds lower than those in urine extraction. In the capillary electrophoresis procedures [8,9] the quality of separation was dependent upon the sample diluent used [8] and only basic drugs are screened from blood [9] while most of the spectrophotometric

*Author for correspondence

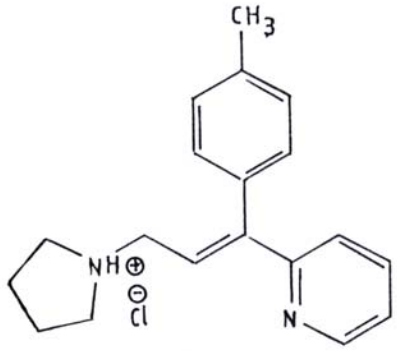

Triprolidine hydrochloride

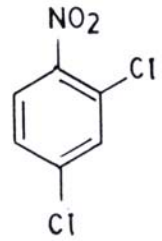

2, 4- dichloronitrobenzene

Fig. 1. Structural formula of triprolidine hydrochloride and 2, 4-dichloronitrobenzene.

procedures [10-13] are carried out in the UV region. Long and tedious procedures are involved in chemiluminescent nitrogen detection in conjunction with reversed phase HPLC, UV and MS [14] and TLC/MS [15] exhibiting an average error of ± 10 over the entire linear range of absorbance [14]. Triprolidine (trip) ion selective electrodes of three types, i.e. conventional polymer membrane, graphite coated and carbon pasted based on the ion pair of triprolidine hydrochloride with sodium tetraphenylborate were also employed [16]. A kinetic method based on the alkaline oxidation of triprolidine with $KmnO_4$ has also been reported [17].

During the studies it was found that triprolidine-HCl reacts with dichloronitrobenzene in alkaline media to give an orange colour having maximum absorbance at 440nm. The reaction obeys Beers Law and has 0.005 $mgml^{-1}$ as visual limit of identification. The colour reaction has not been reported in the literature. The present method is simple, accurate, precise and sensitive. Percentages of other drugs have also been studied.

Materials and Methods

Apparatus and reagents

Cecil CE-2041 spectrophotometer with 1cm Quartz cell was used to measure the absorbance and graduated pipettes were employed. Analytical grade chemicals and doubly distilled water were used. Triprolidine-HCl (Glaxo Wellcome, Karachi, Pakistan) standard solution (w/v) (1.0$mgml^{-1}$) was prepared by dissolving triprolidine HCl (100mg) in ethyl alcohol (20 ml) (BDH) and the volume was made up to 100ml with distilled water to give a stock solution, which was diluted further as required. A 1% (w/v) dichloronitrobenzene (BDH) was prepared in ethyl alcohol and 1.0 N sodium hydroxide was prepared in distilled water.

General procedure

To an aliquot of triprolidine-HCl containing 0.005 mg to 0.15 $mgml^{-1}$ was added 2 ml of 1% dichloronitrobenzene, 1ml of 1.0N of sodium hydroxide and the contents were heated for 45 s in a water bath at 65°C, cooled and the volume was made up to 10 ml with ethyl alcohol. The resulting absorbance of the orange colour was measured 440 nm, employing all reagents except triprolidine-HCl as a blank. The experiment was repeated with different volumes of standard triprolidine-HCl solution and a calibration curve was prepared (Fig.2). The colour reaction obeys Beer's Law from 0.005 to 0.15 mg/ml^{-1} of triprolidine-HCl.

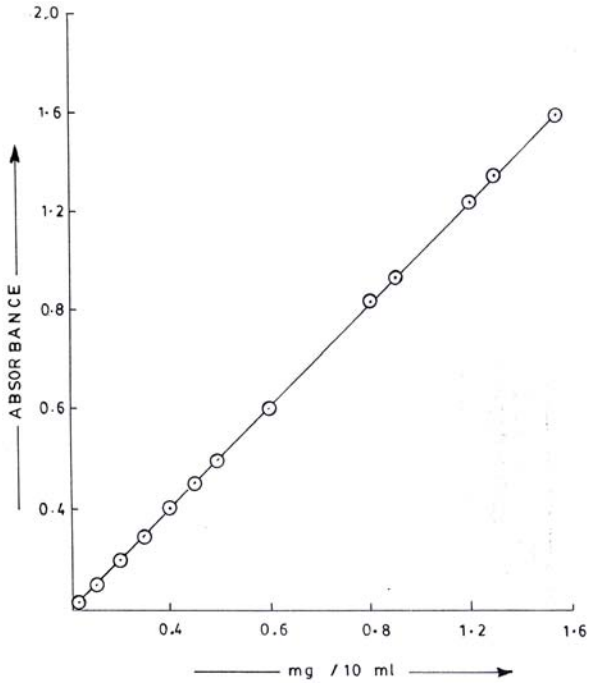

Fig. 2. Calibration curve of triprolidine — HCl with dichloronitrobenzene.

Procedure for studying the interfering compounds

To an aliquot containing 1.0 $mgml^{-1}$ of triprolidine-HCl, different amounts of various compounds (1.0 $mgml^{-1}$) were added individually until the solution showed the same(± 0.01) absorbance as that of pure triprolidine-HCl solution without the addition of the organic compound, under experimental conditions, as described in the general procedure. The value was calculated as the percentage of organic compound with respect to the amount of triprolidine-HCl.

Procedure for the determination of triprolidine-HCl in pharmaceautical preparations

Tablets containing 1.25, 1.5 and 2.5mg of triprolidine-HCl were powdered, weighed, dissolved in ethyl alcohol and filtered. The filtrate was diluted with distilled water to get a 1 mg/ml^{-1} solution of triprolidine-HCl. An aliquot containing 0.005 to 0.15 $mgml^{-1}$ was taken and the procedure was followed as described above and the absorbance was measured at 440 nm. The quantity per tablet was calculated from the standard calibration curve.

Syrup containing 0.25 $mgml^{-1}$ of triprolidine-HCl was weighed, dissolved in distilled water and filtered. If turbidity persisted, the contents were centrifuged until a clear supernatant was obtained. After filtration a 1.0 $mgml^{-1}$ solution of triprolidine-HCl was prepared. An aliquot containing 0.005 to 0.15 $mgml^{-1}$ was taken, the above procedure was followed and the absorbance was measured at 440 nm. The quantity of triprolidine-HCl per 5 ml of syrup was calculated from calibration curve.

Results and Discussion

Absorption spectrum of the coloured complex

Triprolidine-HCl reacts with dichloronitrobenzene when heated for 45s at 65°C in basic media to give an orange complex, the absorption spectra of which under optimum condition lies at 440 nm (Fig. 3).

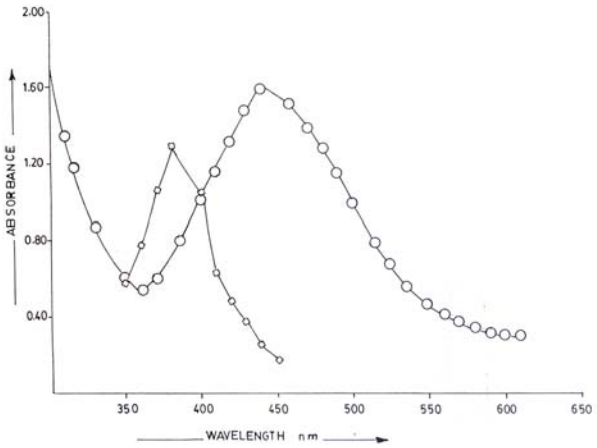

Fig. 3. ○ Absorption spectrum of triprolidine hydrochloride with 2, 4-dichloronitrobenzene.
□ Absorption spectrum of reagent blank.

Effect of colour producing reagent

Dichloronitrobenzene was used as a colour producing reagent. It was found that 2.2 mgml^{-1} of dichloronitrobenzene gave maximum colour (Fig. 4), above and below this concentration the colour intensity diminished and the colour became unstable. Effect of pH is shown in Fig. 5. Maxium colour intensity was obtained at pH 13.6. This pH was maintained by the addition of 1ml of 0.1N sodium hydroxide. The probable mechanism (Fig. 8) of the colour reaction is that on addition of sodium hydroxide, pyridine moiety is generated thus furnishing a pair of electrons for interaction with electron deficient dichloronitrobenzene. A charge transfer complex is formed having a $\ddot{e}_{max}$ at 440nm. Charge transfer complexes are formed by interaction between the basic N of antihistamine as electron donor and the electron acceptor in this case dichloronitrobenzene [18].

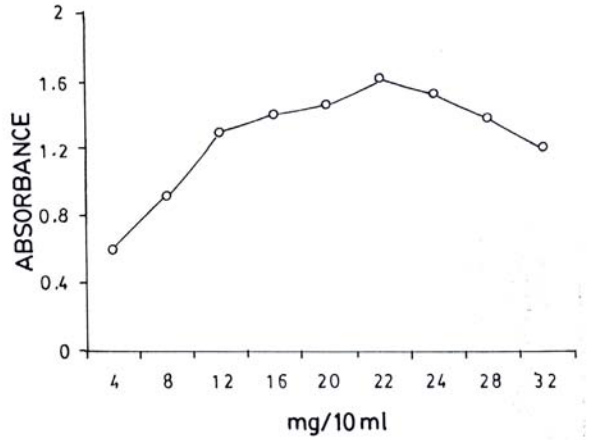

Fig. 4. Effect of reagent.

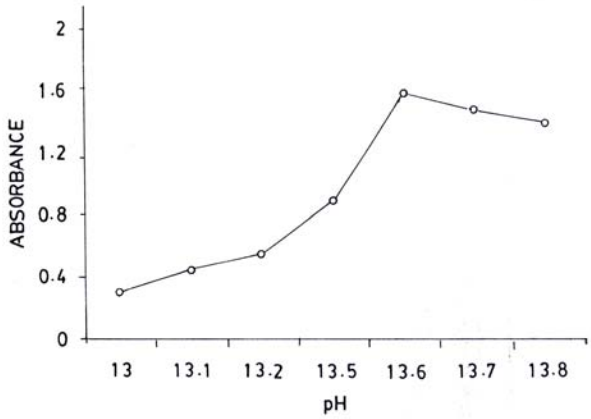

Fig. 5. Effect of pH.

Effect of temperature and heating time

The effect of temperature is shown in Fig. 6. With the rise of temperature the colour intensity increased and was stable at 65°C. The colour did not develop at room temperature. The absorbance of the developed colour was stable for more than 24 h. A water bath was used to carry out the temperature studies. The effect of heating time on colour intensity is shown in Fig. 7. It was found that heating for 45 s at 65°C gave maximum colour, above and below this time the colour intensity decreased and was unstable.

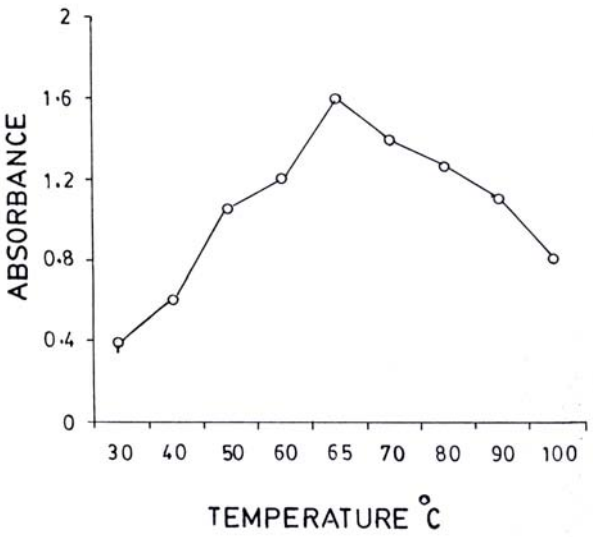

Fig. 6. Effect of temperature.

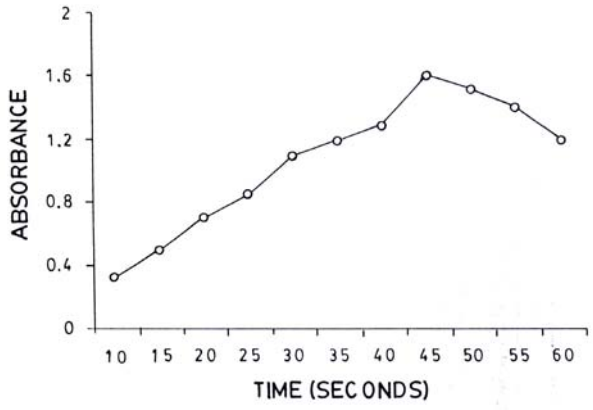

Fig. 7. Effect of heating time.

Effect of organic solvents

Different organic solvents such as choloroform, n-hexane, xylene, acetone, benzene, dichloro-methane, dioxane, formaldehyde and tetra hydrofuran, were tested for colour extraction and for stability, but none was effective and therefore no organic solvent was employed.

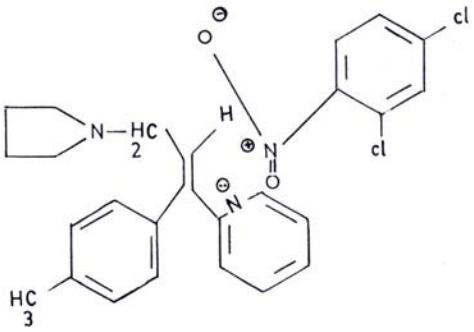

Fig. 8. Effect of pH.

Analytical Figures of Merit

The results for the determination of triprolidine-HCl are shown in Tables 1 and 2, which show the sensitivity, validity and repeatability of the method. It is also reasonably precise and accurate, as the amount taken from identical samples is known and the amount found by the above procedure does not exceed the relative standard deviation of 0.60% which is the replicate of five determinations (Table 1). The optimization has been done at lower analyte concentration. The calibration graph is linear in the range of 0.005 mg to 0.15mgml^{-1}. The apparent molar absorptivity calculated was 2.81 x 10^3 and the regression [19] was calculated by the method of least squares from ten points, each of which was the average of five determinations. The regression cofficient of determination (r^2) comes out to be 0.978.

Interferences

The quantitative assessment of tolerable amount of different organic compounds under the experimental conditions is given in Table.3. Various amounts of diverse interfering compounds were added to a fixed amount of triprolidine-HCl (Imgml^{-1}) and the recommended procedure for the spectrophotometric determination was followed. Other common interferences, like buscopan, zantac, septran, cimet,semidine and glucophage did not interfere.

Table 1.
Determination of triprolidine - HCl from pure solution.

Triprolidine-HCl taken mg/10ml	Triprolidine-HCl found *mg/10ml	Percentage Recovery
0.100	0.102 (± 0.60)	102.0
0.150	0.151 (± 0.58)	100.6
0.200	0.203 (± 0.50)	101.5
0.300	0.290 (± 0.39)	96.6
0.500	0.504 (± 0.31)	100.8
1.000	1.042 (± 0.10)	104.2
1.200	1.210 (± 0.08)	100.8
1.500	1.515 (± 0.06)	101.1

*Every reading is an average of five independent measurements

Table 2.
Optical characteristics precision and accuracy of the proposed method.

Parameters	Values
λ_{max} (nm)	440
Molar absorptivity (mol^{-1} cm^{-1})	0.2814x 10^4
Regression equation (Y)*	
Slope (b)	0.7676
Intercept (a)	0.0021
Regression coefficient of determination (r^2)	0.978
Relative standard deviation (RSD%)**	0.60 %
% Range of error (confidence limit) at 95% confidence level	1.25+ 0.0022 %

*Y = a + bC where C is the concentration of analyte (mg/10 ml) and Y is the absorbance unit.

**Calculated from five determinations.

Table 3.
Quantitative assessment of tolerable amount of other drugs.

Drugs	Maximum Amount Not Interfering* (%)
Aspirin	200
Marzine	100
Diclofenac sodium	100
Flubiprofen	100
Avil	150
Phenytoin sodium	150
Indomethacin	200
Propranolol-HCl	150
Metamizole sodium	100
Paracetamol	100
Ibuprofen	100
Buscopan	150
Bricanyl	100
Fluoxetine-HCl	100

*The value is the percentage of the drug with respect to 1mg/ 10ml of triprolidine-HCl that causes +0.01 change in absorbance.

Application

In conclusion, the proposed method has been successfully applied for the quality control of pure triprolidine-HCl and in the pharmaceutical dosage form (Table 4). The spectrophotometric method for the determination of Triprolidine-HCl is simple, reliable, sensitive and less time consuming. The statistical analysis is in good agreement with those of the official British Pharmacopeia 1988. The colour reaction is selective for Triprolidine-HCl. The method can be successfully applied to the micro determination of Triprolidine-HCl either in pure or in pharmraceutical preparations. The colour reaction has 0.005 $mgml^{-1}$ as visual limit of identification. The advantage of the present procedure is that it does not require many solvents whereas the HPLC procedures [7-9] are long, tedious and expensive, involving many reagents and solvents showing high RSD value i.e. 12% [9] and the colour stability varied

Table 4.
Determination of triprolidine-HCl from pharmaceutical preparations.

Drug	**Trade Name**	**Pharmaceutical preparations**	**Labeled (mg)**	**Amount found* (mg)**	**Amount Percentage recovery (%)**
Triprolidine – HCl	Actidil (Glaxo Wellcome Pharmaceutics, Karachi, Pakistan)	Tablet	2.5	2.52	100.6
Triprolidine – HCl	Actified P (Glaxo Glaxo Wellcome Pharmaceutics, Karachi, Pakistan)	Tablet	1.5	1.51	100.6
Triprolidine – HCl	Actified -DM (Glaxo Wellcome Pharmaceutics, Karachi, Pakistan)	Tablet	1.25	1.24	99.2
Triprolidine – HCl	Actidil (Glaxo Wellcome Pharmaceutics, Karachi, Pakistan) Elpomide (Elite Pharama, Pakistan)	Syrup	1.25 mg/ 5ml	1.246mg/ 5ml	99.6

* Every reading is an average of five determinations

from five to sixty minutes in the TLC procedure [3]. The literature indicates that this colour reaction has not been reported previously. The present method is precise, accurate and other compounds like buscopan, zantac, septran, cimet and semidine do not interfere. A significant advantage of a spectrophotometric determination is its application to the determination of individual compounds. This aspect of spectrophotometric analysis is of major interest in the analytical pharmacy, since it offers a distinct possibility of quality control in the assay of pharmaceutical dosage formulations.

References

1. **Swinyard, E.A.** 1985. Histamine and antihistamine. In: *Remington's Pharmaceutical Sciences*, 17th Edition; pp.1130 Mack Publishing Co. Pennsylvania ,USA.
2. **Reynolds, J.E.F.** 1982. Promethazine and other antihistamines. In: *Martindale: The Extra Pharmacopoeia*, 28th Edition, pp. 1294. The Pharmaceutical Press, London.
3. **Bhatia, M.S., Kaskhedikar, S.G. and Chaturvedi, S.C.** 2000. Chromatographic estimation of dextromethorphan hydrobromide, pseudoephedrine hydrochloride and triprolidine from multicomponent tablets. *Indian J. Pharm*. Sci. 62: 61-63.
4. **De Orsi, D., Gagliardi, L., Balasco, A. and Tonelli, D.** 1996. Simultaneous determination of triprolidine, pseudoephedrine, paracetamol and dextromethorphan by HPLC. *Chromatographia* 43:496-500.
5. **He, W., Parisis, N. and Kiratzidis, T.** 1998. Determination of benzodiazepines in forensic samples by HPLC with photodiode array detections. *J. Forensic Sci*. 43:1061-1067.
6. **Akhtar, M.J., Khan, S. and Hafiz, M.** 2002. High performance liquid chromatographic assay for the determination of paracetamol, pseudoephedrine hydrochloride and triprolidine hydrochloride. *J. Pharm. Bio Med. Anal*. 27:851-860.
7. **Nishikawa, M., Seno, H., Tshii, A., Suzuki, 0., Kumazawa, T., Watanabe, K. and Hattori, H.** 1997. Simple analysis of diphenylmethane antihistaminies and their analogs in body fluids by headspace solid phase micro extraction-capillary gas chromatography. *J. Chromatogr*. *Sci.* 35: 275-279.
8. **Altaria, K.D.**1999. Application of microemulsion electrokinetic chromatography to the analysis of a wide range of pharmaceuticals and excipients. *J. Chromatogr*. 844: 371-386.
9. **Hudson, J.C., Golin, M. and Malcolm, M.** 1995. Capillary zone electrophoresis in a comprehensive screen for basic drugs in whole blood. *J.Can. Soc. Forensic Sci*. 28:137-152.
10. **Sachan, A. and Trivedi, P.** 1999. Spectrophotometric determination of triprolidine hydrochloride and phenylpropanolamine hydrochloride. *East-Pharm*. 42:107-110.
11. **Gangway, S. and Trivedi, P.** 1999. Extractive Spectrophotometric determination of dextromethorphan hydrobromide and triprolidine hydrochloride in liquid dosage form. *Asian J. Chem*. 11:922-926.
12. **Mohasana, R., Kawathekar, N. and Chaturvedi, S. C.**1996. Simultaneous spectrophotometric estimation of triprolidine hydrochloride and pseudoephedrine hydrochloride in pharmaceutical dosage form. *Indian J. Pharm. Set*. 58: 93-95.
13. **Dine, E. and Onur, F.** 1998. Comparison of ratio spectra derivative spectrophotometry, derivative spectrophotometry and Vierordt's method applied to quantitative analysis of pseudoephedrine hydrochloride and triprolidine hydrochloride in tablets. *S.T.P. Pharma Sci*. 8:203-208.
14. **Taylor, E.W., Qian, M.G. and Dollinger, G.D.** 1998. Simultaneous online characterization of small organic molecules derived from combinational libraries for identity, quantity and purity by reversed phase HPLC with chemiluminescent nitrogen, UV and mass spectrometric detection. *Anal. Chem*. 70:3339-3347.
15. **Brzezinka, H., Dallakian, P. and Budzikiewicz, H.**1999. Thin-layer chromatography and mass spectrometry for screening of biological samples for drugs and metabolites. *J. Planar Chromatog. Mod. TLC* 12:96-108.
16. **Zayed, S.I.** 2004. New plastic membrane and carbon paste ion selective electrodes for the determination of triprolidine. *Anal. Sci*. 20:1043-1048.
17. **Metwally, F.H.** 2002. Kinetic spectrophotometric methods for the quantitation of triprolidine in bulk and in drug formulations. *Int. J. Pharm*. 232:131-137.
18. **Moon, H.S. and Baik, C. S.** 1989. Spectrophotometric determination of antihistamines by using iodine as electron acceptor. *Yakhar Hoechi* 33:141-148.
19. **Christian, G.D.** 2004. *Data handling and spread sheets in analytical chemistry.* 6th Edition, pp 102-106. John Wiley and Sons, New York.

Proc. Pakistan Acad. Sci. 42(4):261-264.2005

LANDAU LIFSHITZ ENERGY MOMENTUM PSEUDOTENSOR FOR METRICS WITH SPHERICAL SYMMETRY

J. H. Caltenco, J. I. López-Bonilla, R. Peña-Rivero and J. Rivera-Rebolledo

Sección de Estudios de Posgrado e Investigación, Escuela Superior de Ingeniería Mecánicay Eléctrica, Instituto Politécnico Nacional, Edif. Z-4, 3er Piso, Col. Lindavista, C.P. 07738 México, DF

Received September 2005, accepted November 2005

Communicated by Prof. Dr. Kamaluddin Ahmad

Abstract: We have calculated the Landau-Lifshitz pseudotensor for various spherically symmetric systems as preparation for a later study for the case of rotation, which may be of interest in astrophysics. The systems we considered are the static spherical star, the Schwarzschild geometry, the collapsing spherical dust ball of uniform density and the general pulsating or collapsing star.

Keywords: Landau-Lifshitz psudotensor, spherically symmetric systems, Schwarzschild geometry

Introduction

The point to point distribution of energy-momentum in the gravitational field is non-unique [1,2] in the theory of general relativity. This is inescapable because it is always possible to change coordinates to make the frame locally Lorentz at any chosen event. Gravitation must, however, make a contribution to the energy of a system since, for example, the mass of a star is less than the sum of the rest masses of its individual particles. In proving conservation laws of momentum and angular momentum for isolated systems, one can construct entities, which describe the energy-momentum content of the gravitational field. These entities are called energy-momentum pseudotensors [3-10]. The distribution of energy-momentum depends [1] on the choice of pseudotensor and on the choice of coordinates. Besides, the total momentum and angular momentum or the total energy radiated into the asymptotically flat space surrounding an isolated source also depends on the choice of pseudotensor or coordinates used in the calculation [11].

E-mail: jlopezb@ipm.mx

Einstein [12] was the first to introduce a pseudotensor, which is not symmetric and does not give a volume integral for the total angular momentum. In this work we have chosen the Landau-Lifshitz pseudotensor [2,13,14], which is symmetric and leads to volume integrals for momentum and angular momentum. Pseudotensors have been used [15,17] in studies of gravitational self-energy.

Landau-Lifshitz energy-momentum pseudotensor

The Landau-Lifshitz (LL) pseudotensor $t_{LL}^{\mu\nu}$ is defined by writing the Einstein equations in the form [2,13,14]:

$$H_{LL}^{\mu\alpha\nu\beta}{}_{,\alpha\beta} = 16\pi(-g)\left(T^{\mu\nu} + t_{LL}^{\mu\nu}\right) = 16\pi\, T_{LL\ eff}^{\mu\nu} \tag{1}$$

where

$$H_{LL}^{\mu\alpha\nu\beta} = q^{\mu\nu}\, q^{\alpha\beta} - q^{\alpha\nu}\, q^{\mu\beta} \quad , \quad q^{\mu\nu} = \sqrt{-g}\, g^{\mu\nu} \tag{2}$$

and

$$16\pi(-g)t_{LL}^{\alpha\beta} = q^{\alpha\beta}{}_{,\lambda}\, q^{\lambda\mu}{}_{,\mu} - q^{\alpha\lambda}{}_{,\lambda}\, q^{\beta\mu}{}_{,\mu} + \frac{1}{2} g^{\alpha\beta} g_{\lambda\mu} \cdot q^{\lambda\nu}{}_{,\rho}\, q^{\rho\mu}{}_{,\nu} - g_{\mu\nu} q^{\mu\rho}{}_{,\lambda} \cdot$$
$$\cdot \left(g^{\alpha\lambda} q^{\beta\nu}{}_{,\rho} + g^{\beta\lambda} q^{\alpha\nu}{}_{,\rho}\right) + g_{\lambda\mu} g^{\nu\rho} q^{\alpha\lambda}{}_{,\nu}\, q^{\beta\mu}{}_{,\rho} + \frac{1}{8}\left(2g^{\alpha\lambda} g^{\beta\mu} - g^{\alpha\beta} g^{\lambda\mu}\right) \cdot \tag{3}$$
$$\cdot \left(2g_{\nu\rho} g_{\sigma\tau} - g_{\rho\sigma} g_{\nu\tau}\right) q^{\nu\tau}{}_{,\lambda}\, q^{\rho\sigma}{}_{,\mu}$$

The conserved momentum and angular momentum of an isolated system are given by:

The conserved momentum and angular momentum of an isolated system are given by:

$$P^{\mu} = \int T_{LL\ \ eff}^{\mu 0}\ d^3x\,, \qquad (4)$$

$$J^{\mu\nu} = \int \left(x^{\mu} T_{LL\ \ eff}^{\nu 0} - x^{\nu} T_{LL\ \ eff}^{\mu 0}\right) d^3x\,,$$

with the conservation law $T_{LL\ eff}^{\mu\nu}{}_{,\nu} = 0$ In the expressions above, x^{μ} are asymptotically Minkowskian coordinates.

Some geometries with spherical symmetry

a) The metric for a spherically symmetric star is given by:

$$ds^2 = -e^{2\Phi} dt^2 + \left(1 - \frac{2m(r)}{r}\right)^{-1} dr^2 + r^2 d\Omega^2. \qquad (5)$$

We change coordinates t, r, θ, φ to t, x^1, x^2, x^3 where $r^2 = \left(x^1\right)^2 + \left(x^2\right)^2 + \left(x^3\right)^2$. In the new asymptotically Minkowskian coordinates the metric takes the form:

$$ds^2 = -e^{2\Phi} dt^2 + g_{ij}\, dx^i\ dx^j \qquad (6)$$

such that

$$g_{ij} = \frac{A}{r^2} x_i x_j + \delta_{ij} \quad , \quad A = \left(1 - \frac{2m(r)}{r}\right)^{-1} - 1 \qquad (7)$$

A short calculation yields the following result for the effective energy density:

$$-g\left(T^{00} + t_{LL}^{00}\right) = \frac{1}{8\pi r^2}(rA)_{,\,r} \qquad (8)$$

b) We consider next the Schwarzschild geometry with metric:

$$ds^2 = \frac{32M^3}{r} e^{-\frac{r}{2M}} \left(du^2 - dv^2\right) + r^2\, d\,\Omega^2 \qquad (9)$$

in Kruskal-Szekeres coordinates [2,18,19]; *r(u,v)* is the Schwarszchild radial coordinate.

The coordinate transformation:

$$\bar{u} = 2M\, Ln\left[(u+a)^2 - v^2\right] \quad , \quad \bar{v} = 4M \tanh^{-1}\frac{v}{u+a} \qquad (10)$$

which covers the region $(u+a) \rangle |v|$

where $a > 0$, puts the metric in the form

$$ds^2 = \frac{2M}{r} e^{-\frac{r}{2M}} \left[(u+a)^2 - v^2\right]\left(d\bar{u}^2 - d\bar{v}^2\right) + r^2\, d\,\Omega^2 \qquad (11)$$

The additional coordinate transformation from $\bar{v}, \bar{u}, \theta, \varphi$ to asymptotically Minkowskian coordinates $\bar{v}, x^1, x^2, x^3$

where $(\bar{u})^2 = \left(x^1\right)^2 + \left(x^2\right)^2 + \left(x^3\right)^2$, gives

$$ds^2 = -\frac{2M}{r} e^{-\frac{r}{2M}} \left[(u+a)^2 - v^2\right] d\bar{v}^2 + \left(A\delta_{ij} + \frac{B}{\bar{u}^2} x_i x_j\right) dx^i dx^j \qquad (12)$$

with $A = \frac{r^2}{\bar{u}^2}$ and $B = -g_{\bar{v}\bar{v}} - A$. The following expression is obtained for the LL energy density:

$$-g\, t_{LL}^{00} = \frac{1}{16\pi\bar{u}^2}\left[2(\bar{u}AB)_{,\bar{u}} - \left(\bar{u}\left(A^2\right)_{,\,\bar{u}}\right)_{,\,\bar{u}}\right] \qquad (13)$$

The space-like hypersurface $\bar{v} = constant$ includes the singularity at $r = 0$ when $\bar{v}$ is larger than a positive number which depends on *a*. The integral of $-g\, t_{LL}^{00}$ over any of these hypersurfaces gives *M*, as it should.

c) We now repeat the calculation for the case of the Schwarszchild metric in comoving coordinates.

This is appropriate to connect to an interior Friedman solution for the case of a collapsing ball of dust. In Novikov coordinates [20], the metric is written as:

$$ds^2 = -d\tau^2 + \left(\frac{R^{*2}+1}{R^{*2}}\right)\left(\frac{\partial r}{\partial R^*}\right)^2 dR^{*2} + r^2\, d\,\Omega^2 \qquad (14)$$

and in terms of the new radial variable $R = 2M\left(R^{*2} + 1\right)$:

$$ds^2 = -d\tau^2 + f(\tau, R) dR^2 + r^2(\tau, R) d\,\Omega^2 \qquad (15)$$

The new coordinates τ, x^1, x^2, x^3, where

$R^2 = (x^1)^2 + (x^2)^2 + (x^3)^2$ are asymptotically Minkowskian and thus (15) adopts the form:

$$ds^2 = -d\tau^2 + \left(A\delta_{ij} + \frac{B}{R^2} x_i x_j \right) dx^i\, dx^j \qquad (16)$$

being $A = \frac{r^2}{R^2}$ and $B = f - A$. Then the *LL* energy density, is given by a relation similar to (13):

$$-g\, t^{00}_{LL} = \frac{1}{16\pi R^2}\left[2(RAB)_{,R} - \left(R(A^2)_{,R}\right)_{,R}\right]. \qquad (17)$$

d) The collapsing uniform density ball of dust has an interior Friedman solution:

$$ds^2 = -d\tau^2 + a^2(\tau)\left[d\chi^2 + Sin^2\chi\, d\Omega^2\right], \qquad (18)$$

with $a(\tau) = \frac{1}{2} a_m (1 - Cos\,\eta)$ and

$\tau = \frac{1}{2} a_m (\eta + Sin\,\eta)$. This geometry connects at the surface χ_0 of the ball with the exterior Schwarzschild solution (15) using the radial coordinate $R = a_m Sin\,\chi$, then (18) implies:

$$ds^2 = -d\tau^2 + \left(\frac{a^2}{a_m^2 - R^2} \right) dR^2 + \frac{a^2 R^2}{a_m^2} d\Omega^2 \qquad (19)$$

We further change the coordinates τ, R, θ, φ to τ, x^1, x^2, x^3, where $R^2 = (x^1)^2 + (x^2)^2 + (x^3)^2$, then the new coordinates connect to the exterior asymptotically Minkowskian coordinates which were used in (16). Thus the *LL* effective energy density $-g\left(T^{00} + t^{00}_{LL}\right)$ is given by (17) with:

$$A = \frac{a^2}{a_m^2} \quad , \qquad B = \frac{a^2}{a_m^2 - R^2} \ . \qquad (20)$$

The interior contribution to the total energy *M* on a τ = constant hypersurface is

$$\frac{MR_0}{16(R_0 - 2M)} (1 + Cos\,\eta)^4 , \qquad (21)$$

where R_0 is the radial (comoving) coordinate of the surface of the ball. This contribution decreases and becomes zero when the dust hits the singularity at $a(\tau) = 0$ for $\tau = \frac{\pi}{2} a_m$. The exterior contribution to the total energy is *M* minus the value above for $\tau < \frac{\pi}{2} a_m$ and *M* for later times.

Finally, the *LL* effective energy density of any metric of the form (15) is given by expression (17) setting $A = \frac{r^2}{R^2}$ and $B = f - A$.

References

1. **Trautman, A.** 1962. Gravitation: an Introduction to Current Research. Ed. Witten, L. Wiley, New York.
2. **Misner, C.W., Thorne, K.S. and Wheeler, J.A.** 1973. *Gravitation*. *W.H.* Freeman, San Francisco, USA.
3. **Moeller, C.** 1958. On the localization of the energy of a physical system in the general theory of relativity. *Ann. Phys.* 4:347-371.
4. **Goldberg, J.N**. 1958. Conservation laws in general relativity. *Phys. Rev*. 111:315-320.
5. **Dirac, P.A.M**. 1975. *General theory of relativity*. John Wiley, New York.
6. **Stachel, J**. 1977. A variational principle living gravitational superpotentials, the affine connection, Riemann tensor and Einstein field equations. *Gen. Rel. Grav*. 8:705-715.
7. **Persides, S.** 1979. Energy and momentum in general relativity. *Gen. Rel. Grav*. 10:609-622.
8. **Palmer, T.N**. 1980. Gravitational energy-momentum: The Einstein pseudotensor reexamined. *Gen. Rel. Grav*. 12:149-154.
9. **Chang, C.C., Nester, J. and Chen, C.M.** 1999. Pseudotensors and quasilocal energy-momentum. *Phys. Rev. Lett.* 83:1897-1901.
10. **Babak, S.V. and Grishchuk, L.P**. 2000. The energy-momentum tensor for the gravitational field. *Phys. Rev*. D61:24-38.
11. **Horowitz, G.T. and Tod, K.P**. 1982. A relation between local and total energy in general relativity. *Commun. Math. Phys*. 85:429-447.
12. **Einstein, A.** 1916. Die grundlage der allegemeinen relativitätstheorie. *Ann. Der Physik* 49:769-822.
13. **Landau, L.D. and Lifshitz, E.M.** 1962. The Classical Theory of Fields. Addison-Wesley, Reading Mass.,

USA.

14. **Synge, J.L.** 1976. *Relativity: The general theory.* North-Holland Pub., Amsterdam.
15. **Einstein, A**. 1918. Der energiesatz in der allgemeinen relativitätstheorie. *Berliner Berichte* 349:448-459.
16. **Einstein, A. and Rosen, N.** 1935. The particle problem in the general theory of relativity. *Phys. Rev*. 48:73-77.
17. **Treder, H.J. and Yourgrau, W**. 1977. On self-gravitation. *Phys. Lett*. 64:25-28
18. **Kruskal, M.D**. 1960. Maximal extension of Schwarzschild metric. *Phys. Rev.* 119:1743-1745.
19. **Szekeres, G**. 1960. On the singularities of a Riemannian manifold. *Publ. Mat*. *Debrecen* 7:285-301.
20. **Zel´dovich, Ya., B. and Novikov, I.D.** 1974. *Relativistic Astrophysics*. Vol. I: Stars and Relativity. University Chicago Press, USA.

ON CERTAIN CLASS OF ANALYTIC FUNCTIONS

Nailah Abdul Rahman Al Dihan

Mathematics Department, Girls College of Education, P.O. Box 61410, Riyadh 11567, Saudi Arabia

Received February 2005, accepted September 2005

Communicated by Prof. Dr. Q. K. Ghori

Abstract: $P_k^{\alpha}[A,B]$ and $Q_{\alpha}^{k}[A,B]$ denote classes of functions analytic in the disc $E=\{z:|z|<1\}$ defined by a bounded radius rotation functions. In this paper we have obtained the distortion theorems, coefficients estimate, some radius problems, geometrical properties and studied convolution conditions.

***Keywords**:* Analytic, starlike, convex, positive real part function, bounded radius rotation, convolution

Introduction

Let A denote the class of analytic functions f(z) in $E=\{z:|z|<1\}$, given by

$$f(z)=z+\sum_{n=2}^{\infty}a_n z^n\ , \tag{1}$$

and let S, S* and C be classes of functions in A, which are respectively univalent, starlike and convex in the unit disc E.

Janowski [4] introduced the class $P[A,B]$ as follows:

Definition 1

An analytic function in E given by the form $P(z)=1+C_1Z_1+C_2Z^2+\ldots$ belongs to $P[A,B]$ if it satisfies the condition

$$p(z)=\frac{1+Aw(z)}{1+Bw(z)},\ -1\le B<A\le 1,$$

where, w(0)=0 and $|w(z)|\le 1$.P[1,-1]=P (the class of analytic function with positive real part satisfying Rep(z)>0).

E-Mail N_Al-Dihan@Hotmail.com

Definition 2

An analytic function in E given by (1) belongs to S*[A,B],-1≤B<A≤1, if and only if, $\frac{zf'(z)}{f(z)} \in P[A,B]$ and S*[1,-1]= S*. Also it is well known that an analytic function given by (1) belongs to C[A,B] , if and only if, $\frac{(zf'(z))'}{f'(z)} \in P[A,B]$ and C[1,-1]=C.

Definition 3

A function f∈A is close to convex denoted by K[A,B,C,D] if ∃ a starlike function g(z)∈S*[C,D] such that $\frac{zf'(z)}{g(z)} \in P[A,B]$ and K[1,-1,1.-1]=K (the well known close to convex class due to Kaplan).

Definition 4

Let $P_k(\alpha)$, $k \geq 2$ and 0<α≤1, be the class of functions p analytic in E and have the representation

$$p(z) = \frac{1}{2}\int_{-\pi}^{\pi} \frac{1+(1-2\alpha)ze^{-it}}{1-ze^{-it}} d\mu(t) \quad ,$$

where $\mu(t)$ is a function with bounded variation on $[-\pi,\pi]$ and satisfies the conditions $\int_{-\pi}^{\pi} d\mu(t) = 2$, $\int_{-\pi}^{\pi} |d\mu(t)| \leq k$. We note that $k \geq 2$ and $P_2(\alpha) = P[1-2\alpha,-1] = P(\alpha)$ are the class of analytic function with positive real part greater than α . It can easily be seen [5] that $p \in P_k(\alpha)$, if and only if, there exist two analytic functions $p_1, p_2 \in P(\alpha)$ such that

$$p(z) = \frac{k+2}{4} p_1(z) - \frac{k-2}{4} p_2(z)$$

Let $R_k(\alpha)$ denote a subclass of A of functions of bounded radius rotation of order α . Then f∈ $R_k(\alpha)$, if and only if,

$$\frac{zf'(z)}{f(z)} \in P_k(\alpha) \quad , \quad k \geq 2 \quad , \quad z \in E. \tag{2}$$

I t is clear that $R_2(\alpha)$ =S*(α).

Let f be given by (1) and g given by $g(z) = z + \sum_{n=2}^{\infty} a_n z^n \in$ A . Then the convolution f*g is

defined by (f∗g) (z) $= z + \sum_{n=2}^{\infty} a_n b_n z^n$.

Definition 5

Let f∈A. Then f belongs to $P_k^{\alpha}[A, B]$ if it satisfies the condition

$$\frac{f(z)}{g(z)} = \frac{1 + Aw(z)}{1 + Bw(z)},$$

where g ∈ $R_k(\alpha)$, $-1 \le B < A \le 1$, $w(z)$ is regular, w(0)=0 and w(z)≤1 and 0<α ≤1.

Definition 6

Let $Q_k^{\alpha}[A, B]$ denote the class of functions $F(z) = z^{-1} + c_0 + c_1 z + c_2 z^2 + \ldots$, which are regular in $0 < |z| < 1$ and satisfy the condition

$$\frac{F(z)}{G(z)} = \left[\frac{1 + Aw(z)}{1 + Bw(z)}\right]^{-1},$$

where $-1 \le B < A \le 1, w(z)$ is regular in $0 < |z| < 1$ and $G(z) = z^{-1} + d_0 + d_1 z + d_2 z^2 + \ldots$, is of bounded radius rotation of order α, i.e.

$$-\frac{zG'(z)}{G(z)} \in P_k(\alpha) \qquad , \qquad 0 < |z| < 1.$$

Distortion theorem for the class $P_k^{\alpha}[A, B]$

Theorem 1

If $f \in P_k^{\alpha}[A, B]$, then for $|z| = r$, $0 < r < 1$

$$\frac{1 - Ar}{1 - Br} \frac{(1 - r)^{(k-2)(1-\alpha)/2}}{(1 + r)^{(k+2)(1-\alpha)/2}} \le |f(z)| \le \frac{1 + Ar}{1 + Br} \frac{(1 + r)^{(k-2)(1-\alpha)/2}}{(1 - r)^{(k+2)(1-\alpha)/2}} \qquad \ldots \qquad (3)$$

This result is sharp.

Proof

Since $f \in P_k^{\alpha}[A, B]$, we have

$$\frac{f(z)}{g(z)} = \frac{1+Aw(z)}{1+Bw(z)} \quad , \quad -1 \le B < A \le 1 \quad .,$$

where g$\in$. $R_k(\alpha)$. By Schwarz's lemma, we have $|w(z)| \le |z|$.

If $p(z) = \frac{1+Aw(z)}{1+Bw(z)}$, $-1 \le B < A \le 1$, then it is well known [4] that p $\in$ P[A,B] and satisfies

$$\frac{1-Ar}{1-Br} \le |p(z)| \le \frac{1+Ar}{1+Br} \quad \ldots \quad (4)$$

Further if $g(z)$ is a function of bounded radius rotation of order α , then by [7]

$$\frac{(1-r)^{(k-2)(1-\alpha)/2}}{(1+r)^{(k+2)(1-\alpha)/2}} \le |g(z)| \le \frac{(1+r)^{(k-2)(1-\alpha)/2}}{(1-r)^{(k+2)(1-\alpha)/2}} \quad \ldots \quad (5)$$

equations (4),(5) together imply the inequality (3).

This result is sharp, if we take

$$p(z) = \frac{1+Az}{1+Bz} \text{ and } g(z) = \frac{(1+\theta_1 z)^{(k-2)(1-\alpha)/2}}{(1+\theta_2 z)^{(k+2)(1-\alpha)/2}} \quad , \quad |\theta_1| = |\theta_2| = 1 .$$

Remarks

1. On taking $k = 2$, we have a result of Ganesan [2].
2. On taking $k = 2$, $B = -\lambda\beta$ and $A = \beta$ with $w(z)$ replaced by $-w(z)$, we get the result of Goel and Sohi [3].

Coefficient estimates for the class $P_k^{\alpha}[A,B]$

To find the coefficient estimates for the class $P_k^{\alpha}[A,B]$, we need the following lemmas:

Lemma 1 [4]

Let $p \in P[A,B]$ and $p(z) = 1 + \sum_{n=1}^{\infty} c_n z^n$. Then $|c_n| \le A - B$.

Lemma 2

If $p \in P_k(\alpha)$, $p(z) = 1 + \sum_{n=1}^{\infty} c_n z^n$, then $|c_n| \le k(1-\alpha)$.

Proof

This can be easily seen using Lemma 1 and the relation

$$p(z)=\frac{k+2}{4}p_1(z)-\frac{k-2}{4}p_2(z)$$

with A= 1- 2α and B=-1.

Using Lemma 2, we can prove Lemma 3

Lemma 3

Let $g \in R_k(\alpha), g(z)=z+b_2z^2+b_3z^3+\ldots$. Then

$|b_2| \le k(1-\alpha)$ and $|b_3| \le \frac{k(1-\alpha)}{2}(k-k\alpha+1)$.

Proof

Let $g \in R_k(\alpha)$. Then $zg'(z)=P(z)g(z), P(z) \in P_k(\alpha)$. If $g(z)=z+b_2z^2+\ldots$ and $p(z)=1+c_1z+c_2z^2+\ldots$, then

$$z+2b_2z^2+3b_3z^3+\ldots=(z+b_2z^2+b_3z^3+\ldots)(1+c_1z+c_2z^2+\ldots)$$

Equating the coefficient of z^2 and z^3 on both sides and using Lemma1 and Lemma 2, we have

$$2b_2=c_1+b_2$$
$$|b_2|=|c_1| \le k(1-\alpha)$$

and $3b_3=b_3+c_1b_2+c_2$

$$|b_3|=\left|\frac{b_2c_1+c_2}{2}\right| \le \frac{k^2(1-\alpha)^2+k(1-\alpha)}{2}=\frac{k(1-\alpha)}{2}(k(1-\alpha)+1).$$

Theorem 2

Let $f \in P_k^{\alpha}[A,B]$, where $f(z)=z+\sum_{n=2}^{\infty}a_nz^n$. Then

$$|a_2| \le (1-\alpha)k+(A-B)$$

and

$$|a_3| \le (A-B)+k(1-\alpha)(A-B)+\frac{k(1-\alpha)}{2}(k-k\alpha+1)$$

These bounds are sharp.

Proof

Since $f \in P_k^{\alpha}[A,B]$, there exists a function $g \in R_k(\alpha)$ such that $f(z) = g(z)p(z)$, $p \in P[A,B]$.

If $g(z) = z + \sum_{n=2}^{\infty} b_n z^n$

and $p(z) = 1 + c_1 z + c_2 z^2 + \ldots,$

then

$$z + a_2 z^2 + a_3 z^3 + \ldots = (z + b_2 z^2 + b_3 z^3 + \ldots)(1 + c_1 z + c_2 z^2 + \ldots)$$

Equating the coefficient of z^2 and z^3 on both sides and using Lemma 1 and Lemma 3 we have

$$a_2 = b_2 + c_1$$
$$|a_2| = (1-\alpha)k + (A - B)$$

and $a_3 = c_2 + b_2 c_1 + b_3$

$$|a_3| \le (A - B) + k(1-\alpha)(A - B) + \frac{k(1-\alpha)}{2}(k - k\alpha + 1).$$

This result is sharp as can be seen by the function

$$f(z) = \frac{(1-z)^{(k-2)(1-\alpha)/2}}{(1+z)^{(k+2)(1-\alpha)/2}} \frac{1+Az}{1+Bz}.$$

Remarks

i. If $k = 2$, this result agrees with the result of Ganesan [2] and when $k = 2$, $A = \beta$, $B = -\lambda\beta$, these results correspond to the result of Goel and Sohi [3].

ii. If $B = 0$, we get $\frac{f(z)}{g(z)} = 1 + Aw(z)$ and if $k = 2$ in E, the inequality $|a_n| \le A(n-1) + n$, $n \ge 2$ with sharp bounds as discussed in [3] is also obtainable.

Argument of $\frac{f(z)}{z}$ when $f \in P_k^{\alpha}[A,B]$

To discuss the argument of the class $P_k^{\alpha}[A,B]$, we need the following Lemma:

Lemma 4

Let $f \in R_k(\alpha)$. Then

$$\left|\arg\frac{f(z)}{z}\right| \le k(1-\alpha)\sin^{-1} r .$$

Proof

It is well known that if $f \in R_k(\alpha)$, then there exist two functions $s_1, s_2 \in S^*(\alpha)$ such that

$$f(z) = \frac{(s_1(z))^{\frac{k+2}{4}}}{(s_2(z))^{\frac{k-2}{4}}} .$$

Thus
$$\left|\arg\frac{f(z)}{z}\right| = \left|\frac{k+2}{4}\arg\frac{s_2(z)}{z} - \frac{k-2}{4}\arg\frac{s_2(z)}{z}\right|$$
$$\le \frac{k+2}{4}\left|\arg\frac{s_2(z)}{z}\right| + \frac{k-2}{4}\left|\arg\frac{s_2(z)}{z}\right| .$$

It is known [8] that if $s \in S^*(\alpha)$, then

$$\left|\arg\frac{s(z)}{z}\right| \le 2(1-\alpha)\sin^{-1} r .$$

Hence
$$\left|\arg\frac{f(z)}{z}\right| \le k(1-\alpha)\sin^{-1} r .$$

Sharpness is satisfied for $f(z) = \dfrac{(1+\theta_1 z)^{(1-\alpha)\left(\frac{k-2}{2}\right)}}{(1+\theta_2 z)^{(1-\alpha)\left(\frac{k+2}{2}\right)}}$.

Lemma 5 [4]

Let $p \in P[A, B]$. Then

$$\left|\arg\frac{p(z)}{z}\right| \le \sin^{-1}\frac{(A-B)r}{1-ABr^2} .$$

Using Lemma 4 and Lemma 5, we can prove

Theorem 3

Let $f \in P_k^{\alpha}[A,B]$. Then

$$\left|\arg\frac{f(z)}{z}\right| \le k(1-\alpha)\sin^{-1} r + \sin^{-1}\frac{(A-B)r}{1-ABr^2}.$$

Proof

Since $f \in P_k^{\alpha}[A,B]$, therefore

$f(z) = g(z)p(z)$, $p(z) \in P[A,B]$ and $g \in R_k(\alpha)$. By Lemma 4, we have

$$\left|\arg\frac{g(z)}{z}\right| \le k(1-\alpha)\sin^{-1} r \qquad \ldots \qquad (6)$$

and by Lemma 5, we have

$$\left|\arg p(z)\right| \le \sin^{-1}\frac{(A-B)r}{1-ABr^2} \qquad \ldots \qquad (7)$$

Using (6) and (7), we have the result.

Sharpness follows by taking

$$\frac{f(z)}{g(z)} = \frac{1+A\theta_1 z}{1+B\theta_1 z} \quad , \quad |\theta_1| = 1 \qquad \ldots \qquad (8)$$

and

$$g(z) = \frac{(1+\theta_2 z)^{(1-\alpha)(k-2)/2}}{(1+\theta_2 z)^{(1-\alpha)(k+2)/2}} \quad , \quad |\theta_2| = 1.$$

Then

$$\arg\frac{f(z)}{g(z)} = \sin^{-1}\frac{(A-B)r}{1-ABr^2}$$

and

$$\arg\frac{g(z)}{z} = \arg(1+\theta_2 z)^{(1-\alpha)(k-2)/2} + \arg(1+\theta_2 z)^{(1-\alpha)(k+2)/2}$$

Using Lemma 4, we have

$$\arg\frac{g(z)}{z} = (1-\alpha)k\ \sin^{-1} r \qquad \ldots \qquad (9)$$

Using (8) and (9), we have that

$$\arg\frac{f(z)}{z} = (1-\alpha)k\ \sin^{-1} r + \sin^{-1}\frac{(A-B)r}{1-ABr^2}.$$

Remark

For $k = 2$ again this result agrees with the result in [2], and when $A = \beta > 0$, $B = -\lambda\beta$ and replacing $w(z)$ by $-w(z)$, we have the result of Goel and Sohi [3].

Some radius problems for $P_k^{\alpha}[A,B]$

Lemma 6 [1]

Let $p \in P[A,B]$. Then for $z \in E$

$$\mathrm{Re}\left\{\alpha p(z) + \beta\frac{zp'(z)}{p(z)}\right\} > \begin{cases} \dfrac{\alpha - [(A-B)\beta + 2\alpha A]r + \alpha A^2 r^2}{(1-Ar)(1-Br)} & \text{if} \quad R_1 < R_2, \\ \beta\dfrac{A+B}{A-B} + \dfrac{2}{(A-B)(1-r^2)}\left\{(L_1K_1)^{1/2} - \beta(1-ABr^2)\right\} & \text{if} \quad R_2 < R_1. \end{cases}$$

where

$$R_1 = \left(\frac{L_1}{K_1}\right)^{1/2},\ R_2 = \frac{1-Ar}{1-Br},\ L_1 = (1-A)(1+Ar^2) \text{ and } K_1 = (1-B)(1+Br^2)$$

This result is sharp.

.

Lemma 7 [7]

Let $g \in R_k(\alpha)$. Then

$$\mathrm{Re}\frac{zg'(z)}{g(z)} \geq \frac{1-k(1-\alpha)r + (1-2\alpha)r^2}{1-r^2}.$$

Further, since, $g \in R_k(\alpha)$ implies $\dfrac{zg'(z)}{g(z)} = f(z) \in P_k(\alpha)$, we have for all $f \in P_k(\alpha)$

$$\text{Re f (z)} \geq \frac{1-k(1-\alpha)r+(1-2\alpha)r^2}{1-r^2}.$$

Theorem 4

Let $f \in P_k^{\alpha}[A,B]$. Then

$$\text{Re}\frac{zf'(z)}{f(z)} \geq \begin{cases} M_1(r) & for \quad R_1 \leq R_2 \\ M_2(r) & for \quad R_2 \leq R_1 \end{cases},$$

where

$$M_1(r) = \frac{1-k(1-\alpha)r+(1-2\alpha)r^2}{1-r^2} - \frac{(A-B)r}{(1-Ar)(1-Br)},$$

$$M_2(r) = \frac{1-k(1-\alpha)r+(1-2\alpha)r^2}{1-r^2} + \frac{A+B}{A-B} + \frac{2}{(1-r^2)(A-B)}\left[(L_1K_1)^{\frac{1}{2}1} - (1-ABr^2)\right]$$

and $R_1, R_2, L_1 and K_1$ are defined in Lemma 6 .

Proof

Since $f \in P_k^{\alpha}[A,B]$, there exists a function $g \in R_k(\alpha)$ such that

$$\frac{f(z)}{g(z)} = P(z) \in P[A,B]$$

Using logarithmic differentiation, we obtain

$$\frac{zf'(z)}{f(z)} = \frac{zg'(z)}{g(z)} + \frac{zp'(z)}{p(z)}$$

and

$$\text{Re}\frac{zf'(z)}{f(z)} \geq \min \text{Re}\frac{zg'(z)}{g(z)} + \min \text{Re}\frac{zp'(z)}{p(z)}.$$

Using Lemma 6 with $\alpha = 0$, $\beta = 1$ and Lemma 7, we have the result.

Sharpness of the bounds follow if we choose $g_i(z)(i=1,2)$, of bounded radius rotation of order α such that

Case 1: If $R_1 \le R_2$, we take $P_1(z) = \dfrac{1+Az}{1+Bz}$, and $\dfrac{zg_1'(z)}{g_1(z)} = \dfrac{1+(1-\alpha)z+(1-2\alpha)z^2}{1-r^2}$.

Then $\dfrac{zP_1'(z)}{P_1(z)} = \dfrac{(A-B)z}{(1+Az)(1+Bz)}$ .Thus at z= -r, $\mathrm{Re}\dfrac{zP_1'(z)}{P_1(z)} = \dfrac{-(A-B)r}{(1-Ar)(1-Br)}$.

Case 2: If $R_2 \le R_1$, we take $p_2(z) = \dfrac{f_2(z)}{g_2(z)} = \dfrac{1+Aw_1(z)}{1+Bw_1(z)}$ and

$\dfrac{zg'(z)}{g(z)} = \dfrac{1+k(1-\alpha)w_1(z)+(1-2\alpha)w_1^{\,2}}{1-w^2(z)}$ with $w_1(z) = \dfrac{z(z-c_1z)}{(1-c_1z)}$, where c_1 defined by the condition

$\mathrm{Re}\left[\dfrac{1+Aw_1(z)}{1+Bw_1(z)}\right] = R_1$ at z=-r.

Now $\dfrac{zp_2'(z)}{p_2(z)} = \dfrac{(A-B)zw_1'(z)}{(1+Aw_1(z))(1+Bw_1(z))}$.

In fact from the inequalities $R_2 \le R_1 \le c+p$, where $c = \dfrac{1-ABr^2}{1-B^2r^2}$, $p = \dfrac{(A-B)r}{1-B^2r^2}$ and we have $\dfrac{1-Ar}{1-Br} \le \dfrac{1+AT}{1+BT} \le \dfrac{1+Ar}{1+Br}, T = w_1(-r)$.

Hence $|T| \le r$ and $T^2 \le r^2$ which yields

$$\frac{r^2(r+c_1)^2}{(1+rc_1)^2} \le r^2 \quad . \text{ Thus } |c_1| \le 1$$

Further $|zw_1'(z) - w_1(z)| = \dfrac{|z|^2 - |w(z)|^2}{1-|z|^2}$, for $w_1(z) = \dfrac{z(z-c_1)}{(1-c_1z)}, |c_1| \le 1$.

$w_1(-r) = T = \dfrac{1-R_1}{BR_1 - A} = \dfrac{r(r-c_1)}{(1+c^2{}_1)}$.

Hence $c_1 = \dfrac{r^2-T}{r(T-1)}$ *and* $\dfrac{r^2-T^2}{(1-r^2)} = \dfrac{r^2(1-q^2)}{(1+qr)^2}$ and $[zw_1'(z) - w_1(z)]_{z=1r} = \dfrac{r^2-T^2}{(1-r^2)}$.

Now $\operatorname{Re}\left[\frac{zp_2'(z)}{p_2(z)}\right] = \frac{(A-B)}{(1-AT)(1-BT)}\left\{T - \frac{r^2-T^2}{1-r^2}\right\}$

Using $T = \frac{1-R_1}{BR_1 - A}$ with $R_1 = \sqrt{\frac{(1-A)(1+Ar^2)}{(1-B)(1+Br^2)}}$ (see [1]),

and simplifying, we have $\operatorname{Re}\left[\frac{zp_2'(z)}{p_2(z)}\right]_{z=-r} = \frac{A+B}{A-B} + \frac{2}{(1-r^2)(A-B)}\left\{(L_1K_1)^{\frac{1}{2}} - (1-ABr^2)\right\}$,

where $L_1 = (1-A)(1+Ar^2), K_1 = (1-B)(1+Br^2)$, (see[1]).

Thus the equality in our theorem holds at z=-r for

$f_1(z) = \frac{1+Az}{1+Bz} g_1(z), if R_1 \le R_2$

and for $f_2(z) = \frac{1+Aw_1(z)}{1+Bw_1(z)} g_2(z), if R_2 \le R_1$, where $g_1(z), g_2(z) \in R_k(\alpha)$.

Theorem 5

If $f \in P_k^{\alpha}[A,B]$, then f is starlike in

$$|z| < \begin{cases} r_1 & for \quad R_1 \le R_2 \\ r_2 & for \quad R_2 \le R_1 \end{cases},$$

where R_1 and R_2 are defined as in Lemma 6 and r_1, r_2 are respectively the positive roots of the following two equations

$$(1-k(1-\alpha)r + (1-2\alpha)r^2)(1-Ar)(1-Br) - (A-B)r(1-r^2) = 0$$

$$(1-k(1-\alpha)r + (1-2\alpha)r^2)(A-B) + (1-r^2)(A+B) + 2\left[(L_1K_1)^{1/2} - (1-ABr^2)\right] = 0 \quad ,$$

where K_1 and L_1 are defined in Lemma 6. This result is sharp.

Proof

It follows from Theorem 4 that if $f \in P_k^{\alpha}[A,B]$, then $\operatorname{Re}\frac{zf'(z)}{f(z)} \ge M_1(r), if R_1 \le R_2$ and

$\operatorname{Re}\frac{zf'(z)}{f(z)} \geq M_2(r), if R_2 \leq R_1$. Then

$$\operatorname{Re}\frac{zf'(z)}{f(z)} \geq \frac{(1-k(1-\alpha)r+(1-2\alpha)r^2)(1-Ar)(1-Br)-(A-B)r(1-r^2)}{(1-r^2)(1-Ar)(1-Br)} > 0, forall|z| < r_1$$

If $R_1 \leq R_2$ and

$$\operatorname{Re}\frac{zf'(z)}{f(z)} \geq \frac{(1-k(1-\alpha)r+(1-2\alpha)r^2)(A-B)+(1-r^2)(A+B)+2\left[(L_1K_1)^{\frac{1}{2}}-(1-ABr^2)\right]}{(1-r^2)(A-B)} > 0.$$ for all, if $R_2 \leq R_1$.

For special cases see [2] and [3].

Lemma 8

Let $g_1(z)$ and $g_2(z) \in R_k(\alpha)$. Then $G(z) = (g_1(z))^{\rho}(g_2(z))^{\gamma} z^{1-(\rho+\gamma)}$ belongs to $R_k(\alpha_1)$ where $\alpha_1 = 1-(1-\alpha)(\rho+\gamma)$.

Proof

A logarithmic differentiation yields

$$\frac{zG'(z)}{G(z)} = \rho\frac{zg_1'(z)}{g_1(z)} + \gamma\frac{zg_2'(z)}{zg_2(z)} + (1-(\rho+\gamma))$$

$$= \rho K_1(z) + \gamma K_2(z) + (1-(\rho+\gamma))$$

where $K_1 and K_2 \in P_k(\alpha)$. From the definition of $P_k(\alpha)$, there exists $h_i, i = 1,2,3,4 \in P(\alpha)$ such that

$$\frac{zG'(z)}{G(z)} = \rho\left[\frac{k+2}{4}h_1(z) - \frac{k-2}{4}h_2(z)\right] + \gamma\left[\frac{k+2}{4}h_3(z) - \frac{k-2}{4}h_4(z)\right] + (1-(\rho+\gamma))$$

It is well known that if $h \in P(\alpha)$, then h(z) can be written as

$$h(z) = (1-\alpha)p(z) + \alpha, where \operatorname{Re} p(z) > 0$$

and

$$\frac{zG'(z)}{G(z)} = \rho\left[\frac{k+2}{4}[(1-\alpha)p_1(z)+\alpha]\right] - \rho\frac{k-2}{4}[(1-\alpha)p_2+\alpha] + \gamma\frac{k+2}{4}[(1-\alpha)p_3+\alpha] - \gamma\frac{k-2}{4}[(1-\alpha)p_4+\alpha] + (1-(\rho+\gamma)). \quad (10)$$

Since the class P is a convex set, then

$$\frac{\rho p_1(z)+\gamma p_3(z)}{\rho+\gamma} = H_1(z) \text{ and } \frac{\rho p_2(z)+\gamma p_4(z)}{\rho+\gamma} = H_2(z),$$

where $\operatorname{Re} H_I(z) > 0, i = 1,2.$ Hence(10) can be written as

$$\frac{zG'(z)}{G(z)} = \frac{k+2}{4}[(1-\alpha)(\rho+\gamma)H_1(z) + [1-(1-\alpha)(\rho+\gamma)]] - \frac{k-2}{4}[(1-\alpha)(\rho+\gamma)H_2(z) + [1-(1-\alpha)(\rho+\gamma)]]$$
$$= \frac{k+2}{4}T_1(z) + \frac{k-2}{4}T_2(z), T_1, T_2 \in P(\alpha_1) \text{ and } \alpha_1 = 1-(1-\alpha)(\rho+\gamma)$$

This shows that $G \in R_k(\alpha_1)$.

Theorem 6

Let $f_1, f_2 \in P_k^{\alpha}[A,B]$. Then

$$F(z) = (f_1(z))^{\rho}(f_2(z))^{\gamma} z^{1-(\rho+\gamma)}$$

belongs to $P_k^{\alpha_1}[A,B]$, where $\alpha_1 = 1-(1-\alpha)(\rho+\gamma)$.

Proof

Let G (z) be given by $G(z) = (g_1(z))^{\rho}(g_2(z))^{\gamma} z^{1-(\rho+\gamma)}$. Then

$$\frac{F(z)}{G(z)} = \left(\frac{f_1(z)}{g_1(z)}\right)^{\rho}\left(\frac{f_2(z)}{g_2(z)}\right)^{\gamma}$$
$$= (h_1(z))^{\rho}(h_2(z))^{\gamma} \quad , \quad (\rho+\gamma) \le 1,$$

where $h_1, h_2 \in P[A,B]$.

Hence $F \in P_k^{\alpha_1}[A,B]$, $\alpha_1 = 1-(1-\alpha)(\rho+\gamma)$.

.

Some geometrical properties

In this part we shall investigate the behavior of $\arg f(z)$ at a point $w(\theta) = F(re^{i\theta})$ to the image Γ_r of the circle $Cr = \{z : |z| = r\}$, $0 \le r < 1$ and where θ is any number of the interval $(0, 2\pi)$ under the mapping by means of function f from the class $p_k^{\alpha}[A,B]$. We have

Theorem 7

If $F \in P_k^{\alpha}[A,B]$ and $0 \le r < 1$, then for $\theta_2 < \theta_1, \theta_1, \theta_2 \in [0, 2\pi]$

$$\arg f(re^{i\theta_2}) - \arg f(re^{i\theta_1}) = \int_{\theta_1}^{\theta_2} \mathrm{Re}\left[\frac{re^{i\theta} f'(re^{i\theta})}{(re^{i\theta})}\right]$$

$$\ge -\pi + \{1-(1-\alpha)k + (1-2\alpha)\}(\theta_2 - \theta_1) + 2arcC\,\mathrm{os}\frac{A-B}{1-AB}$$

where -1≤B<A≤1 and 0<α≤1 .

Proof

If $f \in P_k^{\alpha}[A,B]$, then $\frac{f(z)}{g(z)} = p(z)$, where $p \in P[A,B]$.

Thus

$$\mathrm{Re}\,\frac{zf'(z)}{f(z)} = \mathrm{Re}\,\frac{zg'(z)}{g(z)} + \mathrm{Re}\,\frac{zp'(z)}{p(z)} \qquad \ldots \qquad (11)$$

Let $z = re^{i\theta}$, $0 < r < 1$, $\theta \in [0, 2\pi]$. Integrating (11) with respect to θ in the interval $l[\theta_1, \theta_2]$, $\theta_1 < \theta_2$, we have

$$\int_{\theta_1}^{\theta_2} \mathrm{Re}\frac{re^{i\theta} f'(re^{i\theta})}{f(re^{i\theta})} d\theta = \arg f(re^{i\theta_2}) - \arg f(re^{i\theta_1})$$

$$= \int_{\theta_1}^{\theta_2} \mathrm{Re}\frac{re^{i\theta} g'(re^{i\theta})}{g(re^{i\theta})} d\theta + \int_{\theta_1}^{\theta_2} \mathrm{Re}\frac{re^{i\theta} p'(re^{i\theta})}{p(re^{i\theta})} d\theta$$

Since $f \in R_k(\alpha)$, it follows that

$$\min_{g \in R_k(\alpha)} \int_{\theta_1}^{\theta_2} \mathrm{Re}\frac{re^{i\theta} g'(re^{i\theta})}{g(re^{i\theta})} d\theta \ge \frac{1-k(1-\alpha)r + (1-2\alpha)r^2}{1-r^2}(\theta_2 - \theta_1), \quad \text{See [7].}$$

Now in the second integral, we observe that

$$\frac{\partial}{\partial\theta}\arg p(re^{i\theta}) = \frac{\partial}{\partial\theta}\mathrm{Re}\left\{-i\,\ln p(re^{i\theta})\right\} = \mathrm{Re}\frac{re^{i\theta}p'(re^{i\theta})}{p(re^{i\theta})}.$$

Consequently

$$\int_{\theta_1}^{\theta_2}\mathrm{Re}\left[\frac{re^{i\theta}p'(re^{i\theta})}{p(re^{i\theta})}\right]d\theta = \arg p(re^{i\theta_2}) - \arg p(re^{i\theta_1})$$

and

$$\max_{p\in P[A,B]}\left|\int_{\theta_1}^{\theta_2}\mathrm{Re}\frac{re^{i\theta}p'(re^{i\theta})}{p(re^{i\theta})}d\theta\right| \le \max_{p\in P[A,B]}\left|\arg p(re^{i\theta_2}) - \arg p(re^{i\theta_1})\right|$$

Using Lemma 5, we have

$$\max_{p\in P[A,B]}\arg p(re^{i\theta}) = \sin^{-1}\frac{(A-B)r}{1-ABr^2}$$

$$\max_{p\in P[A,B]}\left|\int_{\theta_1}^{\theta_2}\mathrm{Re}\frac{re^{i\theta}p'(re^{i\theta})}{p(re^{i\theta})}d\theta\right| \le \max_{p\in P[A,B]}\left|\arg p(re^{i\theta})\right| - \min_{p\in P[A,B]}\left|\arg p(re^{i\theta})\right|$$

$$\le 2\sin^{-1}\frac{(A-B)r}{1-ABr}$$

$$= \pi - 2\cos^{-1}\frac{(A-B)r}{1-ABr}$$

Hence

$$\arg f(re^{i\theta_2}) - \arg f(re^{i\theta_1}) \ge -\pi + 2Cos^{-1}\frac{(A-B)r}{1-ABr^2} + \frac{1-k(1-\alpha)r+(1-2\alpha)r^2}{1-r^2}(\theta_2-\theta_1).$$

The value of the right side is depending on the value of r and it takes its smallest value at $r=1$. Thereby we obtain the required result.

A convolution conditions for $p_k^{\alpha}[A,B]$

In 1973, Rushweyh and Sheil-Small [9] proved the polya-Schoenberg conjecture, namely, if f is convex or starlike or close to convex and ϕ is convex then $f * \phi$ belongs to the same class. In the following we shall prove the analogue of this conjecture for the class $p_k^{\alpha}[A,B]$ and give some of its applications. We need the following lemma with simple modification.

Lemma 9 [6]

Let f $\in R_k(\alpha)$. Then G = $f * \phi \in R_k(\alpha)$ where ϕ is convex in E

Theorem 8

Let $F \in P_k^{\alpha}[A,B]$ and ϕ is convex. Then $F * \phi \in P_k^{\alpha}[A,B]$.

Proof:

Let F$\in P_k^{\alpha}[A,B]$. Then F (z)=P(z) g(z) , where g belongs to $R_k(\alpha)$ and P(z)$\in$P[A,B]. It follows from the Lemma 9 that g$\star\varphi \in R_k(\alpha)$ .Then $\frac{F*\phi}{g*\phi} \in P[A,B]$.

Remark

As an application of Theorem 8, we have the following

(1) The family $P_k^{\alpha}[A,B]$ is invariant under the following operators.

$$F_1(f) = \int_0^z \frac{f(\xi)}{\xi} d\xi = (f * \phi_1)(z)$$

$$F_2(f) = \frac{2}{z}\int_0^z f(\xi) d\xi = (f * \phi_2)(z)$$

$$F_3(f) = \int_0^z \frac{f(\zeta) - f(x\zeta)}{\zeta - x\zeta} d\zeta \quad , \quad |x| \le 1 \quad , \quad x \ne 1$$

$$= (f * \phi_3)(z)$$

$$F_4(f) = \frac{1+c}{c}\int_0^z \xi^{c-1} f(\xi) d\xi \quad , \quad \mathrm{Re}\, c > 0$$

where $F(f_i(z)) = (f * \phi_i)(z)$ and $\phi_i (i = 1,2,3,4)$ are convex univalent functions which satisfy

$$\phi_1(z) = \sum_{n=1}^{\infty} \frac{1}{n} z^n = -\log(1-z),$$

$$\phi_2(z) = \sum_{n=1}^{\infty} \frac{2}{n+1} z^n = \frac{-2[z + \log(1-z)]}{z},$$

$$\phi_3(z) = \sum_{n=1}^{\infty} \frac{1-x^n}{n(1-x)} z^n = \frac{1}{1-x}\log\frac{1-xz}{1-z} \quad , |x| \le 1, x \ne 1,$$

$$\phi_4(z) = \sum_{n=1}^{\infty} \frac{1+c}{n+c} z^n \quad , \mathrm{Re}\, c > 0.$$

Now let $D_\lambda F(z) = (1-\lambda)F(z) + \lambda z F'(z) = (\psi_\lambda * F)(z)$ .....(12)

where λ>0 and let $\psi_\lambda(z) = \dfrac{z[1-(1-\lambda z)]}{1-z^2}$. Then $\psi_\lambda(z)$ is convex if

$$|z| = r_\lambda = \frac{1}{2\lambda + \sqrt{4\lambda^2 - 2\lambda + 1}} \qquad \ldots \qquad (13)$$

Thus, we have

(2) Let $F(z) \in P_k^\alpha[A,B]$. Then $D_\lambda F(z) = \psi_\lambda * F$ belongs to the same class for $|z| < r_\lambda$, where r_λ is given by (13).

Now let $\mu(F) = zF'(z)$. This differential operator can be written as $\mu(F) = \phi * F$,

where

$$\phi(z) = \sum_{n=1}^{\infty} nz^n = \frac{z}{1-z^2} \qquad \ldots \qquad (14)$$

It can be easily verified that the radius of convexity of ϕ is given by $r_c(\phi) = 2-\sqrt{3}$. This fact together with Theorem 8 yields

(3) If $f \in P_k^\alpha[A,B]$ then $\phi * f \in P_k^\alpha[A,B]$ where ϕ is given by (14) if $|z| = r_c < 2-\sqrt{3}$.

Radius of starlikeness for the class $Q_k^\alpha[A,B]$

Now we generalize the result of Goel and Sohi [3] and Ganesen [2] for the class $Q_k^{\alpha}[A,B]$. The following lemma can be easily derived.

Lemma 9

Let $s_i, i = 1,2$ be given by $s_1(z) = z^{-1} + c_\circ + c_1 z + c_2 z^2 + \ldots$ and $s_2(z) = z^{-1} + d_\circ + d_1 z + d_2 z^2 + \ldots$, and let $s_i, i = 1,2$ satisfy $-\mathrm{Re}\dfrac{zs_i'(z)}{s_i(z)} > \alpha$. If $G(z) = z^{-1} + b_\circ + b_1 z + b_2 z^2 + \ldots$ such that

$$G(z) = \frac{(s_1(z))^{\frac{k+2}{4}}}{(s_2(z))^{\frac{k-2}{4}}} \qquad \ldots \qquad (15)$$

then

$$-\frac{zG'(z)}{G(z)} \in P_k(\alpha) \ .$$

Proof

Differentiating (15) logarithmically yields

$$\frac{zG'(z)}{G(z)} = \frac{k+2}{4}\frac{zs_1'(z)}{s_1(z)} - \frac{k-2}{4}\frac{zs_2'(z)}{s_2(z)} \ .$$

This implies that

$$-\frac{zG'(z)}{G(z)} = \frac{k+2}{4}\left(-\frac{zs_1'(z)}{s_1(z)}\right) - \frac{k-2}{4}\left(-\frac{zs_2'(z)}{s_2(z)}\right)$$

or $$-\frac{zG'(z)}{G(z)} = \frac{k+2}{4}p_1(z) - \frac{k-2}{4}p_2(z) \ ,$$

where $\operatorname{Re} p_i(z) > \alpha \ , i = 1, 2$ and $-\frac{zG'(z)}{G(z)} \in P_k(\alpha)$.

Theorem 9

If $F \in Q_k^{\alpha}[A, B]$, then for $|z| = r < 1$

$$-\operatorname{Re}\frac{zF'(z)}{F(z)} \geq \begin{cases} \{M_1(r), \ for R_1 \leq R_2 \\ M_2(r), \ for R_2 \leq R_1 \end{cases} ,$$

where

$$M_1(r) = \frac{1 - k(1-\alpha)r + (1-2\alpha)r^2}{1-r^2} - \frac{(A-B)r}{(1-Ar)(1-Br)},$$

$$M_2(r) = \frac{1 - k(1-\alpha)r + (1-2\alpha)r^2}{1-r^2} + \frac{A+B}{A-B} + \frac{2}{(1-r^2)(A-B)}\left[(L_1K_1)^{\frac{1}{2}1} - (1-ABr^2)\right]$$

and $R_1, R_2, L_1 and K_1$ are defined in Lemma 6 .

Proof

Since $F \in Q_k^{\alpha}[A, B]$, therefore

$$p(z)=\left[\frac{F(z)}{G(z)}\right]^{-1}=\frac{1+Aw(z)}{1+Bw(z)}\text{ , where } -1\le B<A\le 1 \qquad \ldots \qquad (16)$$

$w(z)$ is analytic in E and satisfies $w(0)=0$, $|w(z)|<1$,

Differentiating (16) logarithmically, we have

$$\frac{zp'(z)}{p(z)}=-\frac{zF'(z)}{F(z)}+\frac{zG'(z)}{G(z)}$$

or $$-\frac{zF'(z)}{F(z)}=-\frac{zG'(z)}{G(z)}+\frac{zp'(z)}{p(z)} \ .$$

Using Lemma 6, we have

$$-\mathrm{Re}\frac{zF'(z)}{F(z)}\ge-\mathrm{Re}\frac{zG'(z)}{G(z)}-\frac{(A-B)r}{(1-Ar)(1-Br)} \quad if \quad R_1\le R_2$$

$$\ge-\mathrm{Re}\frac{zG'(z)}{G(z)}+\frac{(A+B)}{(A-B)}+\frac{2\left[(L_1K_1)^{1/2}-(1-ABr^2)\right]}{(A-B)(1-r^2)}$$

and since G is of bounded radius rotation of order α , using Lemma 7 we have

$$\mathrm{Re}-\frac{zG'(z)}{G(z)}\ge\frac{1-(1-\alpha)kr+(1-2\alpha)r^2}{1-r^2},|z|<r \qquad \ldots \qquad (17)$$

Using (17), we have the required result. The bounds are sharp. This can be seen by choosing $G_1(z)$ of bounded radius variation of order α such that

$$-\frac{zG'(z)}{G(z)}\ge\frac{1-(1-\alpha)kz+(1-2\alpha)z^2}{1-z^2} \quad if \quad R_1\ge R_2,$$

$$-\frac{zG'(z)}{G(z)}\ge\frac{1-(1-\alpha)kw_1(z)+(1-2\alpha)w_1^2(z)}{1-w_1^2(z)} \quad if \quad R_2\ge R_1$$

and take $F_1(z)$ such that it satisfies

$$p_1(z)=\left[\frac{F_1(z)}{G_1(z)}\right]^{-1}=\frac{1+Az}{1+Bz} \quad if \quad R_1\le R_2$$

$$= \frac{1 + A w_1(z)}{1 + B w_1(z)} \quad if \quad R_2 \le R_1 ,$$

where $w_1(z) = \dfrac{z(1 - c_1 z)}{1 - c_1 z}$ with $|c_1| \le 1$. Proceeding in the same way as in proving the sharpness of Theorem 4, we can prove that this result is sharp.

Theorem 10

If $F \in Q_k^{\alpha}[A, B]$, then F is starlike for $|z| = r_i < 1$,i=1,2

i. $0 < |z| < r_1 \quad for \quad R_1 \le R_2$
ii. $0 < |z| < r_2 \quad for \quad R_2 \le R_1$

where r_1 and r_2 are the smallest positive roots of the following equations respectively

$$\left[1 - k(1-\alpha)r + (1-2\alpha)r^2\right](1 - Ar)(1 - Br) - (A - B)r(1 - r^2) = 0$$

$$\left[1 - k(1-\alpha)r + (1-2\alpha)r^2\right](A - B) + (1 - r^2)(A + B) + 2\left[(L_1 K_1)^{1/2} - (1 - ABr^2)\right] = 0$$

Proof

Using Theorem 9, we have

$\text{Re} - \dfrac{zF'(z)}{F(z)} \ge M(r)_1, when R_1 \le R_2$ and $\text{Re} - \dfrac{zF'(z)}{F(Z)} \ge M_2(r) when R_2 \ge R_1$. Hence

$\text{Re}\dfrac{zF'(z)}{F(z)} > 0$ For $|z| < r_i, i = 1,2$, and this gives a sufficient condition for any function F to be starlike. Proceeding in the same way as in Theorem 5, we obtain the required result.

Acknowledgements

The author is grateful to the referee for his valuable comments and suggestions.

References

1. **Anh, A. and Tuan, P.** 1979. On β -convexity of certain starlike functions. *Rev. Roum. Math. Pures Appl.* 25:1413-24.
2. **Ganesan, M.** 1982. On certain classes of analytic functions. *Indian J. Pure Appl. Math*. 13:47-57.
3. **Goel, R . and Sohi, N.** 1980. On certain analytic functions. *Indian J. Pure Appl. Math*. 11:1308-1324.

4. **Janowski, W**. 1973. Some external problems for certain families of analytic functions I. *Ann. Polon. Math*. 18:298-326.
5. **Noor, K**. 1992. On subclasses of close to convex functions of higher order. *Inter. J. Math. Math. Sci.* 6:79-290.
6. **Noor, K**. 1996. On some subclasses of functions with bounded radius and bounded boundary rotation. *PanAmer. Math. J*. 6:75-81.
7. **Padmanabhan, K. and Paravatham, R**. 1975. Properties of a class of functions with bounded boundary rotation. *Ann. Polon. Math* .31:311-323.
8. **Pinchuk, B** .1968. On starlike and convex functions of order α. *Duke Math. J*. 35:721-34.
9. **Rusheweyh, S. and Sheil-Small, T**. 1973. Hadamard products of Schlicht functions and the polya-Schoenberg conjecture. *Comment. Math. Helv*. 48:119-135.

Proc. Pakistan Acad. Sci. 42(4):287-295.2005

SEISMIC HAZARD ASSESSMENT OF NW HIMALYAN FOLD AND THRUST BELT, PAKISTAN, USING PROBABILISTIC APPROACH

[1]MonaLisa, [1]Azam A. Khwaja, [2]M. Javed, [2]Yawer S. Ansari and [1]M.Qasim Jan

[1]Quaid-i-Azam University, Islamabad (45320), Pakistan and [2]National Engineering Services, Pakistan

Received November 2005, accepted November 2005

Communicated by Prof. Dr. M. Qasim Jan

Abstract: Seismic Hazard Assessment (SHA) of the entire seismically active NW Himalayan Fold and Thrust Belt Pakistan that incorporates probabilistic approach was carried out. Additional information in the form of earthquake catalogue, delineation of 40 active faults in a structural map, their relationship to the seismicity, establishment of seismotectonic zones was also undertaken and is represented in the form of a map. Distribution of 813 events within study area indicates that seismicity (≥4.0 M_w) appears to be associated with both the surface and blind faults. At the same time, clustering of events in specific parts along the surface faults shows that some fault segments, especially in the hinterland zone are more active. In parts of the active deformational front like Salt Range, southern Potwar and Bannu, lesser seismic activity (≥4.0 M_w) could be due to the damping effect of the thick Precambrian salt. Considering a number of geological and seismological factors, four seismotectonic zones were established. The b value for the Peshawar-Hazara Seismic Zone (PHSZ) is 1.16 followed by 1.12 for the Surghar-Kurram Seismic Zone (SKSZ). The other two, Swat-Astor Seismic Zone (SASZ) and Kohat-Potwar-Salt Range (KPSZ) have identical values of 0.95, thereby indicating occurrence of more events of relatively higher magnitude as compared to the other two seismic zones. Mean activity rate of earthquakes (λ) ranges from 4.26 to 1.73. In decreasing order, the values are 4.26, 2.62, 2.07 and 1.73 for PHSZ, SASZ, KPSZ and SKSZ, respectively. Using 4 regression relationships, the maximum potential magnitude (m_1) has been determined for the 40 Quaternary faults. In each seismic zone, the highest value within the seismic zone represents its m_1. The results show that m_1 is 7.8 in the hinterland (SASZ and PHSZ) and 7.4 in the foreland part (KPSZ and SKSZ). SHA incorporating probabilistic approach was undertaken at 10 sites (Astore, Bannu, Kaghan, Kohat, Mangla, Malakand, Muzaffarabad, Peshawar, Talagang and Islamabad). In the Probabilistic seismic hazard assessment (PSHA), the peak ground acceleration (PGA) values with 10% probability of exceedance in the 50 years i.e. the return period of 475 have been determined using the EZ-FRISK (6.2 beta version) software. Best-estimated seismic hazard parameters (λ, m_1, m_0 and the β value) of the four seismic zones were used as the input parameters. The results were generated in the form of total hazard curves. Values obtained range from 0.08g (for Bannu) to 0.21g (for Malakand and Kohat). For the other sites these are: Astore (0.082g), Kaghan (0.12g), Muzaffarabad (0.13g), Islamabad and Peshawar (0.15g), Talagang (0.16g) and Mangla (0.18g). High population density and more poorly constructed structures in Rawalpindi (twin city of Islamabad) and Peshawar make them even more hazardous. In addition, disaggregation at the assigned amplitude of 0.2g was also carried out for the ten sites.

Keywords: NW Himalayan Fold and Thrust Belt Pakistan, Seismic Hazard Assessment, probabilistic approach, seismic zones, peak ground acceleration, seismicity pattern

Introduction

The NW Himalayan Fold-and-Thrust, Pakistan, which forms the northwestern portion of the Himalayan frontal arc, is seismically one of the most active intercontinental regions anywhere in the world. The Himalayan mountain ranges have been formed due to the continental collision between the Indo-Pak and Eurasian plates. Between 1897 and 1952 there was a phase of very high seismicity when 14 major earthquakes (M≥7.5) occurred, including 5 great earthquakes of M≥8. The study area, which

forms the northern and northeastern portions of Pakistan, has recently been activated on 1st and 20th November 2002 (Bunji Earthquakes), and 14th February 2004 (Batgram Earthquake) with two devastating earthquakes of magnitudes ≥5.5 $M_{w.}$ At the same time the most of the country consists of non-engineered structures, which are a constant threat to lives and property. It is not the purpose of present study to device a new building code, but to provide information in the form of seismic zonation and seismic hazard assessment (SHA) of the area that may prove useful in revision of such a code and help to mitigate earthquake disaster in the study area. For this purpose a total of ten sites i.e. Astor, Bannu, Islamabad, Kaghan, Kohat, Mangla, Malakand, Muzaffarabad, Peshawar and Talagang have been selected and Seismic Hazard Assessment (SHA) has been carried out using probabilistic approach.

The present work is based on the available historic and instrumental data along with geological and tectonic information. The results that are in the form of peak ground acceleration (PGA) curves are based on the statistical behaviour. Therefore, representing the first ever comprehensive study of the area, the results ought to be used with some caution. Notwithstanding, this work serves as a good starting point for further study.

Tectonic Setting of the Area

The active fold and thrust belt along the northwestern margin of the Indo-Pakistan plate is divisible into two parts—the Sulaiman belt and the NW Himalayan fold and thrust belt. The former is believed to be along a zone of transpression, whereas the latter is associated with the main zone of Himalayan convergence [1]. Transpression is considered to be the result of the 80 to 900 km long Chaman and Ornach-Nal Fault Zones [2] and forms the western plate boundary. In the Himalayan zone of convergence (Fig.1), the Main Karakoram Thrust (MKT, also known as the Shyok Suture Zone), Main Mantle Thrust (MMT, also known as the Indus Suture Zone), Main Boundary Thrust (MBT) and the Salt Range Thrust (SRT) delineate the major subdivisions of the collision zone [3,4].

From the above-mentioned major tectonic subdivisions of the Himalayan zone of convergence, the area between the MMT and SRT with its westward extensions (Surghar, Marwat, Bhittani and Manzai ranges) is referred to as the NW Himalayan Fold and Thrust Belt [5]. According to Gee [6] and later workers, the southern sides of these ranges are also marked by thrusts. The tectonic domains of Hazara-Kashmir Syntaxis and the Nanga Parbat Haramosh Massif comprise its eastern boundary. The western limit is not clearly defined. Besides the Kurram Fault in the southwestern portion, a series of thrusts beyond the borders of Pakistan (e.g. the Sarobi Fault in Afghanistan) are considered to delineate this boundary.

In this nearly 250 km wide and 560 km long fold and thrust belt, the Panjal-Khairabad fault (Fig.1) divides it into a northern hinterland zone and the southern foreland zone. The hinterland zone is also referred to as the Hazara Crystalline Zone [7] and Himalayan Crystalline Zone [8]. In the hinterland zone, which lies between the Main Mantle Thrust (MMT) and Panjal Khairabad Fault, mostly crystalline rocks occur, represented by Proterozoic to Mesozoic metamorphic and igneous rocks. Shearing and imbrication has resulted in a complex deformation pattern. The basement is also involved in thrusting. Treloar *et al*. [9] identified six nappe zones (Mohmand-Swat nappe, Besham nappe, Hazara nappe, Banna nappe, Kaghan nappe and Nanga Parbat-Haramosh massif) separated from each other by prominent shears and thrust faults. Besides the nappe zones, in the lower part of the hinterland zone, south of the Mansehra Thrust (and its probable extension, the Balakot shear zone) and Mohmand-Swat nappe zone the area mostly contains metasediments of Precambrian age. Kazmi and Jan [5] refer to this portion of the hinterland zone as the Khyber-Lower Hazara Meta-sedimentary Fold and Thrust Belt. A subdivision of this Metasedimentary belt is called the Peshawar

Basin (Fig. 1). This intermontane basin is believed to have formed during the Middle Tertiary due to south-verging imbricate thrusting on the MBT [10]. According to Hussain and Yeats [10], steep dips in unlithified Quaternary sediments, suggests that deformation involves both folding and faulting, and that the basement is affected by the high angle faults.

In the foreland zone, between the Panjal-Khairabad Fault and the Salt Range Thrust along with its westward extension, a thick sequence (upto about 8 km thick) of sedimentary rocks ranging in age from Upper Proterozoic to Cenozoic overlie the older crystalline basement rocks [11]. This foreland zone comprises many thrust sheets (decollement zones) with a southward translation of up to 100 Km.

Many workers [5,7,11] have classified this part of the study area into different units based on various geological factors. Following the classification of Kazmi and Jan [5], the foreland zone on the basis of deformation style is divisible in to the Salt Range and Kohat-Potwar fold belt, Kurram-Cherat-Margalla fold and thrust belt and the Hazara-Kashmir Syntaxis.

In this part of Pakistan (NW Himalayan fold and thrust belt), recent work of some workers [12, 13,14] as well as the present study suggests that transpression (strike slip faulting) is also operative in

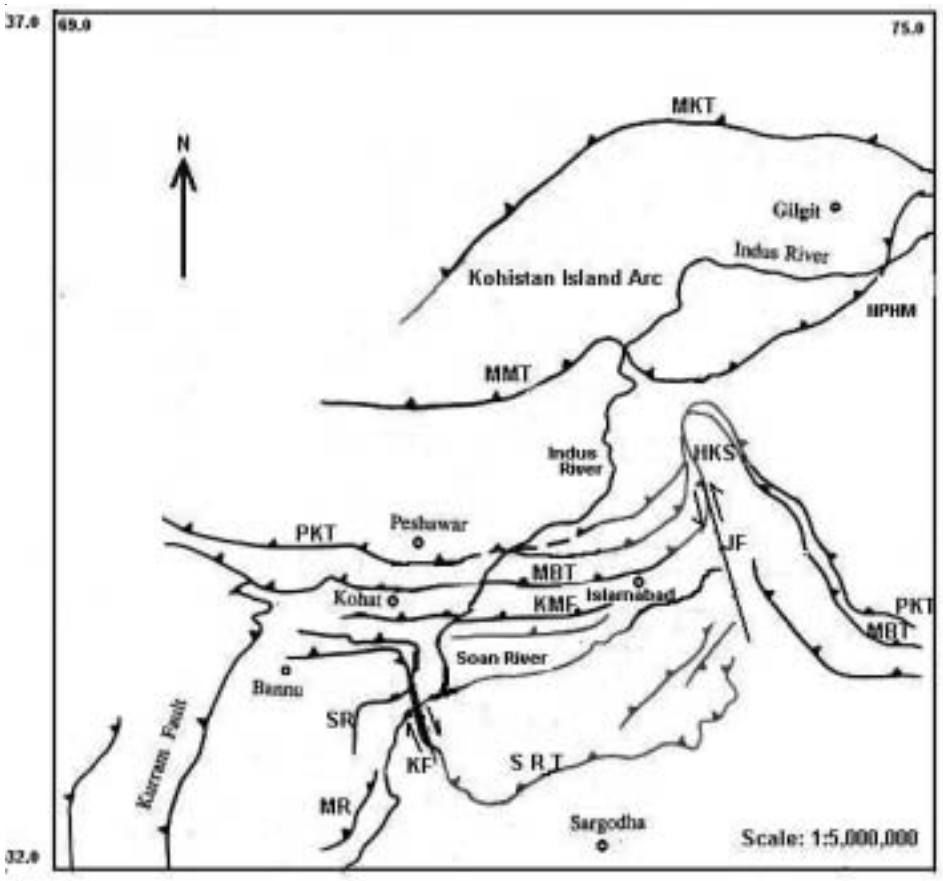

Figure 1. Structural and tectonic map of the study area and adjoining regions. Here MBT=Main Boundary Thrust. MKT=Main Karakoram Thrust. MMT= Main Mantle Thrust. PKT= Panjal Khairabad Thrust. KMF= Khair-I-Murat Fault. SR= Surghar Range. SRT= Salt Range Thrust. JF= Jhelum Fault. HKS= Hazara Kashmir Syntaxis. NPHM=Nanga Parbat Haramosh massif.

this compressional regime.

Quaternary Faults

It is commonly accepted that the recurrence interval of many earthquakes associated with faults is so large that considering only the instrumental (and/or historical) seismicity for evaluating seismic potential of a fault may not be a reliable indicator. At the same time, workers dealing with neotectonics consider all faults that may have been active during the last 10,000 to 12,000 years (i.e. during the Holocene) to be active faults. Thus, the prevailing practice in seismic hazard evaluation is to consider all Holocene faulting to be a part of the active fault system of the area i.e. having the potential of generating earthquakes in the future also.

The structural map (Fig. 2) prepared in the present work shows the 40 major active faults identified by different workers from within the study area. All these forty faults are considered to be seismically active with capability of causing significant damage.

Seismicity of the Area

Pakistan and adjoining countries experience high frequency of earthquakes, which in some cases have resulted in great loss of life and destruction. In Pakistan, besides the two active fold and thrust belts (Sulaiman and NW Himalayan Fold and Thrust Belt), high zones of seismicity exist in other parts of the country also. Available information [5] indicates that the Makran coastal earthquake of 1945 having a magnitude of m_b 8.3 was the severest earthquake to affect Pakistan. This event created a number of offshore islands along the Makran coastline. In the vicinity of the study area, the 1905 Kangra earthquake (in India) of m_b 8.4 activated the MBT, a major fault that extends into the study area also. More recently, Pattan (1974), Rawalpindi (1977), Bunji (2002) and Batgram (2004) earthquakes badly affected the study area.

In the present work, preparation of a composite earthquake catalogue has been undertaken by including all available earthquake data. This catalogue lists a total of 813 earthquakes in chronological order for the period of 1904-2002. The events in this composite catalogue occurred between latitude 32^0-$35^0 30'$N and longitudes 70^0-$75^0 15'$E and have moment magnitude (M_w) ≥ 4.0. Some further information about the catalogue preparation is provided below.

A report was made available by Pakistan Meteorological Department of the Mangla Joint Venture that was submitted to Pakistan Water and Power Development Authority in 2002 and revised in 2003. It includes a composite catalogue containing 631 earthquakes of ≥ 4.0 M_w between latitude 31^0-$35^0 30'$N and longitudes 70^0-76^0E for the period of 1904-2002. This catalogue has been prepared by Prof. N.N. Ambraseys of Imperial College, London. In our view this composite catalogue is the most reliable as it was prepared by incorporating data from the previous catalogues [15,16] and many other local as well international sources. The epicentral locations given in the catalogue for events prior to 1964 are the same as those determined by [16]. For later events, locations and depths recomputed by [17] were adopted. In the case of magnitude, a single scale i.e. moment magnitude (M_w) was adopted by using the relationships of Ambraseys and Bommer [18].

This catalogue contains 182 additional events to those 631 events catalogued by Prof. Ambraseys. The Tarbela, Mangla and microseismic network of Pakistan Atomic Energy Commission (PAEC) provided data for these events. Hypo71 and Hypo inverse softwares were used to compute epicentral locations and depths. For earthquake events from 2000 onwards, PAEC used the SEISAN software [19]. The local observatory data of Tarbela and Mangla has an error of less than 2.5km for location and depths; whereas the data of PAEC has an error of 2 to 5km. This data, for moment magnitude, was converted by using the relationships of Ambraseys

and Bommer [18] given above. This has helped to create uniformity in the catalogue.

In the seismicity map (attached map and prepared using the above mentioned data), there are areas such as the Salt Range, Southern Potwar near Talagang and the Bannu Basin with little or no epicentral distribution. One reason is that in spite of general agreement of Salt Range and southern Potwar being a part of an active deformational front, only low magnitude levels (≤ 4.0 m_b) have been recorded as previously observed by Seeber and Armbruster [20] and Quittmeyer *et al.* [16]; whereas in the seismicity map only events having magnitude ≥4 have been plotted. Another reason may be the presence of a thick sequence of EoCambrian salt in the Salt Range and Potwar area that may be having a damping effect. Further, the lithologies occurring in the Salt Range/Potwar are believed to be extending into the Bannu Basin also [11] thereby implying the presence of salt in this part also.

Seismotectonic Zonation

For any seismic hazard assessment to be carried out, seismotectonic zonation is considered to be an essential prerequisite. In order to establish the seismotectonic zones a number of factors related to seismological characteristics, geology and geophysics of the region of interest are taken into consideration. According to Udias [21], the characteristics of the occurrence of earthquakes in relation to regional tectonics and general geodynamic conditions form part of seismotectonic studies. This includes geographic distribution of epicentres, magnitude, depth, focal mechanism solutions and their correspondence to various types of faults, stress orientations and kinematic aspects of tectonics. In the present work using all these parameters, a seismotectonic map has been compiled (Fig. 2). Information related to the tectonics, seismological characteristics that aid in establishing the seismic zones have been provided in the previous sections. In this section a brief account of the previous work regarding zonation, their seismological characteristics and statistical analysis dealing with seismic hazard parameters is described.

Workers from the Columbia University [20, 22] based on microseismicity data from the Tarbela Observatory recognized three seismic zones (Indus Kohistan Seismic Zone, Hazara Lower Seismic Zone and Tarbela Seismic Zone) in parts of the study area. Quittmeyer *et al.* [16] divided the whole of Pakistan into 15 seismotectonic provinces out of which 5 covered the study area. Of these 5 zones, excepting one (namely the Hazara region), the others (Sulaiman Range; Gardez, Kunar and Safed Koh Fault Zone; Salt Range and the Himalayas) only partly cover the study area. Their division is based on the interpretation of the regional tectonic evolution and patterns of seismicity (including magnitude).

From amongst the unpublished reports, the report of the Mangla Joint Venture (2001) and subsequent reports of the Mangla Observatory contain 6 seismotectonic zones (MBT, Riasi, Hazara, Potwar, Salt Range and Punjab Seismic Zones) for this part of Pakistan. From these 6 zones, Riasi only partly covers the study area whereas the Punjab Seismic Zone lies beyond the southern boundary. Also, parts of the study area such as the Kohat and adjacent regions in the west and those located in the northern portion are not covered. These zones (area sources) were considered to be homogenous in their tectonic and seismic characteristics.

Presently Formulated Seismotectonic Zonation

Initially in the present study, the tectonic subdivisions of Kazmi and Jan [5] were taken to be representing the seismotectonic zonation of the study area also. The problem in adopting such an approach has been lack of sufficient earthquake events in most of these subdivisions for undertaking statistical analysis leading to high statistical uncertainty.

Considering the geological and seismological information provided in the previous sections, the following four seismotectonic zones have been

established (Fig. 2): Swat-Astor Seismic Zone (SASZ), Peshawar-Hazara Seismic Zone (PHSZ), the Kohat-Potwar-Salt Range Seismic Zone (KPSZ) and the Surghar-Kurram Seismic Zone (SKSZ). These zones contain several tectonic features (faults) within them.

Overall, they are a combination of the tectonic subdivisions of Kazmi and Jan [5] in which nearly similar subdivisions like their different crystalline nappe zones and HKS have been grouped into the Swat-Astore Seismic Zone. However, each seismic zone if compared with each other differs in their lithological/stratigraphic/structural/tectonic characteristics. At the same time, there are differences in their seismicity behaviour and in other statistically dependent seismic parameters. Further, as performance of statistical analysis is a prerequisite in any seismic hazard assessment, the seismic zones should contain sufficient number of events for carrying out such an analysis. In the present case, the best estimated seismic hazard parameters i.e. λ, m_1 and the β parameter for every seismic zone were determined for use in seismic hazard assessment. The results are summarized in Tables 2-5 (see Fig.2). The symbol β although not discussed previously is a substitute for the b value, where $\beta = b \ln 10$. The threshold magnitude (m_0) is taken as 4.0 and the focal depth given for each zone is the average for all instrumentally recorded earthquakes of that particular zone.

Evaluation of Peak Ground Accelerations (PGA) Using the Probabilistic Approach

Commonly there are two approaches are used for the determination of seismic hazard assessment (SHA) i.e. Deterministic Seismic Hazard Assessment (DSHA) and Probabilistic Seismic Hazard Assessment (PSHA). The DSHA is comparatively simple and does not account for the uncertainties and probability of occurrence of an earthquake. The PSHA is denoted by the probability that ground motion (acceleration) reaches certain amplitudes or seismic intensities exceeding a particular value within a specified time interval. Inverse of the probability of exceedance is known as the return period for that acceleration and is used to define the seismic hazard. In probabilistic hazard evaluation, the seismic activity of seismic sources (line or area) is specified by a recurrence relationship, defining the cumulative number of events per year versus their magnitude. Distribution of earthquakes is assumed to be uniform within the source zone and independent of time [23]. Seismic hazard calculated for different sites can be used to generate maps or curves (hazard curves) with intensities or ground accelerations expected with a given probability for a specified interval of time. In the present work, four seismic zones were established and their PSHA was carried out.

On the basis of the seismic hazard parameters evaluated in the preceding section, PSHA was carried out on ten sites i.e. Astor, Bannu, Islamabad, Kaghan, Kohat, Mangla, Malakand, Muzaffarabad, Peshawar and Talagang selected for this purpose using the EZ-FRISK software. Further information about the specific contributory parameters was obtained by applying disaggregation (deaggregation).

Generally, it is recommended that high quality accelerograms data be used in the relationships. However, this type of data is lacking or limited in quantity for most regions of the world. In such areas where an attenuation relationship is yet to be established, one or more than one relationship derived for other regions, preferably with similar or nearly similar tectonics is used. Criteria for selection of an appropriate attenuation relationship are available [24]. Similar situation of lack of a relationship also exists in Pakistan. According to [25], the first accellerographs were installed in 1990. Insufficient data have been generated so far. This strong motion data has previously been incorporated by Ambraseys and Bommer [26] and Ambraseys [24] in their database for the derivation of attenuation equation in Europe. It formed only a small portion (3%) of their database.

Bommer [25] in his detailed work on

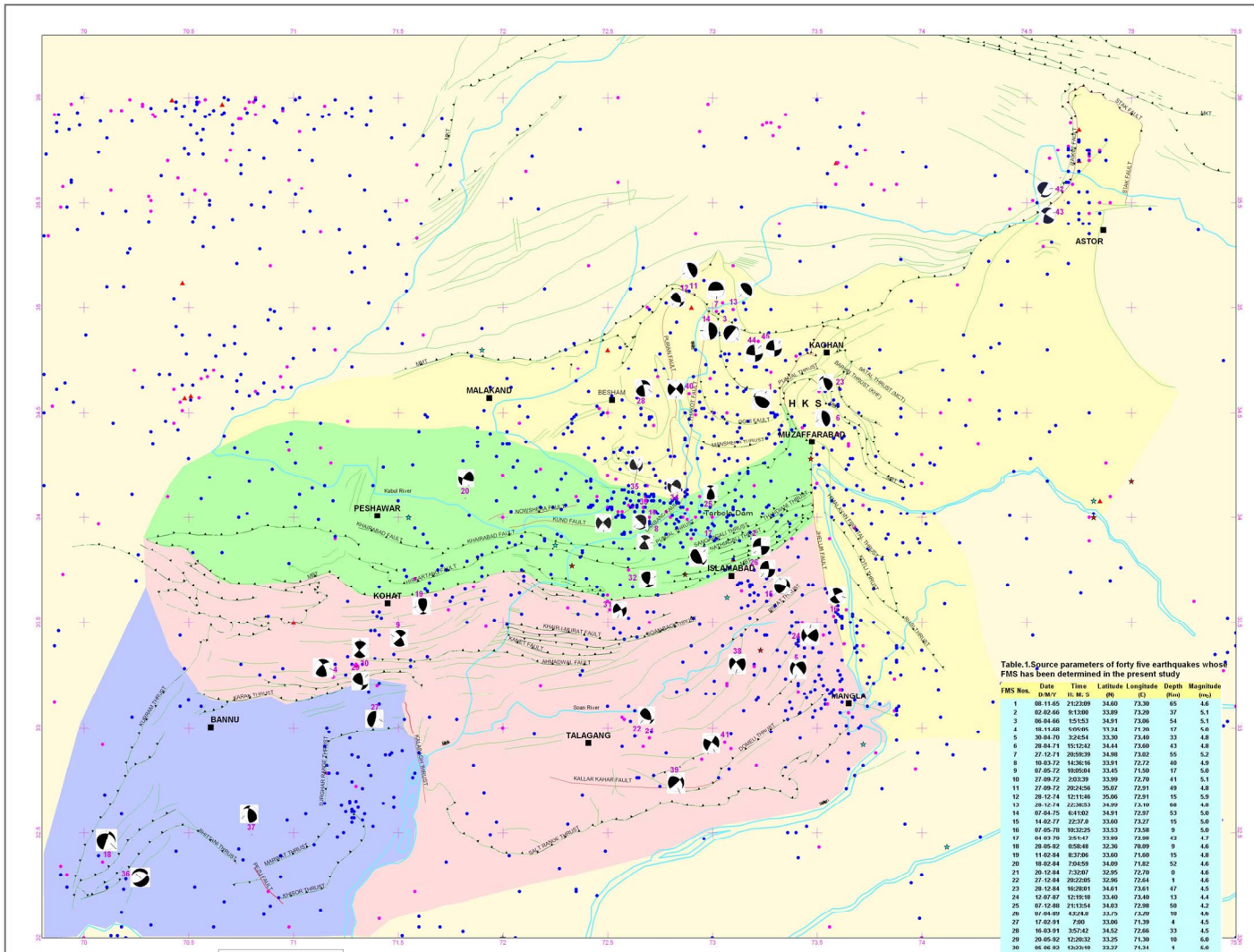

FIG 2
SEISMOTECTONIC MAP OF NW HIMALAYAN FOLD AND THRUST BELT

Mona Lisa, Azam A. Khawaja, M. Javed, Yawer S. Ansari and M. Qasim Jan (2006)

1:1000000

50 0 50 Kilometers

Table.1.Source parameters of forty five earthquakes whose FMS has been determined in the present study

FMS Nos.	Date D/M/Y	Time H: M: S	Latitude (N)	Longitude (E)	Depth (Km)	Magnitude (m_b)
1	08-11-05	2:52:39	34.60	73.30	65	4.6
2	02-02-66	9:13:00	33.89	73.20	37	5.1
3	06-04-66	1:51:53	34.91	73.06	54	5.1
4	18-11-68	5:06:45	34.34	71.39	17	5.0
5	30-04-70	3:24:54	33.30	73.40	33	4.8
6	28-04-71	15:12:42	34.44	73.60	43	4.8
7	27-12-71	20:59:39	34.98	73.82	55	5.2
8	10-03-72	14:36:16	33.91	72.72	40	4.9
9	07-05-72	10:05:04	33.45	71.50	17	5.0
10	27-09-72	2:03:39	33.99	72.70	41	5.1
11	27-09-72	20:24:56	35.07	72.91	49	4.8
12	28-12-74	12:11:46	35.06	72.91	15	5.9
13	29-12-74	22:36:53	34.99	73.10	68	4.8
14	07-04-75	6:41:02	34.91	72.97	53	5.0
15	14-02-77	22:37:0	33.60	73.27	15	5.0
16	07-05-78	10:32:25	33.53	73.58	9	5.0
17	04-03-79	2:51:47	33.99	72.90	43	4.7
18	28-05-82	0:58:48	32.36	70.89	9	4.6
19	11-02-84	8:37:06	33.60	71.60	15	4.8
20	18-02-84	7:04:59	34.09	71.82	52	4.6
21	20-12-84	7:32:07	32.95	72.70	0	4.6
22	27-12-84	20:22:05	32.96	72.64	1	4.6
23	28-12-84	16:28:01	34.61	73.61	47	4.5
24	12-07-87	12:19:18	33.40	73.40	13	4.4
25	07-12-88	21:13:54	34.03	72.98	50	4.2
26	07-04-89	4:24:43	33.75	73.29	10	4.6
27	17-02-91	7:00	33.86	71.39	4	4.5
28	16-03-91	3:57:42	34.52	72.66	33	4.5
29	29-05-92	12:26:32	33.25	71.30	10	6.0
30	06-06-92	13:33:10	33.27	71.31	1	5.0
31	17-02-93	16:06:07	33.55	72.50	7	4.9
32	08-06-93	14:36:37	33.68	72.62	8	4.8
33	20-02-96	2:55:52	34.04	72.67	46	4.7
34	08-08-96	14:58:19	34.06	72.82	21	4.8
35	12-07-96	5:54:00	34.11	72.63	27	5.0
36	23-01-99	9:53:00	32.27	70.20	15	5.5
37	16-04-99	22:11:00	32.49	70.80	10	4.8
38	28-04-99	13:00:00	33.33	73.12	5	4.7
39	15-07-99	4:29:00	32.76	72.82	0	3.8
40	17-07-00	5:26:00	34.59	72.89	10	5.0
41	16-07-01	16:07:06	32.93	73.06	32	5.2
42	01-11-02	22:09:29	35.62	74.66	23	5.3
43	26-11-02	21:32:00	35.51	74.69	45	6.2
44	14-02-04	11:56:58	34.81	73.19	10	4.9
45	14-02-04	10:30:22	34.83	73.26	10	5.0

Table. 2.The a-and b-values for the 4 determined seismic zones in the study area and its vicinity using the threshold magnitude (m0) of 4.0 Mw

Zone No.	Name	b value	$M_w \geq 4.0$ a value	No. of events
1	The Swat-Astore (SASZ)	0.95	4.34	207
2	The Peshawar-Hazara (PHSZ)	1.16	5.43	333
3	The Kohat-Potwar-Salt Range (KPSZ)	0.96	4.23	194
4	The Surghar-Kurram (SKSZ)	1.12	4.85	79

Table.3. The annual activity rate of occurrence of earthquakes for Mw 4.0

Zone No.	Name	Annual activity rate (l)
1	The Swat-Astore (SASZ)	2.62
2	The Peshawar-Hazara (PHSZ)	4.26
3	The Kohat-Potwar-Salt Range (KPSZ)	2.07
4	The Surghar-Kurram (SKSZ)	1.73

Table. 4. The maximum potential magnitudes assigned to the four seismotectonic (seismic) zones

Seismotectonic Zone	Most Critical Tectonic Feature	Maximum Potential Magnitude (M_{max})
Swat-Astor Seismic Zone (SASZ)	Main Mantle Thrust (MMT)	
	Main Boundary Thrust (MBT)	7.8
Peshawar-Hazara Seismic Zone (PHSZ)	Main Boundary Thrust (MBT)	7.8
Kohat Potwar–Salt Range Seismic Zone (KPSZ)	Kurram Thrust	
	Khair-i-Murat Fault (KMF)	7.4
Surghar-Kurram Seismic Zone (SKSZ)	Kurram Thrust	7.4

Table.5. The best-estimated seismic hazard parameters assigned to four seismotectonic (seismic) zones

Seismic Zone	b value	β value	λ	m_o	m_t	Focal Depth (km)
SASZ	0.95	2.19	2.62	4	7.8	25
PHSZ	1.16	2.67	4.26	4	7.8	20
KPSZ	0.96	2.19	2.07	4	7.4	10
SKSZ	1.12	2.58	1.73	4	7.4	10

Table.6. Peak Ground Accelerations (PGA) with 10% probability of exceedance in the 50 years i.e. the return period of 475 years calculated by using the attenuation equations of Ambraseys et al., (1996) and Boore et al., (1997) for the ten sites

Name of the Site	PGA (g) values calculated in the present study		Most Contributing Seismic Zone
	Ambraseys et al., (1996)	Boore et al., (1997)	
Astor	0.07	0.082	SASZ
Bannu	0.06	0.08	SKSZ
Kaghan	0.09	0.12	SASZ
Kohat	0.2	0.21	KPSZ
Mangla	0.16	0.18	KPSZ
Muzaffarabad	0.1	0.13	SASZ
Peshawar	0.14	0.15	PHSZ
Talagang	0.15	0.16	SKSZ
Islamabad	0.1	0.15	KPSZ
Malakand	0.2	0.21	SASZ

Table. 7. Ten sites, most critical tectonic feature, closest distance from the sites and associated maximum potential magnitudes using empirical relationships

Name of the Site	Tectonic Features	Closeet Distance to Faults (Kms)	Maximum potential magnitudes evaluated from the empirical relationships
Astore	MMT	25.00	7.8
Bannu	Karak Thrust	15.00	7.0
Kaghan	MMT	12.00	7.8
Kohat	MBT	1.61	7.8
Mangla	Dil Jabba Fault	11.00	7.1
Muzaffarabad	MBT	0.00	7.8
Peshawar	Khairabad Fault	12.00	7.5
Talagang	Kalar Kahar Fault	10.00	7.1
Islamabad	MBT	4.00	7.8
Malakand	MMT	20.00	7.8

attenuation equations for Pakistan concluded that there are no equations available even from neighbouring countries that can be adopted for seismic hazard assessment. The attenuation equations of Ambraseys *et al*. [27] and Boore *et al*. [28] have previously been utilized for the computation of peak ground accelerations (PGA) at the Mangla Dam [25]. Also, Jain *et al*. [29] concluded that their regression analysis for Central Himalayas closely fits the equation of Boore *et al*. [28].

PSHA has been carried out using the software called EZ-FRISK (6.2 beta version, 2004 modified form). The program calculates the earthquake hazard at a site under certain assumptions specified by the user. These assumptions involve identifying where earthquakes will occur, what their characteristics will be, and what will be the ground motions generated. These capabilities allow a wide range of seismic hazard problems to be solved, with straightforward specification of input. Its easy use allows in identifying the critical inputs and decisions affecting seismic hazard evaluations. The results of probabilistic calculations are annual frequencies of exceedance of various ground motion levels at the site of interest.

Further, seismic hazard is determined using the standard methodology described in McGuire [30]. The range of values used as input parameters can account for multiple hypotheses and computation of uncertainty in the resultant hazard values. The earlier mentioned seismic hazard parameters i.e.l, m_1, m_0 and the b parameter of each seismic zone i.e. area sources have been taken as input parameters in the present study. Besides representing the total hazard curves this software has aided in determining the most contributory seismic source zone and in carrying out deaggregation also.

Results and Discussion

Probabilistic results (Fig. 2) of seismic hazard assessment, as mentioned previously, have been generated in the form of hazard curves for the 10 selected sites that were distributed within the 4 seismic source zones. An alternate approach could have been the representation of the acceleration values in the form of contours on maps.

The hazard curve is a plot showing the change in ground motion amplitudes relative to return period. Ground motion amplitude always increases with increasing return period in Poisson hazard models. It may be noted that the maximum distance in PSHA is 200km radius. The total hazard curves, in the form of peak horizontal ground acceleration (PGA) at each and individual site versus their annual frequency of exceedance, were obtained. Results based on the attenuation equation of Ambraseys *et al*. [27] are in all cases less and are shown only to help in comparison with the values obtained through use of the equation of Boore *et al*. [28]. The reasons for preferring the latter have already been discussed earlier. At the same time, it is reiterated that instead of using representative equations derived for other places, an attenuation equation of Pakistan is needed. From these curves, acceleration values for different return periods can be determined. Following normal practice, the PGA values with 10% probability of exceedance in the 50 years i.e. the return period of 475 years are generally quoted.

The PGAs determined for the 10 selected sites range from 0.08g to 0.21g as shown in Tables 6 and 7 (see Fig. 2). In the present case, Kohat and Malakand depict the highest values of 0.21g whereas the lowest are obtained for Bannu. Critical tectonic features that may affect these sites have already been identified (Table 7, see Fig. 2). Islamabad and Peshawar although having relatively lower values (0.15g) have a higher population density as compared to the other sites with higher PGAs (Kohat and Malakand). However, Peshawar and Rawalpindi (twin city of Islamabad) are big cities of Pakistan with more poorly constructed structures and can experience appreciable damage as compared to the other less populated sites with higher PGAs. Therefore, an earthquake affecting them would pose a greater hazard as compared to the other sites.

All results obtained from this study have been used in the compilation of a seismotectonic map of the area (Fig. 2), which displays the focal mechanism solutions of 45 earthquakes occurred during the period of 1964-2004, 40 active faults, seismicity from 25 AD-2002, statistical parameters (Tables 2-5, see Fig. 2), most critical tectonic features with maximum potential magnitudes for major ten locations and peak ground accelerations (PGAs) for ten sites using Probabilistic Seismic Hazard Assessment (PSHA). This map, it is hoped would serve as a guide to the different organizations engaged in obtaining a better understanding of the tectonics of the area and in mitigating loss/damage to lives and property. It can certainly be further improved if larger coverage by local networks is undertaken. Strong motion data can also further improve the results. Determination of velocity structure and further subsurface information, based on other geophysical techniques, can also help.

References

1. **Ambraseys, N.N. and Bommer, J.** 1991.The attenuation of ground accelerations in Europe. E*arthquake Engineering and Structural Dynamics* 20:1179-1202.
2. **Ambraseys, N.N. and Bommer, J.J.** 1991. The attenuation of ground accelerations in Europe. *Earthquake Engineering and Structural Dynamics* 5:18-37.
3. **Ambraseys, N.N.** 1995. The prediction of earthquake peak ground accelerations in Europe. *Earthquake Engineering and Structural Dynamics* 24:1179-1202.
4. **Ambraseys, N.N., Simpson, K.A. and Bommer, J.J**. 1996. Prediction of horizontal response spectra in Europe. *Earthquake Engineering and Structural Dynamics* 25:371-400.
5. **Armbruster, J.G., Seeber, L. and Jacob, K.K.** 1978. The northwest termination of the Himalayan mountain front: active tectonics from micro earthquakes. *J. Geophys. Res.* 83:269-282.
6. **Boore, D.M., Joyner, W.B. and Fumal, T.E.** 1997. Equations from estimating horizontal response spectra and peak acceleration from western North American earthquakes: a summary of recent work. *Seismological Research Letters* 68:128-153.
7. **Bender, F.K. and Raza, H.A.** 1995. *Geology of Pakistan*. Tutt Drukerei GmbH, Salzweg-Passau, Germany.
8. **Cornell, A.C.** 1968. Engineering seismic risk analysis. *Bull. Seism. Soc. Am.* 58:1583-1606.
9. **Engdahl, R., Hilst, R.V. and Buland, R.** 1998. Global teleseismic earthquake relocation with improved travel times and procedures for depth determination. *Bull. Seism. Soc. Am.* 88:722-743.
10. **Gee, E.R.** 1980. Pakistan Geological Salt Range Series; (6 sheets, scale 1: 50,000). *Directorate of overseas surveys, UK, for the Government of Pakistan & Geological Survey of Pakistan.*
11. **Havskov, J**. 1997. SEISAN (version 6.0). *Earthquake analysis software for the IBM-PC and SUN*. Institute of Solid Earth Physics, University of Bergen, Norway.
12. **Hussain, A. and Yeats, R.S.** 2002. Active faulting in the southern Peshawar basin, Pakistan. *Geological Bulletin, University of Peshawar* 35:113-124.
13. **Jadoon, I.A.K.** 1992**.** Thin-skinned tectonics on continent/ocean transitional crust, Sulaiman Range, Pakistan. Ph.D. thesis, Geology Department, Oregon State University, USA.
14. **Jain, S.K., Roshan, A.D., Arlekar, J.N. and Basu, P.C.** 2000. Empirical attenuation relationships for the Himalayan earthquakes based on Indian strong motion data. *Proceedings of the Sixth International Conference on Seismic Zonation, Palm Springs, USA.*
15. **Kazmi, A.H. and Abbas, S.G.** 2001. *Metallogeny and mineral deposits of Pakistan.* Graphic Publishers, Karachi, Pakistan.
16. **Kazmi, A.H. and Jan, M.Q.** 1997. *Geology and tectonics of Pakistan.* Graphic Publishers, Karachi, Pakistan.
17. **Kemal, A.** 1992. Geology and New trends for petroleum exploration in Pakistan. In: *Proceedings of International Petroleum Seminar on New Directions and Strategies for Accelerating Petroleum Exploration and Production in Pakistan*. Ed. Ahmad, G., pp.16-57.
18. **Lawrence, R.D. and Yeats, R.S.** 1979. Geological reconnaissance of the Chaman Fault in Pakistan. In: *Geodynamics of Pakistan, E*ds. Farah, A. and DeJong, K.A., pp. 351-357.
19. **McGuire, R.K.** 1993. Computation of seismic hazard. Global Seismic Hazard Assessment Program. *Annali Di Geophysica* 34:181-200.
20. **MonaLisa, Khwaja, A.A. and Qaiser, M**. 2002. Focal Mechanism Studies of Kohat and Northern Potwar Deformed Zone. *Geological Bulletin, University of Peshawar* 35: 85-95.
21. **MonaLisa, Khan, S.A. and Khwaja, A.A**. 2004. Focal mechanism studies of North Potwar deformed zone (NPDZ), Pakistan. *Acta Seismologica Sinica, China* 17:255-261.

22. **NESPAK**. 2003. National Engineering Services Pakistan: A report on the Mangla Dam Project.
23. **Nowroozi, A.A.** 1972. Focal mechanism of earthquakes in Persia, Turkey, West Pakistan and Afghanistan and plate tectonics of the Middle East. *Bull. Seism. Soc. Am.* 62:823-850.
24. **Quittmeyer, R.L., Farah, A. and Jacob, K.H**.1979. The seismicity of Pakistan and its relation to surface faults. In: *Geodynamics of Pakistan, Ed*s. Farah, A. and DeJong, K.A., pp. 271-284.
25. **Seeber, L. and Armbruster. J.** 1979. Seismicity of Hazara Arc in northern Pakistan: Decollement vs. Basement Faulting. In *Geodynamics of Pakistan. E*ds. Farah, A. and DeJong, K.A., pp. 131-142.
26. **Tahirkheli, R.A.K., Mattauer, M., Proust, F. and Tapponier, P.** 1979. The India-Eurasia suture zone in northern Pakistan: Some new data for interpretation at plate scale. In: *Geodynamics of Pakistan.* Eds. Farah, A. and DeJong, K.A., pp. 125-130.
27. **Treloar, P.J., Rex, D.C., Guise, P.G., Coward, M.P., Searle, M.P., Windley, B.F., Petterson, M.G., Jan, M.Q. and Luff, I.W.** 1989. K-Ar and Ar-Ar geochronology of the Himalayan collision in NW Pakistan: Constraints on the timing of collision deformation, metamorphism and uplift tectonic. *Tectonics* 4:881-909.
28. **Udias, A.** 1999. *Principles of Seismology*. University press, Cambridge, UK.
29. **Verma, R.K. and ChandraSekhar, Ch.** 1986. Focal mechanism solutions and nature of plate movements in Pakistan. *Jour. Geodyn.* 5:331-351.
30. **Yeats, R.S. and Lawrence, R.D.** 1984. Tectonics of the Himalayan thrust belt in northern Pakistan. In: *Marine geology and oceanography of Arabian Sea and coastal Pakistan,* Eds. Haq , B.U. and Milliman, J.D., pp. 177-200.

Proc. Pakistan Acad. Sci. 42(4):297-304.2005

DESIGN STRCUTURE MATRIX (DSM): NEW DIRECTIONS

***A.H.M. Shamsuzzoha[1] and Nadia Bhuiyan[2]**

[1]Department of Industrial and Production Engineering, Shah Jalal University of Science and Technology, Sylhet-3114, Bangladesh, and [2]Department of Mechanical and Industrial Engineering, Concordia University, Montreal, Quebec, H3G 1M8, Canada

Received August 2005, accepted November 2005

Communicated by Prof. Dr. Abdul Raouf

Abstract: The Design Structure Matrix (DSM) is a compact representation of the information structure of a design process. It is a powerful tool for representing and analyzing task dependencies of a design project. This method provides a major need in engineering design management through documenting information that is exchanged. Analyzing the structure of a design process can identify many opportunities to improve it. Building a DSM model of a project/system, improves the visibility and understanding of project/system complexity through information flows. With the help of a DSM model it can easily convey the process to others in a single snapshot. In this research work, an improvement of the existing DSM tool is proposed which permits design managers to find an optimum way of restructuring complex design tasks, exposing problems, and creating unique solutions that could not be found simply by manually inspecting the design matrix. The improved model/algorithm follows the information-based approach of the design structure matrix (DSM) method, and uses transformed matrix techniques to reduce product development time and cost through optimal task ordering, while maintaining a high level of quality.

Keywords: Product design, special operator, triangular matrix, design iteration, concurrent engineering

Introduction

Advanced technology, fierce market competition and changing demand are forcing companies to design better quality and less expensive products at a rapid time pace. A product is something sold by an enterprise to its customers. Product development (PD) is the set of activities beginning with the perception of a market opportunity and ending in the production, sale and delivery of a product. PD process is the sequence of steps or activities which an enterprise employs to conceive, design and commercialize a product [1]. The PD process in an organization can be a source of competitive advantage in many industries. PD teams today are facing a growing number of concerns, such as production complexity, resource consumption, future upgrades, maintenance, and recycling [2]. A complex PD project involves a large number of activities that may require coordinating the work of hundreds or thousands of people from various disciplines. The work of any one design task can affect many other development decisions throughout the organization. As complexity increases, it becomes very difficult to manage the interactions among tasks and people. It may be even impossible to predict the impact of a single design change throughout the development process [3]. Coordinating design decisions has therefore become a crucial responsibility of engineering management.

Product development process is generally a complex procedure involving information exchange across many tasks in order to execute the work [4]. It requires innovation and innovation requires feedback loops. Product development performance is generally measured by the lead time to develop

*E-mail: zohaipe@yahoo.com

the product, the cost of the development effort, the manufacturing cost of the product, and the product's quality or attractiveness in the market [5]. Analysis of product development (PD) processes allows us to study product development efficiency and to suggest process improvements.

Iteration is a fundamental characteristic of any product development processes [3,6]. It is assumed that the iteration of a task occurs for the following reasons: (1) new information is obtained from overlapped tasks after starting to work with preliminary inputs, (2) inputs change when other tasks are reworked, and (3) outputs fail to meet established criteria. Many traditional project management tools such as CPM [7], Gantt, and PERT [8], models do not represent iterative task relationships very well. Although, these tools allow the modeling of sequential and parallel processes, they fail to address interdependency (feed back and iteration) which is very common in PD projects. To address this issue, a matrix-based tool called the Design Structure Matrix (DSM) has evolved. Steward [9] developed the design structure matrix (DSM) to model the information flow of design tasks and to identify their iterative loops. It differs from conventional project-management tools such as PERT, Gantt charts and CPM network diagrams in that it focuses on representing information flows of a design project rather than on the work flows.

The aim of this research was to examine the existing DSM tool and to develop a mathematical model or algorithm to restructure the complex PD projects in order to develop quality products more quickly and economically. Such improved design procedures offer opportunities to speed up development progress by enhancing inter-task coordination. This model/algorithm follows the information-based approach of the design structure matrix (DSM) method, and uses transformed matrix techniques to reduce product development time and cost through optimal task ordering, while maintaining a high level of quality.

Design structure matrix: an overview

A matrix-based tool called the Design Structure Matrix (DSM) introduced by Donald Steward [9] provides generic framework for information flow in a simple and elegant manner. Both the sequences and technical relationships are performed by using a matrix representation. These relationships define the technical structure of a project, which is then analyzed in order to find alternative sequences of the tasks. A DSM is a compact matrix representation of a project network. The matrix contains a list of all constituent activities and the corresponding information exchange patterns. That is, what information pieces (parameters) are required to start a certain activity and where does the information generated by that activity feed into. The DSM provides insights about how to manage a complex project, and highlights issues of information needs and requirements, task sequencing and iterations.

It is relatively straight forward to construct a DSM of any company's existing or future product development process. The first step is to identify the tasks involved, which is easy and often available as part of the project management documentation. The next step is to correctly identify the information needed of the various tasks. Once all of the task information is ready, the next step is to draw the projects DSM. First, all tasks are listed in the order in which they are presently carried out. These tasks are then arranged in the same order horizontally and vertically to form a matrix of rows and columns. The other tasks that supply the necessary information are marked off across each row corresponding to a task. In other words, looking across a row shows all the information inputs needed to complete a task and looking down a column shows all the information outputs that will be provided to other tasks.

Figure 1 (adopted from [3]) shown below is

an example of DSM construction, where task B supplies input information to tasks C, F, G, J and K, while task D receives output information from tasks E, F and L. All marks above the diagonal are feedback marks. Feedback marks correspond to the required inputs that are not available at the time of executing a task. In this case, the execution of the dependent task will be based on assumptions regarding the status of the input tasks. As the project unfolds these assumptions are revised in the light of new information, and the dependent task is re-executed if needed. It is worth noting how easy it is to determine feedback relationships in the DSM compared to the graph, which makes the DSM a powerful, but simple, graphic representation of a complex system or project. The matrix can be manipulated in order to eliminate or reduce the feedback marks. This process is called partitioning [9,10]. When this is done, a transparent structure for the network starts to emerge, which allows better planning of the PD project. In Fig. 2, it is seen which tasks are sequential, which ones can be done in parallel, and which ones are coupled or iterative.

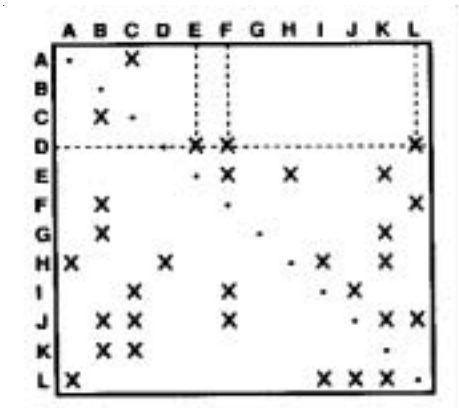

Fig. 1. A binary DSM (partitioned).

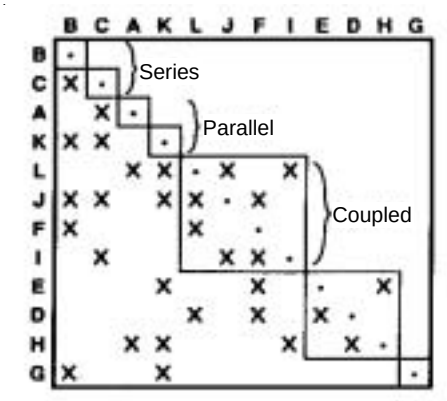

Fig. 2. A binary DSM (unpartitioned)

After portioning the DSM, the tasks in series are identified and executed sequentially. Parallel tasks are also exposed and can be executed concurrently. For the coupled ones, upfront planning is necessary. For example, we would be able to develop an iteration plan by determining what tasks should start the iteration process based on an initial guess or estimate of a missing piece of information. In Fig. 2, block E-D-H can be executed as follows: task E starts with an initial guess on H's output, E's output is fed to task D, then D's output is fed to task H, and finally H output is fed to task E. At this point, task E compares H's output to the initial guess made, and decides if an extra iteration is required or not depending on how far the initial estimate deviated from the latest information received from H. This iterative process proceeds until convergence occurs.

Methodology

The analytical methodology of the design process thus starts with building a structural model using a DSM. The DSM is then sorted out and tasks are rearranged in an attempt to eliminate feedback marks. The DSM is then partitioned into blocks containing task subsets involved in a cyclic information flow. Finally, feedback marks are torn from the DSM to break the cycles to eliminate one or more feedback marks within a coupled block in such a way that the rearrangement of the tasks within the block converts it in lower triangular form.

Results and Discussion

Research Problem: Transformed DSM

In the literature review, it has been observed that after partitioning, some coupled tasks still remain which cause lengthy lead-time and cost. The present research attempted to find a mathematical model or algorithm, which removes all coupled blocks or reduces coupling to a minimum level. To perform this operation, all upper diagonal feedback marks of a DSM had to be brought back to a more appropriate lower triangular form.

In mathematics, we know that if we have a matrix A and if |A| '" 0, then there certainly exists another matrix H, which can make A become diagonalized, if the following calculation is applied:

H^{-1}. A. H = D (is a diagonalised matrix) …..… (i)

As in this example, we desired to find the transformation that can convert a DSM into one, which has the desired features in order to optimize the organization of the design activities. The problem can be solved in other ways, using an 'operator' to express the matrix form. Let's consider the above example again; if A = a given DSM and B = the transformed DSM of A then its operator form becomes:

H^{+}. A. = B ……..…….... (ii)

Similarly, if we can find the expression of H^{+}, it will tell us how to coordinate the design activities to obtain optimal orderings of the DSM.

Here H^{+} is a 'special operator matrix', which can be defined as:

$H^{+}.A.\ A^{-1} = B.\ A^{-1}$,

⇨ $H^{+} = B.\ A^{-1}$ ……..…… (iii)
[$A.\ A^{-1} = I$ (identity matrix)]

In other way, the transformed matrix can be found out which is shown below:

$H^{+}.A.H = B$ …….. (iv)

Here, H^{+} and H are two different operators, which convert A to transformed matrix B. It is therefore, necessary to define these two operators for the DSM transformation.

$H^{+}.\ A.\ H = B$ (is a diagonalised matrix)

Example of Matrix Transformation

Consider matrix A as a work transformation matrix, where the diagonal elements are zero and off diagonal marks represents dependency strengths between tasks. Now the columns of matrix A can be interchanged to bring the higher dependency marks into a lower triangle. This transformation occurs by multiplying matrix A by unit matrix H and different values of H may be used to observe the actual transformation-taking place. Therefore it can be written as:

$A \times H = B$…… (1)

where A is the original matrix and B is new matrix after changing the column or row. The matrix H is the unit matrix, which transforms matrix A to matrix B. Transformation of a sample matrix **A** is shown below.

Let:

$$A = \begin{matrix} 0.0 & 0.1 & 0.2 & 0.3 \\ 0.3 & 0.0 & 0.4 & 0.2 \\ 0.1 & 0.3 & 0.0 & 0.5 \\ 0.1 & 0.1 & 0.2 & 0.0 \end{matrix}$$

$$B1 = \begin{matrix} 0.1 & 0.0 & 0.2 & 0.3 \\ 0.0 & 0.3 & 0.4 & 0.2 \\ 0.3 & 0.1 & 0.0 & 0.5 \\ 0.1 & 0.1 & 0.2 & 0.0 \end{matrix}$$

(We obtained 'B1' after interchange of columns 1& 2 of 'A')

Therefore

$$H1 = B1/A = \begin{matrix} 0 & 1 & 0 & 0 \\ 1 & 0 & 0 & 0 \\ 0 & 0 & 1 & 0 \\ 0 & 0 & 0 & 1 \end{matrix} \quad \text{.....(2)}$$

$$B2 = \begin{matrix} 0.2 & 0.1 & 0.0 & 0.3 \\ 0.4 & 0.0 & 0.3 & 0.2 \\ 0.0 & 0.3 & 0.1 & 0.5 \\ 0.2 & 0.1 & 0.1 & 0.0 \end{matrix}$$

(We obtained 'B2' after interchange of columns 1& 3 of 'A')

$$H2 = B2/A = \begin{matrix} 0 & 0 & 1 & 0 \\ 0 & 1 & 0 & 0 \\ 1 & 0 & 0 & 0 \\ 0 & 0 & 0 & 1 \end{matrix} \quad \text{.....(3)}$$

$$B3 = \begin{matrix} 0.3 & 0.1 & 0.2 & 0.0 \\ 0.2 & 0.0 & 0.4 & 0.3 \\ 0.5 & 0.3 & 0.0 & 0.1 \\ 0.0 & 0.1 & 0.2 & 0.1 \end{matrix}$$

(We obtained 'B3' after interchange of columns 1& 4 of 'A')

$$H3 = B3/A = \begin{matrix} 0 & 0 & 0 & 1 \\ 0 & 1 & 0 & 0 \\ 0 & 0 & 1 & 0 \\ 1 & 0 & 0 & 0 \end{matrix} \quad \text{.....(4)}$$

$$B4 = \begin{matrix} 0.0 & 0.2 & 0.1 & 0.3 \\ 0.3 & 0.4 & 0.0 & 0.2 \\ 0.1 & 0.0 & 0.3 & 0.5 \\ 0.1 & 0.2 & 0.1 & 0.0 \end{matrix}$$

(We obtained 'B4' after interchange of columns 2& 3 of 'A')

$$H4 = B4/A = \begin{matrix} 1 & 0 & 0 & 0 \\ 0 & 0 & 1 & 0 \\ 0 & 1 & 0 & 0 \\ 0 & 0 & 0 & 1 \end{matrix} \quad \text{.....(5)}$$

and so on .....

From the above transformations, it can be observed that the *columns* of matrix A can be interchanged by multiplying matrix H1, H2, H3, H4 and so on, which convert easily to the higher dependency marks in the lower triangular form as necessary.

In another trial, carried out by interchanging the rows of matrix A, the following results were obtained:

$$A = \begin{matrix} 0.0 & 0.1 & 0.2 & 0.3 \\ 0.3 & 0.0 & 0.4 & 0.2 \\ 0.1 & 0.3 & 0.0 & 0.5 \\ 0.1 & 0.1 & 0.2 & 0.0 \end{matrix}$$

$$B'1 = \begin{matrix} 0.3 & 0.0 & 0.4 & 0.2 \\ 0.0 & 0.1 & 0.2 & 0.3 \\ 0.1 & 0.3 & 0.0 & 0.5 \\ 0.1 & 0.1 & 0.2 & 0.0 \end{matrix}$$

(We obtained 'B1' after interchange of rows 1& 2 of 'A')

$$H'1 = B'1/A = \begin{matrix} -1.42 & 0.81 & -1.6 & 0.80 \\ 0.48 & 0.84 & 0.32 & -0.16 \\ 0.96 & -0.32 & 1.6 & -0.32 \\ 0.19 & -0.06 & 0.12 & 0.93 \end{matrix} \quad \text{.....(6)}$$

$$B'2 = \begin{matrix} 0.1 & 0.3 & 0.0 & 0.5 \\ 0.3 & 0.0 & 0.4 & 0.2 \\ 0.0 & 0.1 & 0.2 & 0.3 \\ 0.1 & 0.1 & 0.2 & 0.0 \end{matrix}$$

(We obtained 'B'2' after interchange of rows 1& 3 of 'A')

$$H'2 = B'2/A = \begin{matrix} 0.29 & -1.42 & 1.42 & -1.42 \\ -0.25 & 0.48 & 0.52 & -0.52 \\ 0.48 & 0.96 & 0.03 & 0.96 \\ 0.09 & 0.19 & -1.19 & 1.19 \end{matrix} \quad \text{.....(7)}$$

$$B'3 = \begin{matrix} 0.1 & 0.1 & 0.1 & 0.0 \\ 0.3 & 0.0 & 0.4 & 0.2 \\ 0.1 & 0.3 & 0.0 & 0.5 \\ 0.0 & 0.1 & 0.2 & 0.3 \end{matrix}$$

(We obtained 'B'3' after interchange of rows 1& 4 of 'A')

$$H'3 = B'3/A = \begin{matrix} 0.54 & 0 & 0 & 1 \\ -0.71 & 1 & 0 & 2 \\ 0.08 & 0 & 1 & -0.24 \\ 0.52 & 0 & 0 & -0.55 \end{matrix} \quad \text{.....(8)}$$

$$B'4 = \begin{matrix} 0.0 & 0.1 & 0.2 & 0.3 \\ 0.1 & 0.3 & 0.0 & 0.5 \\ 0.3 & 0.0 & 0.4 & 0.2 \\ 0.1 & 0.1 & 0.2 & 0.0 \end{matrix}$$

(We obtained 'B'4' after interchange of rows 2& 3 of 'A')

$$H'4 = B'4/A = \begin{matrix} 0.80645 & 0.29032 & -0.3871 & 0.29032 \\ 0.83871 & -0.25806 & 1.6774 & -1.2581 \\ -0.32258 & 0.48387 & 0.35484 & 0.48387 \\ -0.06451 & 0.096774 & -0.12903 & 1.0968 \end{matrix} \quad ..(9)$$

and so on .....

From the above transformations, it is evident that rows of matrix A can be interchanged by multiplying matrix H'1, H'2, H'3, H'4, and so on, but it seems that a very complex form of H's is required to convert the higher dependency marks in the lower triangular form than the column interchange of matrix A. In this way, we hoped that after changing each row of any DSM, a generalized mathematical model could be developed for optimal task ordering.

Steps to find the 'Special Operator Matrix' $H^{+:}$

(i) Analyzing published examples of product design using the DSM method and its transformed matrix to find out the relation with the operator matrix.

(ii) Using Mat Lab software to find out the internal relationship between two square matrices and also to find a way how they are transformed into a more convenient coupled or lower triangular form.

The following is an example which shows (Figs. 3 to 8) the way transformation occurs (using equation (i))

	A	B	C	D	E	F	G
A						1	
B				1			1
C					1		
D		1					1
E			1				
F	1						
G		1		1			

Fig. 3. A = Original DSM.

	A	F	G	B	D	C	E
A		1					
F	1						
G				1	1		
B			1		1		
D			1	1			
C							1
E						1	

Fig. 4. B1 = Transformed DSM.

$$A := \begin{bmatrix} 0 & 0 & 0 & 0 & 0 & 1 & 0 \\ 0 & 0 & 0 & 1 & 0 & 0 & 1 \\ 0 & 0 & 0 & 0 & 1 & 0 & 0 \\ 0 & 1 & 0 & 0 & 0 & 0 & 1 \\ 0 & 0 & 1 & 0 & 0 & 0 & 0 \\ 1 & 0 & 0 & 0 & 0 & 0 & 0 \\ 0 & 1 & 0 & 1 & 0 & 0 & 0 \end{bmatrix}$$

Fig. 5. A = Original DSM.

$$B := \begin{bmatrix} 0 & 0 & 0 & 0 & 0 & 1 & 0 \\ 0 & \frac{-1}{2} & 0 & \frac{1}{2} & 0 & 0 & \frac{1}{2} \\ 0 & 0 & 0 & 0 & 1 & 0 & 0 \\ 0 & \frac{1}{2} & 0 & \frac{-1}{2} & 0 & 0 & \frac{1}{2} \\ 0 & 0 & 1 & 0 & 0 & 0 & 0 \\ 1 & 0 & 0 & 0 & 0 & 0 & 0 \\ 0 & \frac{1}{2} & 0 & \frac{1}{2} & 0 & 0 & \frac{-1}{2} \end{bmatrix}$$

Fig. 6. B = Inverse of Matrix A.

$$B1 := \begin{bmatrix} 0 & 1 & 0 & 0 & 0 & 0 & 0 \\ 1 & 0 & 0 & 0 & 0 & 0 & 0 \\ 0 & 0 & 0 & 1 & 1 & 0 & 0 \\ 0 & 0 & 1 & 0 & 1 & 0 & 0 \\ 0 & 0 & 1 & 1 & 0 & 0 & 0 \\ 0 & 0 & 0 & 0 & 0 & 0 & 1 \\ 0 & 0 & 0 & 0 & 0 & 1 & 0 \end{bmatrix}$$

Fig. 7. B1 = Transformed Matrix (Optimized DSM).

H1=transformed matrix (B1) x Inverse of original matrix 'A' (B)

$$H1 = \begin{vmatrix} 0 & 0 & 0 & 0 & 0 & 0 & 1 \\ -½ & 0 & ½ & 0 & ½ & ½ & 0 \\ 0 & 0 & 1 & 1 & 0 & 0 & 0 \\ ½ & 0 & -½ & 0 & -½ & ½ & 0 \\ 0 & 0 & 0 & 1 & 1 & 0 & 0 \\ 0 & 1 & 0 & 0 & 0 & 0 & 0 \\ ½ & 0 & ½ & 0 & ½ & -½ & 0 \end{vmatrix}$$

Fig. 8. H1= Transformed matrix (B1) x Inverse of original matrix'A' (B).

In this way a generalized mathematical model/ algorithm could be developed for the optimized DSM.

Significance of this research

To increase competitiveness, every firm has to develop its products with the importance of improving the efficiency and predictability of their design processes. Since, any process improvement requires process understanding, researchers and practitioners put effort into observing product design and development processes, looking for their important characteristics and developing models that account for those features. Most of the advances in this area assume that the design process has an underlying structure. An important characteristic of product development (PD) processes is that, unlike most business and production processes, they are described by terms like "creative," "innovative," and "iterative." At an interesting level of detail, PD processes do not proceed in a purely sequential fashion. The activities in a PD process interact by exchanging information which is iterative.

Product development is considered to be a process of input information about customer needs and market opportunities into output information, which correspond manufacturability designs and functional tooling for volume production. In practice, the information exchanged between activities takes various forms such as customer specifications, parts dimension, and prototypes. Information exchanged in the engineering stages of product development can often be represented as a collection of parameters [3]. In real life, it is rare that a company will be able to design a process in which all interdependent or coupled tasks can be carried out together. In coupled blocks, a significant number of potential unplanned iterations can occur when errors are discovered during the project development process. This rework would also require the company to redo some intervening tasks. The company then decides what to do about them. The coupled tasks may be so far apart that a delay caused by incorporating late information effectively means starting the whole process again. These situations usually arise because some fundamental mistake in

assumptions was made at the beginning of the project [11].

In this research, an improvement of the DSM tool is proposed that permits managers to find optimum ways of restructuring complex design tasks, exposing problems, and creating unique solutions that could not be found simply by manually inspecting the design matrix. This work will be able to reduce the lead-time of any development project. It can be done through resequencing/reordering the coupled task by using the proposed mathematical model/ algorithm. If the model is developed it will definitely help designers/engineers to organize their works in more efficient ways than ever.

References

1. **Ulrich, K.T. and Eppinger, S.D.** 2004. *Product Design and Development.* ISBN 0-07-247146-8, 3rd Edition, McGraw-Hill, New York.
2. **Smith, R.P. and Eppinger, S.D.** 1997. A predictive model of sequential iteration in engineering design. *Management Science* 43:1104-1120.
3. **Eppinger, S., Whitney, D., Smith, R. and Gebala, D.** 1994. A model-based method for organizing tasks in product development. *Research in Engineering Design* 6:1-13.
4. **Krishnan, V., Eppinger, S.D. and Whitney, D.E.** 1995. Accelerating product development by the exchange of preliminary product design information. *J. Mechanical Design* 117:491-498.
5. **Clark, K.B., Chew, B. and Fujimoto, T.** 1987. *Product development in the world auto industry: performance: strategy, organization and performance*. Brookings Papers on Economic Activity, vol. 3, pp.729-771.
6. **Browning, R.T. and Eppinger, S.** 2002. Modeling the impact of process architecture on cost and schedule risk in product development. *IEEE Trans. Engineering Management* 49:428-442.
7. **Kelley, J. and Walker, M.** 1959. *Critical-path planning and scheduling*. Proceedings of Easter Joint Computer Conference, pp. 160-173.
8. **Malcolm, D., Roseboom, J., Clark, C. and Fazar, W.** 1959. Application of a technique for research and development program evaluation. *Operations Research* 7:646-669.
9. **Steward, D.V.** 1981. The design structure system: a method for managing the design of complex systems. *IEEE Trans. Engineering Management* 28:71-74.
10. **Yassine, A., Falkenburg, D. and Chelst, K.** 1999. Engineering design management: an Information structure approach. *International Journal of Production Research* 37:2957-2975.
11. **Kong, L.** 2003. Determining the value of processes and information structures for new product development. Ph.D. thesis, McGill University, Montreal, Canada.

Proc. Pakistan Acad. Sci. 42(4):305-314.2005

Review

PRESENT STATUS AND FUTURE NEEDS OF TEA INDUSTRY IN BANGLADESH

G.M.R. Islam[1], M. Iqbal[2], K.G. Quddus[3] and M. Y. Ali[4]

[1]Department of Tea Technology, Shah Jalal University of Science & Technology, Sylhet-3114, Bangladesh, [2]Department of Industrial & Production Engineering Shah Jalal University of Science & Technology, Sylhet, Bangladesh, and [3] Agrotechnology Discipline, Khulna University, Khulna-9208, Bangladesh

Received August 2005, accepted November 2005

Communicated by Prof. Dr. M. A. Hafeez

Summary: World tea production has been showing an annual increment of 3 % while in Bangladesh the production has increased by 1.84 % and contributes 1.37 in export in the word tea trade and earns near about 1775 million Taka (Taka 63 = USD 1.00) every year. The activities of tea industry fall into two categories: production of tea and manufacturing & marketing of tea. Low productivity, poor quality and higher cost of production compared to the dividend in price for tea is the crux of the problem. We have to make quality tea, which must satisfy the prescribed criterion of the of the European countries especially Maximum Residue Level (MRL) value of pesticides to restore its name and fame. This paper attempts at focusing on the present condition and support required of tea industry in the country.

Introduction

Tea is one of the most important non-alcoholic beverage drinks worldwide and has been gaining further popularity as an important 'health drink' in view of its purported medicinal value. It is served as morning drink for nearly 2/3rd of the world population daily. The Bangladesh tea industry is one of the major sources of income for the national exchequer. Presently, this industry is facing a multitude of problems. Lack of capital and modern machinery, lower market value of made tea in comparison to increasing production cost, lower yield per hectare in comparison to increasing domestic need and lack of modern techniques for measuring quality of tea constitute some of the nagging problems. There is also lack of perennial water source for irrigation during dry season or during prolonged drought. In addition, some owners of the tea gardens are not using Government. loans properly. Malnutrition among the children of the labour line, security problems of the executives, deterioration of law and order situation of the tea estates (log stealing, political or outsider influence on their internal arrangements, illegal occupation of land by the outsiders), lack of medical facilities for labour and lack of infrastructure (road, quarter, water supply network etc) are some of the other constraints. For successful tea culture, the above problems facing both the manufacturing and the marketing sector need to be addressed immediately. In Bangladesh, there is thus dire need to focus attention on improvements in the manufacturing sector covering quality of tea, its productivity, cost of production as well as the marketing system. The following account reviews the present status of the tea industry in Bangladesh and its support requirements in order to compete with other tea producing countries in the international markets, particularly the European Union.

Tea: an overview

Tea (*Camellia sinensis* L.) belongs to the family Theaceae. It is the oldest non alcoholic caffeine-containing beverage in the world. The Chinese were

E-mail: rabi-ttc@sust.edu

the first to use tea as medicinal drink, later as beverage and have been doing so for the past 3000 years [1]. The cultivated taxa comprise of three main natural hybrids. They are (1) *C. sinensis* (L.) O. Kuntze or China type, (2) *C. assamica* (Masters) or Assam type, and (3) *C. assamica* sub spp *lasiocalyx* (Planchon ex Watt.) or Cambod or Southern type. Tea is an evergreen, perennial, cross-pollinated plant and grows naturally as tall as 15 m. However, under cultivated condition, the bush height of 60–100 cm is maintained for harvesting the tender leaves for even more than 100 years. The flowers are white in colour and grow singly or in pairs at the axils. The fruits are green in colour with 2–3 seeds. The leaf is the main criterion by which the three types of tea are classified as follows.

– Assam type : biggest leaves,
– China type: smallest leaves, and
– Cambod: intermediate leaves

The original home or 'the primary center of origin' of tea was South-East Asia i.e. at the point of intersection between the 29% N (latitude) and 98% E (longitude) near the source of the Irrawaddy river at the confluence of North-East India, North Burma, South-West China and Tibet provinces [2]. Tea thrives well within the latitudinal ranges between 45%N to 34% S, cutting across about 52 countries [3].

Global scenario

In the world, thirty countries are producing more than 2.50 billion kilogram of tea annually (including 0.56 billion kg of green tea varieties manufactured by eight countries) from 2.56 million hectares of plantation. After meeting their domestic consumption, 28 countries export about 1.32 billion kg of tea annually [4]. Production of tea by area, production and export is shown in Fig. 1. Tea production by 12 major tea producing countries of the world is shown in Table 1. Bangladesh is producing more than 54 million kg of tea annually from about 49000 hectares of land. It can earn foreign exchange equivalent to about 1775 million Taka (Taka 63 = US $ 1) annually by exporting about 18 million kg of tea [5]. The world tea production has been showing an annual increment of 3 % [4], while in Bangladesh the production has increased by 1.84 % and contributes 1.37% in export in the word tea trade (Table 2).

Tea cultivation in Bangladesh is spread over the hilly zones on the eastern part mainly in four districts (Sylhet, Moulvibazar, Habibgonj and Chittagong). About 96% annual production (of which 63% is of Moulvibazar district) is contributed by greater Sylhet obtained from 93% (of which 62% is of Moulvibazar district) of plantation area. It is to be noted that Sterling companies produce about 50% of annual crop from about 42% of plantation area [6].

Table 1.
Country wise Productivity of Tea (kg/ha)-2000 AD.

SL No.	Country	Productivity
1	Kenya	1934
2	India	1743
3	Japan	1745
4	Turkey	1494
5	Sri Lanka	1450
6	Bangladesh	1102
7	Argentina	1538
8	China	627
9	Indonesia	1006
10	Vietnam	756
11	Uganda	1381
12	Georgia	382

Source: ITC [4]

Table 2.
Tea production in Bangladesh at different periods.

Year	Area (ha)		Production ('000' Kg)		Yield (Kg/ha)**	
	Total	Increased/ decreased*	Total	Increased/ decreased*		
1947	303533	—	18884	—	62	—
1957	31287	+ 934	25549	+ 6665	817	+ 195
1970	42688	+ 11401	31381	+ 5832	735	– 82
1980	43732	+ 1044	40038	+ 8657	916	+ 181
1992	47781	+ 4049	48930	+ 8892	1040	+ 124
2000	48735	+954	55834	+ 6894	1145	+ 105

Source: BTRI [5]; * Difference from previous total denoted by (+) or (-) sign. ** calculated on the basis of production/total tea area/ha

Economic importance and health benefits

The economic importance of the genus *Camellia* is primarily due to use as tea. Tea was initially used as a medicine and subsequently as beverage and now has proven well to be a future potential as an important raw material for the pharmaceutical industry. Tea is mainly consumed in the form of 'fermented tea' or 'black tea'. However, 'non-fermented' or 'green tea' and semi-fermented or 'oolong tea' are also popular in some countries e.g. Japan and China. Apart from being used as beverage, green leaves are also used as vegetable such as 'leppet tea' in Burma and 'meing tea' in Thailand. Though the oil of tea seeds is used as lubricant, yet extraction from seeds is not economical [7]. Additionally, cakes of tea seed contain saponins, have poor value as fertilizer and are unfit for animal feed due to low nitrogen, phosphorus and potassium content. However, these can be used successfully in the manufacture of nematocide [7]. Tea leaves have more than 700 chemical constituents, among which flavanoides, amino acids, vitamins (C, E, K), caffeine and polysaccharides are important to human health. Importantly, the vitamin C content in leaves is comparable to that of lemon. Tea drinking is now being associated with cell-mediated immune responses of the human body and reported to improve the growth of beneficial microflora in the intestine [8]. Tea also imparts immunity against intestinal disorders, protects the cell membranes from oxidative damages, prevents dental caries due to presence of fluorine, normalizes blood pressure, prevents coronary heart diseases due to lipid depressing activity, reduces the blood-glucose activity and normalizes diabetes [8]. Tea also possesses germicidal and germistatic activities against various gram-positive and gramnegative human pathogenic bacteria such as *Vibrio cholera, Salmonella sp., Clostridium sp.*[9]. Both green and black tea infusions contain a number of antioxidants like catechins and have anti-carcinogenic, anti-mutagenic and anti-tumorous properties. Among the different catechins, epigallo catechin-gallate is the most active component. Several epidemiological studies have also proved that tea consumption plays a protective role against human cancer.

Production of tea

Varieties and improvement

Genome diversity

The genus *Camellia* had 82 species in 1958

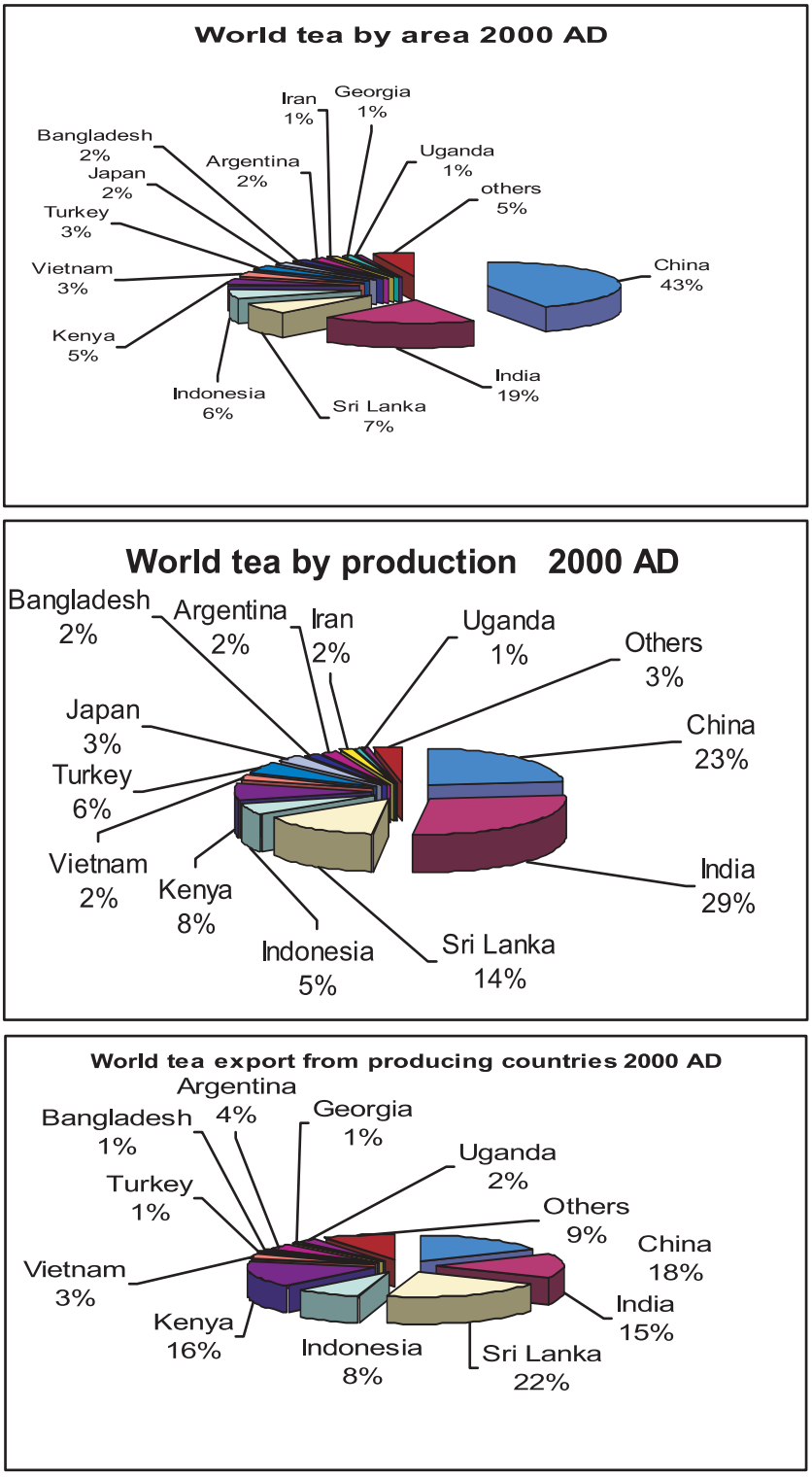

Fig. 1. Top: Country wise percent area under tea cultivation; **middle:** Country wise production of tea; **bottom:** Country wise export of tea.

[10] and accounts for more than 325 species in 2002 [11] that indicates genetical instability and high out-breeding nature of the genus. Presently, over 600 cultivated varieties world-wide are available, of which many have unique traits (Table 3). Owing to extensive internal hybridization between different *Camellia* taxa, several intergrades, introgressants and putative hybrids have been formed. These can be arranged in a gradient based on morphological characters that extend from China types through intermediates to those of Assam types. Indeed, because of the extreme homogenization, existence of the pure archetypes of tea is doubtful [12]. Till date, numerous hybrids currently available are still referred to as China, Assam or Cambod tea depending on morphological proximity to the main taxon [13]. Tea breeds well with wild relatives and thus taxonomists have always been interested in identifying such hybrids due to suspected involvement in tea genetic pool. Two particularly interesting taxa are *C. irrawadiensis* and *C. taliensis* whose morphological distribution overlaps with that of tea [13]. It has also been postulated that some desirable traits such as anthocyanin pigmentation or special quality characters of Darjeeling tea might have been introduced from wild species [14]. Other *Camellia* species, which are suspected to have contributed to the tea genetic pool by hybridization, include *C. flava* (Pifard) Sealy, *C. petelotii* (Merrill) Sealy [15] and possibly *C. lutescens* Dyer [16]. The role of *C. taliensis* is, however, not clear because the species itself is considered to be a hybrid between *C. sinensis* and *C. irrawadiensis* [12,14]. Therefore, it is generally agreed that at least three taxa i.e. *C. assamica*, *C. sinensis*, *C. assamica* sub sp. *lasiocalyx* and to an extent *C. irrawadiensis* have mainly contributed to the genetic pool of tea. The term 'tea' should therefore, cover progenies of these taxa and the hybrids thereof or between them.

Table 3.
Description of tea cultivars with special characters [5,18].

Serial	Special characters	Clone	Originator
1	Wind tolerance	UPASI-2, UPASI-10	UPASI-TRF, India
2	Drought resistance	9 UPASI	UPASI -TRF, India
3	Frost resistance /tolerance	B-26	HPKV-TES, India
4	Smallest leaf	CH-1	IHBT, India
5	Biggest leaf	Betjan	Betjan T.E, India
6	Blister blight tolerance	TRI-2043, DT-1	TRI, Sri Lanka
7	High pubescence content	TRI-2043	TRI, Sri Lanka
8	High anthocyanin pigmentation	TRI-2025	TRI, Sri Lanka
9	High tolerance to pH	TN-14-3	TRF, Kenya
10	Poor fermenter	12/2	TRF, Kenya
11	Mite tolerance	7/9	TRF, Kenya
12	Scale insect tolerant	TN 14-3	TRF, Kenya
13	High polyphenol content (53.7%)	Luxi white tea	TRI, China
14	High amino acid content (6.5%)	Anji white tea	TRI, China
15	Low caffeine content (0.14%),	Guangdong tea	TRI, China
16	High caffeine content (6.96%)	Wild tea at Yunnan	TRI, China
17	Water logged tolerant	TV-9	TES, India
18	Very good pruning recovery and large leaf size	BT-13, BT-16	BTRI, Bangladesh

Conventional propagation and breeding

Tea is propagated either through seeds or cuttings. Usually seeds are collected from orchard, stratified in sand and then sown in polythene sleeves in the nursery where it takes 12–18 months before transferring to the field. Nevertheless, seed-grown plants show a high degree of variability. Therefore, the alternative choice is through vegetative propagation of the elite variety wherein single leaf internode cuttings, with an axillary bud are planted in polythene sleeves under shade for 12–18 months followed by the transfer of these rooted plants to the field. Recently, as an alternative propagation technique, grafting has gained considerable popularity. In this technique, fresh single leaf internode cuttings of both root-stock and scion are generally taken. Scion, commonly a quality cultivar, is grafted on root-stock, which is either drought tolerant or high yielding cultivar. Upon grafting, the scion and stock influence each other for the characters and thus composite plants combine both yield and quality characters resulting in 100% increase of yield with better quality than either of the non-grafted cultivar. Further, a modified improved 'second generation' grafting has been developed where tender shoots are grafted on the young seedlings of tea which have an additional advantage over conventional grafting due to presence of taproot system [17]. Tea breeding consists of hybridization as well as selection. Hybridization can be either natural or hand pollination. In natural hybridization, based on better performance of yield, quality or diseases resistance capability, two parents are planted side by side in an isolated place and allowed to bear fruits. Subsequently seeds (F1) are harvested, raised and planted. If average performance of these plants is found to be better than either parent, then seeds (F1) are released as hybrid seed or biclonal seed. However, some of the outstanding performers among the progenies are marked and verified for multilocational trial and released as clone, if still found suitable. These clones are geographically specific and most of the tea research institutes in the world have generated clones for their own region. Sometimes more than two parents are used and are known as polyclonal seeds. The idea is to introduce more variability among the F1 seeds. Since it is difficult to know about the pedigree of the cultivars (as pollen may come from any male), the chance of reproducibility is low and least preferred presently. Alternatively, pollination or control cross, despite being an important approach, has made a limited success in tea breeding. However, recently, few clones have been released in Kenya and Malawi using this technique. Selection is the most popular, age-old practice in tea breeding. Since commercial tea gardens earlier were established with seeds, lot of variability exits among them. In many instances, the elite plant has been identified in the existing bushes and released as clones. Majority of the tea clones have been developed through selection. However, pedigrees of the clones remain unknown.

Though breeding work is limited up to F1 progenies presently, F2 population holds greater promise for varietals improvement of tea. The advantage of this approach is better segregation of characters and with the help of molecular biology this can be exploited for marker-assisted selections for a particular trait and construction of linkage map which is till not available for tea. Although, conventional tea breeding is well established and has contributed much for tea improvement over the past several decades, the process is slow due to some bottlenecks. Specifically these bottlenecks are:

- perennial nature,
- long gestation periods,
- high inbreeding depression,
- self-incompatibility,
- unavailability of distinct mutant of different biotic and abiotic stress,
- lack of distinct selection criteria,
- low success rate of hand pollination,
- short flowering time (2–3 months),

– long duration for seed maturation (12–18 months), and
- clonal difference of flowering time and fruit bearing capability of some clones.

Similarly, vegetative propagation is an effective method of tea propagation. Yet it is limited by several factors such as:

– slower rates of propagation,
– unavailability of suitable planting material due to winter dormancy, drought in some tea growing area etc.,
– poor survival rate at nursery due to poor root formation of some clones, and
— seasonal dependent rooting ability of the cuttings.

Therefore, micropropagation technique appears to be ideal choice for circumvention of the problems related to conventional propagation. Additionally, transgenic technology has the potential for varietal improvement of tea through means other than conventional breeding. However, central to any successful transgenic technology is an efficient *in vitro* regeneration protocol. While an efficient regeneration protocol is essential for introduction of the foreign gene into plant tissues, micropropagation is important for the transfer of large number of genetically modified plants to the field within a short span of time [18].

In Bangladesh, considerable success has been achieved in the field of clonal selection and tea breeding during the last forty years. Sixteen improved vegetable clones and four biclonal seed stocks and one polyclonal seed stock have been developed and released to the industry [19]. Moreover, some unexplored research areas need to be addressed to increase the relatively low harvest index of tea and the genetic diversity of tea by inducing, recognizing and regenerating chromosomal change through mutation, polyploidy, tissue culture and genetic engineering.

Pruning and Tipping

Pruning is essential in tea to maintain the bush at an operable height as also vegetable vigor. General guidelines on types of pruning (i.e. rejuvenation, hard, medium and light pruning, cut-cross and skiffing) span of time between two pruning and the time of pruning in relation to carbohydrate reserves have been clearly laid out [20] and are adopted with benefit.

Tipping of bush recovering from pruning is an operation aimed at forming a level plucking surface and filling it by a quick production of secondary branches; in other words it is the first round of harvesting young shoots at an operational height and stage [21]. The ideal height of tipping should not only ensure adequate leaf area for maximum photosynthetic efficiency but also fast growth of a mature bush, and in Bangladesh it should be studied for the recommended clones.

Plucking

Removal of young and growing shoots comprising the apical bud and the two internodes immediately below it, which constitute the crop in tea, is called plucking. The tender shoots with growing tips (sinks) and young foliage, which would in normal course have contributed to food reserves (source), are perpetually harvested at short, regular intervals, stimulating a rapid succession of new crop of shoots. There is, thus an intricate relationship between the sink and the source in relation to harvesting in tea which could be altered at will [21]. Plucking system could be designed to determine the severity of the operation as also the amount of maintenance foliage (Source) retained on the bush [23]. The important objective of an efficient system of plucking should be to harvest the maximum possible crop, leaving a minimum period of rest to the buds, while simultaneously ensuring the health of

the bush by retaining adequate maintenance foliage on the bush to meet the carbohydrate requirements of buds in active phase [3]. Too much of maintenance foliage on the bush should be avoided, since it is likely to impose a constraint in obtaining higher yields as pointed out earlier. It has, indeed, been demonstrated that removal of lower layers of mature leaves leads to increased number of shoots per unit area and enhanced size of the harvestable shoot, resulting in increased productivity. This is an indicator of existence of an optimal ratio between the maintenance of foliage and yield, although more critical studies of basic nature are required to determine the precise leaf area that is necessary for higher productivity.

The amount of maintenance foliage retained on the bush could be regulated by optimizing the height of the tipping the bushes recovering from pruning [21] and proper scheduling of plucking system through the pruning cycle [3]. The maintenance leaves retained at the type of tipping should be fully exploited by allowing maximum light penetration during the early part of pruning cycle, when they are photosynthetically most efficient. Further health of the bush should be ensured by retention of new foliage on the bush whenever senility due to aging is suspected to set in among the older leaves. Another away of enhancing the sink activity is to increase the plucking surface area by alternating the canopy architecture into dome or wedge from the conventional flat surface. Such canopies will also facilitate better light penetration and expose more leaf area to the incident light. Yield of 11 and 19 % have been reported due to wedge and dome plucking, respectively [24]. Basic information on the movement photosynthates in shoot and bush is now required for the recommended clone in Bangladesh for a better appreciation of sink-source relationship, so that these operations are further refined to near precision.

Mechanization

True to the situation in the remote, tribal and hilly areas, the plantation industry (particularly tea) relies completely on manual labour. Even a wheelbarrow has not made its appearance in tea estates; the crop and agricultural inputs are still carried on head-loads in the field. A survey of cultural operation reveals the possibility of partial mechanization of at least certain operations like manuring, pruning and plucking 25]. Mechanization, where possible, is necessary not just to reduce the costs in the context of increasing wage-bill, but also to lighten burden of the worker and to make the work more interesting to him. Motorised mechanical aids to prune and skiff, developed in Japan, have been found to be useful [26], but are not available in Bangladesh. Use of hand-operated share shears for harvesting tea has been found to increase the productivity of workers and yield in tea [21], [24]. However they could be used only in high cropping seasons to cope with the labour-shortage. In other seasons, it is not favoured because of the fear of its non-selective harvesting and possible drop in quality. This problem could, perhaps, be overcome by collaborating with the agro-engineering industry.

Tea processing and marketing

Processing

The Engineering industry is more active in the area of tea manufacture than in the field. The machinery required for both orthodox and CTC (Cut, Tear and Curl) manufacture has been developed and standardized 25]. Usually, the tea maker is left with the discretion of deciding whether or not a particular process has been completed, thus leaving scope for an error of human judgment. Sample tests should be formulated to determine, at different stages of manufacture, the biochemical parameters of quality as understood in terms of appearance, color, brightness, briskness, aroma and creaming down, so that uniform standard of the produce is ensured. Measures should be devised to increase the cuppage (number of cups of liquor

Table 4.
MRL Value (ppm) of Various Pesticides in Made Tea [25].

Sl. No.	Technical name of the pesticide	EPA	Codex commission	European Union	German law	Remarks
1	Dicofol	45	8	0.1	2	very very restricted
2	Ethion	10	5	2(proposed 0.1)	-	-do-
3	Sethion	10	5	2	-	-do-
4	Bromopropylate	-	5	-	-	-do-
5	Dimethoate	-	-	0.2	-	-do-
6	Endosulfan	24	30	30	30	Restricted
7	Fenvelerate	-	-	0.1	-	very very restricted
8	Cypermethrin	-	-	0.1	-	-do-
9	Deltamethrin	-	-	5	-	-do-
10	Chlorpyriphos	-	-	0.1	-	-do-
11	Propargite	-	-	0.1	-	-do-
12	Malathion	-	-	0.1	-	-do-

MRL: Maximum Residue Level, EPA: Environmental Protection Agency

per unit weight of made tea) by enhancing the solubility of made tea and manufacturing methods developed for reducing waste.

Marketing

Consumer acceptance of tea as a drink for all times cannot be taken for granted because of the changing tastes and the availability of wide range of aroma of beverages in the market. Incisive market research into consumer preferences and testes would facilitate the introduction of tea in convenient packs, instant tea powder, value added teas, carbonated tea beverages and other consumable packs[27]. Such a generic promotion in conjunction with specific promotion of Bangladesh tea in brands can sustain tea consumption at increasing levels. Still in Bangladesh there is no instrument to measure Maximum Residue Level (MRL) of various pesticides. It will create a serious problem on export volume or sales promotion, since European countries (especially the west European countries) are very conscious about their health and hygiene.

Conclusion

Tea industries in Bangladesh are facing numerous problems. Some of these problems concern security problems of the executives, unexpected natural calamity, deterioration of law and order situation of the tea estates, log stealing, political or outsider influence on their internal arrangements, illegal occupation of land by the outsiders, lack of medical facilities, unhealthy atmosphere in the labour lines, over consumption of wine by the labourer, lack of infrastructure (road, quarter, water supply network etc), lack of capital and modern machineries, lower market value of made tea in comparison to increasing production cost, lower yield per hectare in comparison to increasing domestic need, lack of instrument for measuring MRL value, improper use of Govt. loans by some owners of the tea gardens, lack of perennial water source for irrigation during dry season and also in prolonged drought, lack of

educational institutions, malnutrition among the children of the labour line. For successful tea culture the above problems must be solved. To reduce production cost we have to produce quality tea with eye catching bright orange-red colour liquor with flavour or have to increase yield. We have to make clone tea with high yielding variety having good quality. We must remove the screen of distrust and suspicion of the European countries by establishing a clean image such as achieved by the Sri Lankan Tea Research Institute.

References

1. **Eden, T**. 1958 The development of tea culture. In: *Tea*. Ed. Eden, T., pp. 1–4, Longman, London.
2. **Wight, W**. 1959. Nomenclature and classification of tea plant. *Nature* 183: 1726–1728.
3. **Sana, D.L**. 1989.*Tea Science*. Ashrafia Boi Ghar, Dhaka, pp. 248-266.
4. **ITC**. 2001. *International Tea Committee report* 2001.
5. **BTRI**. 2003. *Biennial Report*. Bangladesh Tea Research Institute, Government of People's Republic of Bangladesh, pp. 94-98, Srimangal, Moulvibazar, Bangladesh.
6. **BBS.** 2000. *Statistical Year Book of Bangladesh*. Bangladesh Bureau of Statistics. Ministry of Planning, Government of People's Republic of Bangladesh, pp.81 & 327. Dhaka, Bangladesh.
7. **Wealth of India.** 1950. *A directory of Indian raw materials and industrial products*. Vol. II. S.S. Bhatnagar. Chairman, Editorial Committee, pp. 26–51. Council of Scientific and Industrial Research, New Delhi, India.
8. **Chen, Z.** 1999. Pharmacological functions of tea. In: *Global Advances in Tea Science*. Ed. Jain, N.K., pp.333-358, Aravali Books International (pvt) Ltd., India.
9. **Chengyin, L., Weihua, L. and Mingjun, R.** 1992. Relationship between the evolutionary relatives and the variation of esterase isozymes in tea plant. *J. Tea Sci.* 12:15–20.
10. **Sealy, J.R.** 1958. A revision of the genus *Camellia*. *R. Hortic. Soc. London* 19:519-524.
11. **Mondal, T.K., Bhattacharya, A. and Ahuja, P.S.** 2002. Induction of synchronous secondary embryogenesis of tea (*Camellia sinensis*). *J. Plant Physiol*. 158:945–951.
12. **Visser, T.** 1969. Tea (*Camellia sinensis* (L.) O. Kuntze). In: *Outlines of perennial crop breeding in the tropics*. Eds. Ferwerdu, E.P. and Wit, F., pp. 459–493. Veenaran and Zonen, Wageningen, The Netherlands.
13. **Banerjee, B.** 1992. Botanical classification of tea. In: *Tea cultivation to consumptio*n. Eds. Wilson, K.C. and Clifford, M.N., pp. 25–51. Chapman and Hall, London.
14. **Wood, D.J. and Barua, D.N.** 1958. Species hybrids of tea. *Nature* 181:1674–1675.
15. **Wight, W.** 1962. Tea classification revised. *Curr. Sci.* 31:298–299.
16. **Sharma, V.S. and Venkataramani, K.S.** 1974. The tea complex.I. Taxonomy of tea clones. *Proc. Ind. Acad. Sci*. 53:178–187.
17. **Prakash, O., Sood, A., Sharma, M. and Ahuja, P.S.** 1999. Grafting micropropagated tea (*Camellia sinensis* (L.) O. Kuntze) shoots on tea seedling- a new approach to tea propagation. *Plant Cell Rep*. 18:137–142.
18. **Mondal, T.K., Bhattacharya, A., Laxmikumaran, M. and Ahuja, P.S**. 2004. Recent advances of tea (*Camellia sinensis*) biotechnology. *Plant Cell, Tissue Culture* 76:195–254.
19. **Alam, A.F.M**. 2002. *Research on varietal improvement of tea and their utilization in the tea industry of Bangladesh*. Proceedings of the International Seminar on "Varietal development of Tea in Bangladesh*", 13 July 2002*. Organized by Bangladesh Tea Research Institute, Srimangal-3210, Maulvibazar, Bangladesh, pp 7-26.
20. **Sharma, V.S**. 1984. Pruning of tea—precepts and practices. *UPASI Tea Sci. Dep. Bull.*39:63-67.
21. **Sharma, V.S., Ramachandran, K.V. and Venkata Ram, C.S.** 1981. Tipping in relation to pruning height and its effect on the yield of *tea (Camellia spp.) J. Plant Crops* 9:112-118.
22. **Sharma, V.S**. 1983. Plucking styles. *UPASI Tea Sci. Dep. Bull.*38:33-38.
23. **Wettasinaghe, D.T., Nathaniel, R.K. and Kroon, D.D.** 1981. Effect of severity of plucking on the growth and yield of low-grown tea. *Tea Quart*. 50:123-130.
24. **Reddy, G.P.** 1983. Areas for exploitation in harvesting technology to enhance productivity in tea. *UPASI Tea Sci. Dep. Bull.* 38:53-56.
25. **Khisa, P. and Iqbal, I.** 2001. *Tea manufacturing in Bangladesh: Problems and prospects*. Proceedings of the International Conference on "Mechanical Engineering", 26-28 December 2001, Department of Mechanical Engineering, Bangladesh University of Science and Technology, Dhaka.
26. **Sharma, V.S. and Venkata Ram, C.S**.1980. Motorized mechanical aids to prune/skiff tea (*Camellia L. spp) Proc. PLACROSYM-III*:283-288.
27. **Sharma, V.S. and Ranganathan, V.** 1985. The word of today: *Outlook of agriculture* 14:35-41.

Proc. Pakistan Acad. Sci. 42(4):315-323.2005

Review

ADVERSE EFFECTS OF PESTICIDES AND RELATED CHEMICALS ON ENZYME AND HORMONE SYSTEMS OF FISH, AMPHIBIANS AND REPTILES: A REVIEW

M. Zaheer Khan* and Francis C.P. Law

Department of Biological Sciences, Simon Fraser University, Burnaby, British Columbia, Canada V5A IS6

Received February 2005, accepted October 2005

Communicated by Prof. Dr. M. A. Hafeez

Summary: The enzyme and hormone disrupting capabilities of pesticides and related chemicals are suspected to be some of the factors contributing to the decline of fish, amphibian, and reptile populations. Globally frogs and other amphibians have been disappearing at an alarming rate. In most cases, the cause or causes are unknown, but are assumed to result from man-made pollutants in the aquatic environment. Some current reports have indicated that many pesticides in the aquatic environment are capable of disrupting the endocrine systems of animals. Some pesticides and related chemicals are persistent in the environment and are accumulated in the fatty tissue of organisms and increase in concentration as they move up through the food web. These chemicals are substances that can cause adverse effects by interfering in some way with the body's hormones or chemical messengers. A recent study indicated that the atrazine effected the sexual development of frogs, even at extremely low doses. Some pesticides reduce the cholinesterase activity of amphibians and reptiles. Some chemicals may cause disease and reproductive failure in fish populations, because they bioaccumulate in the higher trophic levels. Therefore, brown trout exposed to environmental pollutants have been shown to have decreased egg size and low growth rate of the larvae.

Keywords: Pesticides, enzymes, hormones, amphibian, reptile, fish

Introduction

Pesticides and related chemicals destroy the delicate balance between species that characterizes a functioning ecosystem. Pesticides produce many physiological and biochemical changes in freshwater organisms by influencing the activities of several enzymes. Alterations in the chemical composition of the natural aquatic environment usually affect behavioral and physiological systems of the inhabitants, particularly those of the fish [1].

Hormone-disrupting effects in biota as a result of chemicals are caused by a wide variety of mechanisms. Pesticides and related chemicals are substances that can cause adverse effects by interfering in some way with the body's hormones or chemical messengers. These substances are therefore called hormone disruptors or endocrine disruptors, as it is the endocrine glands that secrete the hormones. Hormones play a crucial role in guiding normal cell differentiation in early life forms, and so exposure to endocrine disrupting substances in the egg or in the womb (mammals) can alter the normal process of development. Lately, most attention has been focused on estrogens; natural or synthetic compounds that elicit a feminizing effect by binding to the cellular estrogen receptor in organisms. The interaction between an estrogenic compound and its receptor causes a number of

*To whom correspondence and reprint requests should be addressed.

reactions and development. Environmental problems with estrogenic compounds seem to occur primarily in the aquatic environment, like feminization of male fish [2]. Adult animals can also be affected, but it is the embryonic stages that are especially vulnerable. Exposure at this sensitive time may cause effects in mammalian systems that are not evident until later in life, such as effects on learning ability, behavior, reproduction and increased susceptibility to cancer and other diseases.

The pesticides and related chemicals originating from human activity or agricultural farming are discharged directly or indirectly into the receiving waters. The presence of these chemicals in the environment has become a global issue. Field studies have shown that the reproduction, growth and development of wildlife species, including invertebrates, amphibians, reptiles, fish, birds and mammals may have been impacted by chemicals that interact with the endocrine system. Pesticides at low concentrations may act as blockers of sex hormones, causing abnormal sexual development, abnormal sex ratios, and unusual mating behavior. Pesticides can also interfere with other hormonal processes, such as thyroid and its influence on bone development [3]. This paper reviews the adverse effects of pesticides and related chemicals on enzyme and hormone systems in fish, amphibians and reptiles.

Effects on fish

Fish species are sensitive to enzymic and hormone disruptors. Chronic exposure to low levels of pesticides may have a more significant effect on fish populations than acute poisoning. Doses of pesticides that are not high enough to kill fish are associated with subtle changes in behavior and physiology that impair both survival and reproduction [4]. Biochemical changes induced by pesticidal stress lead to metabolic disturbances, inhibition of important enzymes, retardation of growth and reduction in the fecundity and longevity of the organism [5]. Liver, kidney, brain and gills are the most vulnerable organs of a fish exposed to the medium containing any type of toxicant [6]. The fish show restlessness, rapid body movement, convulsions, difficulty in respiration, excess mucous secretion, change in color, and loss of balance when exposed to pesticides. Similar changes in behavior are also observed in several fishes exposed to different pesticides [7].

The Great Lakes fish are contaminated with chlorinated organic compounds such as PCB and dichlorodiphenyl dichloroethene, pesticides such as mirex and dieldrin, and trace amounts of metals such as lead and mercury [8]. Lake trout, which became extinct in the Great Lakes in the 1950s, has been shown to be very sensitive to dioxins and (polychlorinated biphenyls) PCBs when exposed as embryos. Several species of salmon introduced into the Great Lakes have severely enlarged thyroid glands, which is strong evidence of hormone disruption. Salmon in the Lake Erie show a variety of reproductive and developmental problems, for example, early sexual development and a loss of the typical male secondary sexual characteristics, such as heavy protruding jaws and red coloration on the flanks.

Some agrochemicals can indirectly affect fish by interfering with their food supply or altering the aquatic habitat, even when the concentrations are too low to affect the fish directly. Other agricultural chemicals are capable of killing salmon and other aquatic animals directly and within a short period of time. For example, in 1996 the herbicide acrolein was responsible for the death of approximately 92,000 steel-head, 114 juvenile coho salmon, 19 resident rainbow trout, and thousands of non-game fish in the Bear Creek, a tributary of the Rogue River [3]. Several laboratory experiments show that sublethal concentrations of agrochemicals can affect many aspects of salmon biology, including a number of behavioral effects [3].

Under experimental conditions, rainbow trout exposed for 18-34 days to a combination of 0.05 mg/l of the organochlorine endosulfan and 0.5 mg/l of the organophosphate disulfoton showed changes in the ultrastructure of hepatic cells, with irregular nuclei, and alterations to the lysozomes and rough endoplasmic reticulum [9]. Some pesticides such as organochlorine, organophosphates and carbamates are known to cause morphological damage to the fish testis. These also affect female fish in the same way. They cause delayed oocyte development and inhibition of steroid hormone synthesis [10]. Experimental exposure of fish to them has been shown to depress protein values in brain, gills, muscle, kidney and liver. In the kidney and the liver there is evidence of significant decrease in the protein content due to stress in elimination and also in metabolism [11].

Interference with endocrine hormones affects reproduction, immune function, development, and neurological functions in several species of wild animals. In fish, endocrine disruptors interrupt normal development and cause male fish to have female characteristics. These outward symptoms of developmental disruption are accompanied by reduced fertility and even sterility in adults, as well as lower hatching rates and viability of offspring. Many studies show a direct relationship between concentrations of pesticides and related chemicals in fish tissues and depressed hormone concentrations. Disruption of the balance of endocrine hormones during development of young fish can also cause defects of the skeletal system, resulting in deformities and stunted growth [3,12].

The common pesticide synergist piperonyl butoxide increases carbaryl toxicity (Carbaryl is a neurotoxic carbamate pesticide). In fish, acute toxicity of a carbaryl- piperonyl butoxide mixture was over 100 times that of carbaryl alone [13]. In addition, carbaryl increases the acute toxicity of the phenoxy herbicide 2,4-D, the insecticides rotenone and dieldrin (an organochlorine) as well as the wood preservative pentachlorophenol [14]**.** Sublethal effects of the organophosphate insecticide phenthoate are also synergized by carbaryl in fish, resulting in AChE inhibition [15] and both morphological and behavioral changes [16]. While the toxicity of combinations of chemicals is rarely studied, the ability of carbaryl to interact with a large number of chemical classes is striking.

Effects on amphibians

Concern over the decline of amphibians globally has highlighted the importance of using this group as a bioindicator of environmental contamination and climate change. Since 1989, there has been a growing realization that amphibian populations have been declining at an alarming rate. The present data show significant declines all over the world. Nearly 600 amphibian populations studied in Western Europe show 53% decline beginning in the 1950s [17]. In North and South America, 54% and 60% of the populations, respectively, have shown significant declines. In Australia and New Zealand, as much as 70% of the amphibian populations studied have declined. According to the 2004 IUCN Red List [18], there are 20 countries with the highest number of threatened amphibians (Table 1). The numbers of threatened species are increasing in all taxonomic groups (Table 2) due to environmental pollution (including pesticides and related chemicals), habitat destruction as well as climate change. During the year 2000 and 2004, the number of extinctions in the fish, amphibian, reptilian, mammalian and avian groups has increased further. There are 338 species which are considered extinct and another 22 species are considered extinct in the wild (Table 3).

Table 1.
Countries with highest number of threatened amphibians [18].

Rank	Country	Threatened Species
1	Colombia	208
2	Mexico	191
3	Ecuador	163
4	Brazil	110
5	China	86
6	Peru	78
7	Guatemala	74
8	Venezuela	68
9	India	66
10	Costa Rica	61
11	Madagascar	55
12	Honduras	53
13	Panama	52
14	USA	51
15	Cameroon	50
16	Philippines	48
17	Australia	47
18	Cuba	47
19	Haiti	46
20	Malaysia	45

Amphibians are important components of aquatic habitats, especially in tropical regions of the world [22]. The mechanisms responsible for the decline of amphibian populations include chemical pollution from pesticides and fertilizers and global climate change [19]. The health of amphibians can suffer from exposure to pesticides [20]. Because of their semipermeable skin, the development of eggs and larvae in water, and the position in the food web, amphibians are prone to adverse effects of waterborne and airborne pollutants in their breeding and foraging habitats [21]. Pesticides may affect amphibian populations in a number of ways [27]; they may kill individual amphibians directly [28] or indirectly through alterations in immune or neurological function [29]. Pesticides may also affect recruitment in amphibian populations by disrupting normal growth and development of the young or by impairing adult reproduction [27]. An extensive research study conducted in Quebec, Canada, shows that hind limb deformities are commonly observed in transformed bullfrogs, green frogs, northern leopard frogs, and American toads [23]. Deformity rates tend to be higher at agricultural areas, suggesting that herbicides and pesticides are the likely causes.

Table 2.
Numbers of threatened species by major taxonomic group [18].

Taxonomic group	Number of described species	Number of species evaluated	Number of threatened species in 2004	Number threatened as % of species described	Number threatened as % of species evaluated
Fish	28,500	1,721	800	3%	46%
Amphibians	5,743	5,743	1,856	32%	32%
Reptiles	8,163	499	304	4%	61%
Mammals	5,416	4,853	1,101	20%	23%
Birds	9,917	9,917	1,213	12%	12%

Table 3.
Numbers of extinct (EX) and extinct in the wild (EW) species by taxonomic group in 2004 [18].

Taxonomic group	Extinct (EX)	Extinct in the wild (EW)	Total
Fish	81	12	93
Amphibians	34	01	35
Reptiles	21	01	22
Mammals	73	04	77
Birds	129	04	133
Total	**338**	**22**	**360**

Because deformities of frogs do not always occur in these areas, a number of other factors may be involved, including the incidence or abundance of certain diseases or parasites [24]. Fifteen amphibian species have been designated as endangered, threatened, or of special concern by the Committee on the Status of Endangered Wildlife Canada due to some threats including chemical contamination [24].

Amphibians are known to be vulnerable to pesticides that are cholinesterase inhibitors [25]. Anticholinesterase pesticides function by binding with this enzyme in animals and disrupting nervous system activity, usually causing death by respiratory failure. Decreased cholinesterase activity can indicate exposure to some commonly used pesticides and can be harmful to wild animals [26]. The anticholinesterase effects of two other pesticides, Lambda cyhalothrin (a pyrethroid) and monocrotophos (an organophosphate), on *Rana cyanophlyctis* (Skittering frog) have been observed in the liver, kidney and brain. About 34.6 - 46.3%, 25.08 - 57.1% and 31.64 - 50.7% of the cholinesterase activities in the liver, kidney and brain, respectively are reduced following exposure to cyhalothrin. For monocrotophos treatment, cholinesterase decreases about 37.7 - 57.7%, 57.5 - 67.5% and 47.6 - 65.9% in the liver, kidney and brain, respectively [38]. The effect of two pyrethroids, Lambda cyhalothrin and Permethrin, on the cholinesterase activity of amphibian *R. cyanophlyctis* and *Rana tigrina* have also been compared. The cholinesterase activities of cyhalothrin treated frogs are decreased 34.6 - 46.3%, 25.08 - 57.1% in the liver and kidney. Permethrin treatment decreases cholinesterase activity 23 - 29% and 6.76 - 35% in the liver and kidney, respectively [39]. Total protein content also decreases in non-target amphibians after pesticide treatment, indicating pesticide-produced changes in the biochemical systems of non-target organisms [40]. The brain cholinesterase activity of *Rana cyanophlyctis* decreases upto 4.10 and 13.84 % under the effect of sandaphos and 5.16 and 23.28% under the effect of b-cypermethrin, respectively [41].

Some pesticides, herbicides, and nematocides are documented to have endocrine-disrupting effects [30]. To date, there are no reports linking endocrine dysfunction with amphibian malformations. However, it is well established that pesticides and related chemicals can be major ecological threats to fish and aquatic wildlife by diminishing productivity and fecundity [30]. The normal growth and development of amphibian larvae rely on functional and uncontaminated aquatic systems. Water sources are

particularly at risk to contamination by pesticides because of the accumulation and distribution of contaminating substances in sediments of rivers, lakes, and ponds. Potential sources of EDCs that impact bodies of water include municipal sewage [31], and agricultural runoff (pesticides and herbicides) [32]. Thus, the EDCs that accumulate in aquatic systems may adversely affect amphibian reproductive processes.

Exposure of amphibians to dimethoate, carbofuran and chlorpyifos can alter vitamin A levels [33] and reduce melanogenesis [34]. Carbaryl, a short-lived carbamate that acts through acetylcholinesterase inhibition, may serve as a model chemical for neurotoxins (i.e., carbamates and organophosphates). The effects of sublethal concentrations are more relevant to amphibian communities because they may directly affect time of and size to metamorphosis, or indirectly affect survival [35].

Some studies have reported that the tadpole stage of *Rana* spp. is sensitive to herbicides, and various types of deformities in the tadpoles serve as possible indicators of such sensitivity. Tadpoles are also highly sensitive to organochlorine pesticides, and toxic effects of these pesticides are evident during metamorphosis [29], a period of marked endocrine change and reduction. In Minnesota, USA, some pesticides or their degradation products have been detected in water and sediment samples in very small quantities [36]. Despite the current documentation of amphibian declines and malformations, there are only few reports on the use of amphibians as models for abnormalities of reproductive processes by exposure to EDCs. In one study, the interactions of gonadal steroids and pesticides (DDT, DDE) on gonoduct growth in larval tiger salamanders, *Ambystoma tigrinum*, were examined [37]. The salamanders were immersed in a solution of DDE, DDT, or injected with estradiol or dihydro-testosterone. Essentially all the compounds tested had some adverse effect on the gonoduct growth in this species of salamanders.

Effects on reptiles

Very rapidly deteriorating status of freshwater turtles and tortoises in Southeast Asia has resulted in an increasing number of these species being listed as threatened in the IUCN Red List; globally 42% of turtle and tortoise species are threatened [18]. The decline in the population of alligator in the Lake Apopka, Florida (USA), is contaminated by organochlorine pesticides that emanate from a chemical spill. Here, a number of disturbing abnormalities were recorded in hatchlings and juvenile alligators, including modifications of enzyme activity, concentrations of sex hormones, abnormal ovarian morphology and unusually small phalluses [42,43]. Because these chemicals are known to be weak androgen receptors, the hypothesis that the individual and the population level effects observed in the alligators are due to chemical disruption of endocrine function seems reasonable [44].

The common snapping turtle (*Chelydra serpentina*) is the largest freshwater turtle occurring in Canada. Snapping turtle eggs from the Great Lakes contain high concentrations of fat-soluble contaminants which are absorbed while food is being digested. These include PCBs, dioxins, furans and organochlorine pesticides. Abnormal development, such as incidence of unhatched eggs or deformed animals, occurs at the highest rates in the sites which are the most contaminated [45]. In addition, a correlation between contaminated eggs and reduced developmental success has also been indicated [46].

The anticholinesterase effects of the phytopesticide, biosal (neem based formulation), on Indian garden lizard (*Calotes versicolor*) have been observed in the kidney and liver. About 13.60 - 18% and 39.52 - 52.61% of the cholinesterase activities in the kidney and liver are reduced following

exposure to biosal [47].

Conclusion

This review shows that pesticides and related chemicals are capable of blocking the action of hormones in fish, amphibians and reptiles and causing reproductive dysfunction and abnormal development. They act on target tissues through hormone receptors or nonreceptors, may influence hormone secretion or its clearance from the body. In the last years, a number of deformed frogs have been found in the eastern US and Canada. The cause of mass deformities of transforming frogs remains elusive, but various factors have been implicated, including pesticides and related chemicals. The role of pesticides and related chemicals in amphibian malformations may be of concern due to the high deformity rates associated with sites where agricultural chemicals have been used. These chemicals can be a major threat to fish, amphibians and reptiles, and aquatic environment by diminishing productivity and fecundity. Further research is needed to evaluate the effectiveness of alternative pesticides and related chemicals to reduce the effects on fish, amphibian and reptilian populations. Globally, studies need to simultaneously consider the benefits to both agricultural and conservation communities; scientists from both communities should provide input to make realistic and informed decisions about the protection and conservation of aquatic biodiversity within agricultural landscapes.

References

1. **Radhaiah, V., Girija, M. and Rao, K.J.** 1987. Changes in selected biochemical parameters in the kidney and blood of the fish, *Tilapia mossambica* (Peters), exposed to heptachlor. *Bull. Environ. Contam. Toxicol.* 39:1006-1011.
2. **Jobling, S., Nolan, M., Tyler, C.R., Brighty, G.C. and Sumpter, J.P.** 1998. Widespread sexual disruption in wild fish. *Environ. Sci. Technol*. 32:2498-2506.
3. **Ewing, R.D.** 1999. Diminishing returns: *Salmon decline and pesticides*. Funded by the Oregon Pesticide Education Network, Biotech Research and Consulting, Inc., Corvallis, OR. 55 pp.
4. **Kegley, S., Neumeister, L. and Martin, T.** 1999. *Ecological Impacts of Pesticides in California*. Pesticide Action Network, California, USA. pp 99.
5. **Murty, A.S.** 1986. *Toxicity of Pesticides to fish. Vols. I and II*. C.R.C Press Inc. 483pp, 355pp.
6. **Jana, S. and Bandyopadhyaya, S.** 1987. Effect of heavy metals on some biochemical parameters in the freshwater fish *Channa punctatus*. *Environ. Ecol*. 5:488-493.
7. **Haider, S. and Inbaraj, M**. 1986. Relative toxicity of technical material and commercial formulation of malathion and endosulfan to a freshwater fish, *Channa punctatus* (Bloch). *Ecotoxicol. Environ. Saf.* 11:347-351.
8. **Susan, L., Schantz, S.L., Gasior, D.M., Polverejan, E., McCaffrey, R.J., Sweeney, A.M., Humphrey, H.E.B. and Gardiner, J.C.** 2001. Impairments of memory and learning in older adults exposed to polychlorinated biphenyls via consumption of Great Lakes fish. *Environ. Health Perspect.* 109:605-611.
9. **Arnold, H., Plutra, H.J. and Braunbeck, T.** 1995. Simultaneous exposure of fish to endosulfan and disulfoton *in vivo*: ultrastructure, sterological and biochemical reactions in hepatocytes of male rainbow trout (*Oncorhynchus mykiss*). *Aquat. Toxicol.* 33:17-43.
10. **Kim, D.E**. 1998. *Endocrine disruption in fish*. Kluwer Academic Publishers, London.
11. **Tilak, K.S., Janardhana Rao, N.H. and Lakshmi, J.** 1991. Effect of pesticides mixed in different ratios to the freshwater *Lareo rohita*. *J. Ecotoxicol. Environ. Monit.*1:49-52.
12. **Goodbred, S.L., Gilliom, R.J., Gross, T.S., Denslow, N.P., Bryant, W.L. and Schoeb, T.R.** 1997. Reconnaissance of 17B-estradiol, 11-ketotestosterone, vitellognin, and gonad histopathology in common carp of United States streams: Potential for contaminant-induced endocrine disruption: U.S Geological Survey, Open-File Report, pp. 96-627.
13. **Singh, D.K. and Agarwal, R.A.** 1989. Toxicity of piperonyl butoxide-carbaryl synergism on the snail *Lymnaea acuminata*. *Int. Revue ges. Hydrobiol*. 74:689-699.
14. **Statham, C.N. and Lech, J.J.** 1975. Potentiation of the acute toxicity of several pesticides and herbicides in trout by carbaryl. *Toxicol. Appl. Pharmacol.* 34:83-87.
15. **Rao, K.R.S.S. and Rao, K.V.R.** 1989. Combined action of carbaryl and phenthoate on the sensitivity of the acetylcholinesterase system of the fish. *Ecotoxicol. Environ. Saf.* 17:12-15.
16. **Rao, K.R.S.S. and Rao, J.C.**. 1987. Independent and combined action of carbaryl and phenthoate on

snake head, *Channa punctatus* (Bloch). *Curr. Sci.* 56:331-332.

17. **Houlahan, J., Findlary, C., Schmidt, B., Meyer, A. and Kuzmin, S.** 2000. Quantitative evidence for global amphibian population declines. *Nature* 404:752-755.
18. **Baillie, J.E.M., Hilton-Taylor, C. and Stuart, S.N.** (editors). 2004. *IUCN Red List of Threatened Species.* A Global Species Assessment. IUCN, Switzerland and Cambridge, UK, pp 191.
19. **Lips, K.R**. 1998. Decline of tropical montane amphibian fauna. *Conserv. Biol.* 12:106-117.
20. **Harfenist, A., Power, T., Clark, K.L. and Peakall, D.B.** 1989. *A review and evaluation of the amphibian toxicological literature.* Technical Report Series No. 61, Canadian Wildlife Service, Ottawa..
21. **Bishop, C.A**. 1992. *The effects of pesticides on amphibians and the implications for determining causes of declines in amphibian population*. Proceeding of a workshop on declines in Canadian amphibian populations: designing a national monitoring strategy. Canadian Wildlife Service, pp 67-70.
22. **McDiarmid, R.W**. 1992. *Standard methods for measuring and monitoring biological diversity of amphibians.* Proceeding of a workshop on Declines in Canadian amphibian populations: designing a national monitoring strategy. Canadian Wildlife Service, pp 80-82.
23. **Ouellet, M., Bonin, J., Rodrigue, J., DesGranges, J.L. and Lair, S**. 1997. Hindlimb deformities (ectromelia, ectrodactyly) in free-living anurans from agricultural habitats. *J. Wildl. Dis.* 33:95-104.
24. **David, S. and Seburn, C**. 2000. *Conservation priorities for the amphibians and reptiles of Canada.* CARCN, 93 pp.
25. **Wang, C. and Murphy, S.D.** 1982. Kinetic analysis of species difference in acetylcholinesterase sensitivity to organophosphate insecticides. *Toxicol. Appl. Pharmacol.* 66:409-419.
26. **Catherine, H. and Gloria, M.** 2000. USGS Research finds that contaminants may play an important role in California amphibian declines. US. Geological Survey, MS119 National Center, Reston,VA, USA.www.usgs.gov/public/press/public_affairs/press_releases/pr1338m.html.
27. **Carey, C. and Bryant, C.J**. 1995. Possible interrelations among environmental toxicants, amphibian development, and decline of amphibian populations. *Environ. Health Perspect.* 103 (suppl 4):13-17.
28. **Kirk, J.J.** 1988. Western spotted frog (*Rana pretiosa*) mortality following forest spraying of DDT. *Herpetol. Rev.* 19:51-53
29. **Cooke, A.S.** 1971. Selective predation by newts on frog tadpoles treated with DDT. *Nature* 229:275-276.
30. **Crain, D.A. and Guillette, L.J. Jr.** 1997. Endocrine-disrupting contaminants and reproduction in vertebrate wildlife. *Rev. Toxicol.* 1:47-70.
31. **Purdom, C.E., Hardiman, P.A., Bye, V.J., Eno, N.C., Tyler, C.R. and Sumpter, J.P**. 1994. Estrogenic effects of effluents from sewage treatment works. *Chem. Ecol*. 8:275-285.
32. **Grute, C. E, Gilbert, P.L. and Seeley, M.E**. 1997. Neurohysiological and behavioral changes in non-target wildlife exposed to organophosphate and carbamate pesticides: thermoregulation, food consumption, and reproduction. *Am. Zool.* 37:369-388.
33. **Keshavan, R. and Deshmukh**, **P.B**. 1984. Vitamin A concentrations in liver and serum of frog, *Rana tigrina*, treated with DDT and sevin. *Indian J. Comp. Anim. Physiol*. 2:32-36.
34. **Arias, E. and Zavanella, T.** 1979. Teratogenic effects of manganese ethylenebisdithiocarbamate (Maneb) on forelimb regeneration in the adult newt, *Triturus cristatus carnifes*. *Bull. Environ. Contam. Toxicol*. 22:279-304.
35. **Boone, M.D. and Semlitsch, R.D**. 2001. Interactions of an insecticide with larval density and predation in experimental amphibian communities. *Conserv. Biol.* 15:228-238.
36. **Jones, P.M., Thurman, E.M., Little, E., Kersten, S., Helgen, J. and Scribner, E.A**., 1999. *Pesticide and metabolite concentrations in sediments and surface and ground water found at sites where frog malformations are present in Minnesota* [abs.]: 7th Symposium on the Chemistry and Fate of Modern Pesticides, Lawrence, KS, USA, September 14-16, 1999.
37. **Clark, E. J., Norris, D. O. and Jones, R. E**. 1998. Interactions of gonadal steroids and pesticides (DDT, DDE) on gonaduct growth in larval tiger salamanders, *Ambystoma tigrinum*. *Gen. Comp. Endocrinol.* 109:94-105.
38. **Khan, M.Z., Maria, Z. and Fatima, F**. 2003. Effect of lambda cyhalothrin (pyrethroid) and monocrotophos (organophosphate) on cholinesterase activity in liver, kidney and brain of *Rana cyanophlyctis*. *Korean J. Biol. Sci.* 7:165-168.
39. **Khan, M.Z., Nazia, M., Fatima, F., Rahilla, T. and Gabol, K**. 2003. Comparison in the effect of lambda cyhalothrin with permethrin on cholinesterase activity in wildlife species *Rana cyanophlyctis* and *Rana tigrina* (Ranidae: Amphibia). *Bull. Pure. Appl. Sci*. 22A:43-49.
40. **Khan, M.Z., Tabassum, R., Naqvi, S.N.H., Erum, Z., Farhana, T., Ahmad, I., Fatima, F. and Khan, M.F**.

2003. Effect of cypermethrin and permethrin on cholinesterase activity and protein content in *Rana tigrina* (Amphibia). *Turkish J. Zool*. 27: 243-246.

41. **Khan, M.Z. and Ghazala, Y**. 2005. Pesticides dependent cholinesterase activity in the brain tissue of *Rana cyanophlyctis*. *J. Exp. Zool. India* 8:135-140.
42. **Guillette, L.J. Jr., Gross, T.S., Masson, G.R., Matter, J.M., Percival, H.F. and Woodward, A.R.** 1994. Developmental abnormalities of the gonad and abnormal sex hormone concentrations in juvenile alligators from contaminated and control lakes in Florida. *Environ. Health Perspect.* 102:680-688.
43. **Guillette, L.J. Jr., Gross, T.S., Masson, G.R., Matter, J.M., Percival, H.F. and Woodward, A.R.** 1999. Serum concentration of various environmental contaminants and their relationship to sex steroid concentrations and phallus size in juvenile American alligators. *Arch. Environ. Contam. Toxicol.* 36:447-455.
44. **Ankley, G.T. and Giesy, J.P**. 1998. Endocrine disruptors in wildlife: a weight of evidence perspective. Proceeding from Principal Processes for Evaluating Endocrine Disruption in Wildlife. *SETAC Press*, pp. 349-367.
45. **Shirose, L., Bishop, C. and Gendron, A.** 1995. *Amphibians and reptiles in Great Lakes Wetlands: Threats and Conservation.* Environment Canada, Catalogue No. En 40-222/4-1996E
46. **Bishop, C.A., Brooks, R.J., Carey, J.H., Norstrom, R.J. and Lean, D.R.S.** 1991. The case for a cause-effect linkage between environmental contamination and development in eggs of the common snapping turtle (*Chelydra s. serpentina*) from Ontario, Canada. *J. Toxicol. Environ. Health.* 33:521-547.
47. **Khan, M.Z., Naqvi, S.N.H., Khan, M.F., Tabassum, R., Ahmad, I., Fatima, F. and Tariq, R.M**. 2003. Determination of Induced effect of phytopesticide biosal (Neem based formulation) on cholinesterase activity and protein content in kidney and liver of *Calotes versicolor* Daudin. *J. Exp. Zool. India* 6:175-179.

INSTRUCTIONS TO AUTHORS

Proceedings of the Pakistan Academy of Sciences publishes original research papers on a broad range of topics of basic and applied sciences. State-of-the-art reviews (~ 20 pages, well supported by recent references) which adequately summarise work in a particular area of science, especially in the context of Pakistan and indicate lines of further research are also considered for publication. All original research articles are classified under 4 sections: **Life Sciences, Physical Sciences, Medical Sciences** and **Engineering Sciences & Technology.** All papers are refereed externally. Authors are not required to be members or fellows of the Academy. Manuscripts may be submitted from any country; however, all manuscripts must be submitted in English.

The authors are requested to read the following instructions carefully before submitting a manuscript. Failure to comply with these guidelines is liable to delay the review process and possible publication of the manuscript.

Manuscript preparation:
Manuscripts should be typewritten, double-spaced on 8.5" x 11" paper with 1" margin on all sides. Two copies should be submitted, including Figures and Tables. Papers are subject to editorial revision for purpose of conformity to the style adopted. Manuscripts should in general not exceed 20 typewritten pages including Tables, Figures and illustrations. The authors must submit a 3.5" high density (HD) diskette containing a copy in **Microsoft (MS) Word** of the final version of the manuscript, or as e-mail attachment preferably to **Sectional Editors** (or Editor-in-Chief) through a fellow of the Academy (see Website).

Each of the following sections of the manuscript should be typed on a separate page and in the sequence shown below:

TITLE PAGE: Should carry: (A) title (in capital letters) of the article to have no more than 160 characters, in a concise but informative style. Do not use abbreviations or acronyms, (B) first name, middle initial, last name of each author, (C): name of the department(s) and institution(s) to which the work should be attributed, (D) name and address of author to whom correspondence should be addressed, include Email address if available, (E) short running title of no more than 50 characters.

ABSTRACT AND KEYWORDS: The second page should carry an **abstract** of 250 words or less. The abstract should be self-explanatory, without reference to the text. The abstract should state the objective of the study, the methods used, main findings and principal conclusions. Abbreviations may be used provided they are defined on first mention in the abstract and in the main text. Review articles may be submitted without an abstract. Please suggest five to eight **keywords** excluding any that are already used in the title.

TEXT: For ***original research articles*** the text should be divided into sections with the headings: Introduction: provide a clear and concise statement of the problem and the aims of the investigation, and cite the relevant literature on the subject. **Materials and Methods:** Provide an adequate account of the procedures including statistical tests (if any). Describe briefly but in such a way that sufficient information is provided to replicate the work. **Results:** to be clearly and concisely described with the help of appropriate tables, figures and other illustrative material. Results should have no repetition of data in figures, tables and text. **Discussion**. Provide a brief interpretation of your results in the light of relevant previous studies. Comments and interpretations should be supported by evidence or references. Do not use more than 3 levels of heads in the text. ***For review articles*** the text can be appropriately sectioned.

ACKNOWLEDGEMENTS: Acknowledge financial support and other types of assistance in a brief statement.

REFERENCES: References must be limited to directly related published papers. Authors bear total responsibility for the accuracy of the references. All references in the text are to be included in the list of References and *vice versa*. Only published articles or articles accepted for publication qualify for references. References to manuscripts submitted to other journals but not yet accepted are not permitted. In the text, references should be cited as consecutive numerals in square brackets, for example. "Brown *et al.* [2] reported ..." or ".. as previously described [3,6-8]". They should be listed in the same numerical order in the References list at the end of the manuscript on a separate sheet or sheets. List all authors.

Examples of references:

a. Articles in Journals-

1 . **Speh, B. and Vogan, D.A.** 1980. Reducibility of generalized principal series representations. *Acta Math*. 145: 227-299.

2. **Williams, R.L., Hilton, D.J., Pease, S., Wilson, T.A., Stewart, C.L., Grearing, D.P., Wagner, .F., Metcalf, D., Nicola, N.A. and Gough, N.M.** 1988. Myeloid leukaemia inhibitory factor (LIF) maintains the developmental potential of embryonic stem cells. *Nature* 336: 684-687

b. Chapters in books

3. **Cox, A.W.** 1988. Solar and geothermal energy. In: *Information Sources in Energy Technology*. Ed. Anthony, L.J. pp. 263-289. Butterworths, London.

4. **Smolen, J.E. and Boxer, L.A.** 1991. Functions of neutrophils. In: *Hematology*. Eds. Williams, W.J., Butler, E. and Litchman, M.A. 4th ed. pp. 3-101. McGraw Hill, New York.

c. Books:

5. **Leeper, G.W.** 1978. *Managing Heavy Metals on the Land*. Marcel Dekker, New York.
6. **Adams, D.O., Edelson, P.J. and Koren, H.S.** 1981. *Methods for studying Mononuclear Phagocytes.* Academic Press, San Diego.

TABLES: Tables must be typewritten on separate sheets and submitted in duplicate. They should be numbered consecutively according to order of citation, using arabic numbers. Each table must have a concise heading and should be comprehensible without reference to the text. The approximate position of each table in text should be indicated. Tables should be as simple as possible. Round off numbers within the table to the nearest whole number or significant digit. Place essential explanatory material below the table. Identify footnotes with superscript letters or symbols keyed to data in the table. Do not use vertical lines. Use horizontal lines only to separate the column heads from the data. Refer to published tables in a recent issue of the journal to verify the appropriate style.

ILLUSTRATIONS: Figures should be carefully and professionally prepared. Two sets of high quality camera-ready illustrative material are required. Number figures consecutively with Arabic numerals (1,2,3) in the order in which they are cited in the text. Glossy prints must be submitted for photomicrographs, gels and other halftones. Photocopies of line drawings are acceptable at submission as long as two sets of high quality camera copies are provided. Figures should be identified by a black lead pencil, on the top or back of each figure with figure number and the last name of the first author. Type **legends**, double-spaced, in numerical order, on a separate sheet or sheets. Use numbers and letters consistent in style with those used in the illustration.

Please note that the Figures may be printed (with or without reduction) in two styles. Figures layouts may either match the columns size of 8.2 x 24.0 cm or the entire page of 16.0 x 24.0 cm maximum size.

Line drawings: Computer generated figures produced on a laser printer are acceptable. Alternatively, original line drawings should be made with black ink on white drawing or tracing paper. Do not use lettering smaller than 9 points or unnecessarily large. Lettering should be proportional on all figures within an article. In graphs, the abscissa and ordinate should be clearly labelled, and the units of measurement given.

Photographs: Photographs must be of the highest quality and provided as glossy prints. They should be mounted if they are to form multiple panels on the journal page. All prints should be trimmed to exclude areas not relevant to the paper and be separated from adjacent photographs by uniform spaces. A scale bar should be included on all photomicrographs or magnification (e.g. x 400, x 8000 etc.) be given at the end of the legend. .

Declaration: Submission of the manuscript must be accompanied by the declaration that the results are original; approval of all authors concerned has been obtained to submit manuscript for consideration; the same material is neither 'in press' nor under consideration elsewhere and that the copyright of the paper will be assigned to the *Pakistan Academy of Sciences* in case the article is accepted for publication.

Manuscripts should be submitted to the following **Sectional Editors** (or to Editor-in-Chief).

Life Sciences
Prof. Dr. S. Irtifaq Ali
B-356, Block 6, Gulshan-e-Iqbal
Karachi, Pakistan
E-mail: flora@super.net.pk

Physical Sciences
Prof. Dr. M. Iqbal Choudhary
HEJ Research Institute of Chemistry
Karachi University
Karachi, Pakistan
E-mail: hej@cyber.net.pk

Medical Sciences
Prof. Dr. Iftikhar A. Malik
129 Hali Road, Westridge-1,
Rawalpindi Cantt.
E-mail: fmcrwp@isb.paknet.com.pk

Engineering Sciences & Technology
Prof. Dr. A. Raouf

Lahore, Pakistan
E-mail: abdulraouf@umt.edu.pk

For enquiries contact:

Prof. Dr. M.A. Hafeez
Editor-in-Chief
Pakistan Academy of Sciences
3-Constitution Avenue, G-5/2
Islamabad, Pakistan

Telephone: 92-51-9207140 and 9207789
Fax: 92-51-9206770
Email: hafeez1937@yahoo.com and pasisb@yahoo.com
Website: www.paspk.org